

EXPERIMENTAL SIMULATION OF DISTILLATION COLUMN PROFILE MAPS

Tshepo Sehole David Modise

A thesis submitted to the Faculty of Engineering and the Built Environment,
University of the Witwatersrand, Johannesburg, in fulfillment of the requirements for
the degree of Doctor of Philosophy.

Johannesburg, 2007

DECLARATION

I declare that this thesis is my own, unaided work. It is being submitted for the degree of Doctor of Philosophy in the University of the Witwatersrand, Johannesburg. It has not been submitted before for any degree or examination in any other University.

Tshepo Sehole David Modise

_____ day of _____ 2007

DEDICATION

This work is dedicated to my family and Seitlotli Ntlatleng, for all the love and support they gave me during the many years I spent studying.

ABSTRACT

One of the most important tasks in the chemical industry is the separation of multicomponent liquid mixtures into one or more high-purity products. Several technologies are feasible for this task, either alone or in combination, such as distillation, extraction, crystallization, ect. Among these, distillation is by far the most widely spread and has a long history in chemical technology. However, until recently, there has been no systematic approach for understanding the separation of complex mixtures where azeotropes and multiple liquid phases may occur.

There has been a growing interest in the use of residue curve and column profiles for the preliminary design of distillation columns. Residue curves and column profile are not only used to predict the composition changes in the distillation column but also to determine the feasibility of the proposed separation. Recently, theory underlying column profile maps has been developed by Tapp, Holland and co-workers. However there has been no direct experimental validation of the predictions of the column profile map theory. The main aim of this thesis is to experimentally verify some of the predictions of column profile map theory.

A simple experimental batch apparatus has been developed to measure residue curve maps (RCMs) by Tapp and co-workers, the apparatus was modified so that it could be used to measure column profile maps (CPMs) in this thesis. CPM theory has shown that CPMs are linear transforms of the residues curve maps (RCMs). A stable node which was the apex of a mass balance triangle (MBT) was introduced inside the MBT, this was done by transforming the RCMs to CPMs using the appropriate distillate composition x_d and reflux ratio R . It was also shown that the saddle point which was on the boundary of the triangle of the RCM can be shifted inside the MBT by transforming the RCM to CPM. This is again in accordance with theoretical predictions of CPM theory.

Residue curves (RCs) and pinch point curves (PPCs) are used to determine the operation leaves and hence the feasible region for distillation columns operating at a specific distillate and bottoms composition for all fixed reflux ratio. The operating leaves were expanded beyond the pinch point curve by varying the reflux ratio from a higher reflux to a lower reflux ratio. This showed that one can effectively cross the pinch point curve hence expanding the operating leave.

Finally the importance of experimentally measuring CPMs is demonstrated. Two thermodynamic models were used to predict the profiles of a complex system. The binary vapor-liquid equilibrium (VLE) diagrams and the residue curves produced from using these two thermodynamic models did not predict the same topology. The composition of the profiles were not the same because there were multiple liquid phases involved in this system, which made it difficult for the researchers to measure the correct profiles. Column profile maps were simulated using the different thermodynamic models, they also showed that there is some discrepancy between the predictions of the two models.

ACKNOWLEDGEMENTS

I would like to thank my supervisors Professor David Glasser and Professor Diane Hildebrandt for their guidance over the past several years of research. They have introduced me to the many aspects of distillation. Their insight and high standards have definitely helped to shape this work. It was a pleasure to have two supervisors who were so joyful and creative in this research. I would also like to thank Dr. Shehzaad Kauchali, for his inputs during our weekly meetings, not forgetting my colleagues (Micheala Vrey, Cameron Wilson, Mark Peters, Kgotsfalo Leeuw, Jean Mulopo and Simon Holland).

Special thanks goes to my friend Geoffrey Ngigi for his help in the Laboratory, with his chemistry knowledge.

Finally I would like to express my gratitude to all my friends (Olufemi Fasemore, Peter Mukoma, Mr.Tabrizi, Bilal Patel, Ngangezwe Khumalo, Tumisang Seodigeng), for their support and encouragement.

Financial assistance from the following organizations (COMPS, NRF, Mellon, and University of the Witwatersrand) is gratefully acknowledged.

TABLE OF CONTENTS

DECLARATION.....	I
DEDICATION.....	II
ABSTRACT.....	III
ACKNOWLEDGEMENTS.....	V
TABLE OF CONTENTS.....	VI
LIST OF FIGURES.....	X
1 INTRODUCTION.....	1
1.1 MOTIVATION AND INDUSTRIAL RELEVANCE.....	1
1.2 OBJECTIVE.....	3
1.3 OUTLINE OF THESIS.....	3
1.4 MAIN CONTRIBUTION OF THE THESIS.....	4
1.5 REFERENCE.....	5
2 LITERATURE REVIEW.....	6
2.1 RESIDUE CURVES.....	7
2.2 COLUMN PROFILES.....	8
2.3 BATCH DISTILLATION COLUMN.....	13
2.3.1 <i>Extractive distillation</i>	13
2.4 NOMENCLATURE.....	15
2.5 REFERENCE.....	16
3 EXPERIMENTAL SIMULATION OF THE STABLE NODE REGION IN A DISTILLATION COLUMN PROFILE MAP USING A BATCH APPARATUS.....	18
ABSTRACT.....	18
3.1 INTRODUCTION.....	19
3.2 RESIDUE CURVES.....	21
3.3 COLUMN PROFILE MAP.....	25
3.3.1 <i>Continuous distillation column</i>	25
3.3.2 <i>Batch distillation column</i>	27
3.4 EXPERIMENT.....	31
3.4.1 <i>Experimental setup</i>	31

3.4.2	<i>Experimental procedure</i>	32
3.5	RESULTS AND DISCUSSION	34
3.6	CONCLUSION	36
3.7	NOMENCLATURE.....	37
3.8	REFERENCES	38
4	CAN THE OPERATING LEAVES OF A DISTILLATION COLUMN REALLY BE EXPANDED?	40
	ABSTRACT.....	40
4.1	INTRODUCTION	40
4.2	THEORETICAL BACKGROUND	43
4.2.1	<i>Operating leaf for constant reflux ratio</i>	43
4.2.2	<i>Operating leaf for non-constant reflux ratio</i>	46
4.2.3	<i>Crossing simple distillation boundaries</i>	50
4.3	EXPERIMENT	51
4.3.1	<i>Experimental setup</i>	52
4.3.2	<i>Experimental procedure</i>	53
4.4	RESULTS	57
4.5	DISCUSSION	59
4.6	CONCLUSION	60
4.7	NOMENCLATURE.....	61
4.8	REFERENCES	62
5	EXPERIMENTAL MEASUREMENT OF THE SADDLE NODE REGION IN A DISTILLATION COLUMN PROFILE MAP BY USING A BATCH APPARATUS.....	65
	ABSTRACT.....	65
5.1	INTRODUCTION	66
5.2	OPERATION LEAVES	67
5.2.1	<i>Closed leaves</i>	70
5.2.2	<i>Open leaves</i>	71
5.3	EXPERIMENT	76
5.3.1	<i>Experimental setup</i>	76
5.3.2	<i>Experimental procedure</i>	77
5.4	RESULTS	79
5.5	CONCLUSION	84
5.6	NOMENCLATURE.....	85

5.7	REFERENCES	86
6	USING DISTILLATION COLUMN PROFILE MAPS TO IDENTIFY SUITABLE THERMODYNAMIC MODEL FOR COMPLEX SYSTEMS.....	88
	ABSTRACT.....	88
6.1	INTRODUCTION	89
6.2	IDEAL SYSTEMS	90
6.3	NON-IDEAL SYSTEM.....	91
6.3.1	<i>The NRTL model</i>	92
6.3.2	<i>The Uniquac model</i>	93
6.4	BINARY VAPOR-LIQUID EQUILIBRIUM.....	95
6.5	RESIDUE CURVES.....	98
6.6	COLUMN PROFILE MAP.....	102
6.7	EXPERIMENT.....	107
6.7.1	<i>Experimental Setup</i>	107
6.7.2	<i>Experimental Procedure</i>	110
6.8	RESULTS AND DISCUSSION	112
6.9	CONCLUSION	115
6.10	NOMENCLATURE.....	116
6.10.1	<i>Greek letters</i>	117
6.11	REFERENCES	118
7	CONCLUSIONS.....	120
7.1	FUTURE WORK	123
	APPENDIX A	124
	DERIVATION OF THE FEED ADDITION EQUATION	124
	APPENDIX B	128
	DERIVATION OF THE COMPOSITION EQUATION FOR GC CALIBRATION	128
	<i>GC calibration</i>	129
	APPENDIX C	131
	THE METHANOL, ETHANOL AND ACETONE SYSTEM.....	131
	<i>Operating conditions for the GC</i>	132
	<i>Computer Program used to determine the response factors</i>	134
	<i>Experimental Results for the column profile map of the stable node, see Chapter 3</i>	141

<i>Experimental Results for the expanding of the operating leaves , see Chapter 4</i>	146
APPENDIX D	154
THE METHANOL, DI-ETHYL ETHER AND BENZENE SYSTEM	154
<i>Operating conditions for the GC</i>	155
<i>GC Calibration Program</i>	157
<i>Experimental Results for the column profile map of the saddle point node, see Chapter 5</i>	165
APPENDIX E	171
THE WATER, ETHANOL AND ETHYL ACETATE SYSTEM	171
<i>Operating conditions for the GC</i>	172
<i>GC Calibration Program</i>	174
<i>Experimental Results for the column profile map, see Chapter 6</i>	181

LIST OF FIGURES

Figure 2.1 : The rectifying and stripping section of a continuous distillation column .	9
Figure 2.2: The column section of a continuous distillation column.....	10
Figure 2.3: A semi-batch apparatus used to measure column profiles of the rectifying section.	11
Figure 2.4: A semi-batch apparatus used to measure column profiles of the stripping section.	12
Figure 3.1: Residue curve map of Acetone, Ethanol, and Methanol system.	21
Figure 3.2: Types of nodes.....	22
Figure 3.3: Identifying pinch points on RCM of methanol, ethanol, and acetone system.....	24
Figure 3.4: The rectifying section of a distillation column.....	25
Figure 3.5 : A batch distillation column	27
Figure 3.6: A distillation column consisting of four column sections.....	28
Figure 3.7: Column profile map, with a fixed reflux ratio of 1.	29
Figure 3.8: A residue curve map showing the transformed mass balance triangle of the column profile map.	30
Figure 3.9: Experimental setup with still pot being the main component.	32
Figure 3.10: Column profiles with the reflux ratio equal to one, starting with different initial compositions x_o but with a fixed feed addition composition x_d . i.e. Column profile map.	34
Figure 3.11: An isotherm plot with the column profile map of the reflux ratio $r = 1$ and a distillate composition $x_d = [0.54, 0.11, 0.35]$	36
Figure 4.1: Column profiles for the Ethanol/ Methanol/ Acetone system using equation 4.1 for different reflux ratios and $x_d = [0.54, 0.11, 0.35]$ with the respective pinch point curve.....	44
Figure 4.2: A column profile with its respective pinch point showing the co-linearity of separation and mixing vector. $x_d = [0.54, 0.11, 0.35]$	46

Figure 4.3: Increasing the reflux ratio along a column profile, $x_d = [0.54, 0.11, 0.35]$	47
Figure 4.4: Decreasing the reflux ratio along the column profile with an $x_d = [0.54, 0.11, 0.35]$	48
Figure 4.5: The greatest extension of the operating leaf with an $x_d = [0.54, 0.11, 0.35]$	49
Figure 4.6: Acetone, Benzene and Chloroform system showing the crossing of a simple distillation boundary with an $x_d = [0.132, 0.2, 0.668]$	51
Figure 4.7: Experimental set-up with the still being the main component	53
Figure 4.8: An isotherm plot showing column profile with a reflux of 5, reflux of 1 and their respective pinch point P_1 and P_2 , $x_d = [0.54, 0.11, 0.35]$	56
Figure 4.9: Experimental results of an extended region of an operating leaf with distillate composition x_d of $[0.54, 0.11, 0.35]$	57
Figure 4.10: Experimental results showing the great extension of the operating leaf with the distillate composition x_d of $[0.54, 0.11, 0.35]$	58
Figure 5.1: Distillation column with no bottoms or distillate withdrawn and no feed	68
Figure 5.2: The rectifying section of a distillation column	69
Figure 5.3: Residue curve map with tangential lines from product showing pinch points	70
Figure 5.4: A branched pinch point curve	71
Figure 5.5: An open leaf, showing the column profiles pinching at different distillation regions	72
Figure 5.6: A slight change in the composition changes the direction of the column profile	73
Figure 5.7: Column profile map of Methanol, Diethyl ether and Benzene using a reflux ratio of three ($r=3$) for a rectifying section of distillation column	74
Figure 5.8: The residue curve map of Di-ethyl ether, Methanol and Benzene in full space	75
Figure 5.9: Experimental setup with still pot being the main component	77
Figure 5.10: Measured experimental profile. Profile 1 in Figure 5.13, at 0.83 bars	79

Figure 5.11: Measured experimental profile. Profile 2 in Figure 5.13, at 0.83 bars...	80
Figure 5.12: The temperature profile of Profiles 1 and 2 versus time, at 0.83 bars....	81
Figure 5.13: Column profiles with the reflux of 3 with the distillate composition of 0.0657 benzene and 0.6944 of Diethyl ether.....	82
Figure 5.14: Column profile map with a reflux ratio of three, starting with different initial points with a fixed distillate composition $x_d = [0.0657 \ 0.6944]$	83
Figure 6.1: Comparison of predicted binary VLE for Water-Ethanol system using the UNIQUAC and NRTL models at a total Pressure of 0,83 bars.	95
Figure 6.2: Comparison of predicted binary VLE diagram for Ethyl-acetate-Ethanol system using the UNIQUAC and NRTL models at a total Pressure of 0,83 bars.	96
Figure 6.3: Comparison of prediction binary VLE for Water-Ethyl acetate system using the UNIQUAC and NRTL models at a total Pressure of 0,83 bars.....	97
Figure 6.4: Predicted RCM for the ethyl acetate-ethanol-water system using UNIQUAC at the total pressure of 0.83 bar.....	100
Figure 6.5: Predicted RCM for the ethyl acetate-ethanol-water system using NRTL at a total pressure of 0.83 bar.	101
Figure 6.6: Comparison of the predicted RCMs for the ethyl acetate-ethanol-water system using the two thermodynamic models, UNIQUAC and NRTL at the total pressure of 0.83 bar.	101
Figure 6.7: Predicted CPM for a reflux ratio of 1 and distillate composition of 80% ethyl acetate, 10 % ethanol and 10% water. Thermodynamics predicted using the NRTL model at the total pressure of 0.83 bar.....	104
Figure 6.8: Predicted CPM for a the reflux ratio of 1 and distillate composition of 80% ethyl acetate, 10 % ethanol and 10 % water. Thermodynamics predicted using the UNIQUAC model at a total pressure of 0.83 bar.	105
Figure 6.9: Comparison of the predicted CPMs for the NRTL and UNIQUAC models at a total pressure of 0.83 bar. A reflux ratio of 1 and distillate composition of 80% ethyl acetate, 10 % ethanol and 10 % water is used for both maps.	106
Figure 6.10: Experimental setup with still pot being the main component.	108

Figure 6.11 Predicted RCM for the ethyl acetate, ethanol and water system with the Liquid-Liquid Envelope at 63 °C, at a total Pressure of 0,83 bars.....	109
Figure 6.12: RCM for the ethyl acetate, ethanol and water system with the LLE envelope at 64.8°C. The total pressure is 0.83 bar.....	109
Figure 6.13: Comparison of the measured and predicted CPM for the ethyl acetate, water and ethanol system using the NRTL thermodynamic model. The total pressure is 0.83 bar.....	112
Figure 6.14: Comparison of the measured and predicted CPM for the ethyl acetate, water and ethanol system using the UNIQUAC thermodynamic model. The total pressure is 0.83 bar.....	113
Figure 6.15: Comparison of the experimentally measured and theoretically predicted CPMs for the ethyl acetate, water and ethanol system. The CPMs were predicted using the NRTL and UNIQUAC models. The total pressure is 0.83 bar.....	114

LIST OF TABLES

Table 3.1: The binary interaction parameters for the Methanol, Ethanol and Acetone system.....	23
Table 5.5.1: NRTL parameters for the Ethyl Ether, Methanol and benzene system. .	84
Table 6.1: Binary interaction parameters for NRTL model.....	98
Table 6.2: Binary interaction parameter for UNIQUAC model	98

1 INTRODUCTION

The separation of multicomponent liquid mixtures has always provided significant challenges to process and design engineers. Most liquid mixtures do not behave ideally, which means that there might be azeotropes or the boiling points of the components are close to each other making the possibilities of separating the components difficult. In this thesis, possibilities and limitations imposed by the azeotropes in liquid mixtures are investigated. These limitations are investigated using the column profile maps, which is a novel way of looking into distillation columns.

1.1 Motivation and Industrial Relevance

It has been said that “An economically optimal design with an average process configuration can be much more costly than an average design using the best configuration.” This can be easily understood when related to the local and global optima. In distillation systems, distillation provides the capabilities to zero in on the best configuration (or global minimum) which can then be optimized instead of optimizing the local minimum which was a result of a guess, Safrit et al (1996). This thesis is motivated by the need to understand and provide novel design tools for distillation columns which are commercially viable. We use the process synthesis approach to systematically understand distillation columns. Such an approach avoids doing unnecessary experimental and simulation work as the engineers iteratively conduct experiments for the design.

Industrial production of chemical involves purification and recovery of the products, by products and unreacted raw materials. Distillation is clearly the dominating separation process, accounting for more application than all the other combined (extraction, adsorption, crystallization, membrane-based technologies and so forth).

In fact, distillation columns consume more than 95% of the total energy used in separations in chemical process industries worldwide. “It is not easy to put a new face on a technology as old as that of distillation, and yet the economic impact of even minor, but general, improvements in the method can be most substantial. We workers in the area have a responsibility to make distillation a more effective separation method-while striving always to recognize those instances when it really is not the best way to take the mixture apart.”, Fair et al (1987).

All liquid mixtures have forces of intermolecular attraction. That is why they form liquids and not gases. The molecular interaction when two or more components are mixed may cause the mixture to form certain “inseparable” compositions where the vapor and liquid compositions at equilibrium are equal within a given pressure and temperature range. These specific mixture compositions are called azeotropes.

Azeotropy plays an important role in vapor-liquid equilibrium separation process such as distillation, similar to eutectics and peritectics in liquid-solid systems such as crystallization. To be able to develop separation processes for azeotropic mixtures, there is a need for insight into the fundamental phenomena of azeotropic phase equilibria. The vapor-liquid envelope of the equilibrium temperature surface defines the feasible operating region in which any real distillation process must operate. The existence of azeotrope complicates the structure of this operating envelope, and the resulting distillation behavior of multicomponent azeotropic mixtures may be very complex. The main interest behind azeotropic phase equilibrium diagrams is to reveal all the physiochemical restrictions imposed on the separation process by nature of the mixture in question. Residue curve maps, for multicomponent mixtures, provide important insight for the optimal choice of separation method and the design and synthesis of azeotropic distillation separation systems, Hilmen et al (2000).

Column Profile Maps (CPMs) are conceptual design tools, the entire investigation of the problem including the discovery of barriers to the required task, generation of

feasible process alternatives, and analysis of the process alternatives so that the best one is chosen based on the available information. The process can tolerate some assumptions that other process cannot. This is true especially in the grassroots designs of novel distillation schemes with components whose behavior is not well understood. For any design undertaken, the initial work done has a profound impact on the economics of the entire project. Thus, there is an incentive to look carefully into the field of residue curve maps and column profile maps for azeotropic mixtures.

1.2 Objective

The main aim of this thesis is to show that a small semi-batch apparatus can essentially produce the same column profiles as its continuous distillation counterparts. The advantages of using a semi-batch apparatus is that it uses small amounts of quantity and the time requirement can be related to the number of stages in a continuous distillation column.

The other important aspect of this thesis is that one can use the experimentally simulated column profile maps to identify suitable thermodynamic model for complex systems.

1.3 Outline of Thesis

The thesis consists of a number of chapters, each of these chapters is a paper that has either been published or is in the process of being published. Chapter three shows the relationship between the residue curve map and the column profile map. The column profile map is a linear transformation of the residue curve. It was shown in this paper that the stable node, which was one of the apexes of the mass balance triangle, can be

moved into the mass balance triangle. This confirmed the concept of moving triangles.

Chapter four shows that column profiles can be used to expand the operating leaves of a distillation column. The operating leaves of the distillation column were expanded by varying the reflux ratio.

Chapter five also shows that the column profile map is a linear transformation of the residue curve map. It was shown that the saddle point can be move inside the mass balance triangle; it was also showed the importance of doing experiments around the saddle point region.

Having showed that the column profile maps are linear transformation of residue curves in Chapters three and five, Chapter six shows the application of using column profile maps. In this chapter, two thermodynamic models are used to predict column profiles which do not predict the same topology. Experiments are used to determine which one of the two thermodynamic models agrees with the experiments. Chapter seven presents some conclusions on the work in this thesis.

1.4 Main contribution of the thesis

It has been shown extensively in the thesis that a batch apparatus can be used to simulate profiles of a continuous distillation column. This was done by experimentally measuring column profiles of a continuous distillation column by using a batch apparatus. The main contribution of the thesis is that, the experimental measurements can be used to distinguish between different thermodynamic models which are something that are new and innovative.

1.5 Reference

1. Fair, J.R., Distillation: Whither, Not whether. I. Chem.E. Symposium series, vol 104, 1987, A613-A627.
2. Hillmen, E., Separation of Azeotropic mixtures: tool for analysis and studies on batch distillation operation, NTNU-Thesis, 2000
3. Safrit, B.T., Synthesis of azeotropic batch distillation separation systems., Carnegie Mellon University- Thesis, 1996

2 LITERATURE REVIEW

An important separation process in the chemical industry is distillation. Liquid mixtures are separated by evaporation and condensation. However not all desired separations are feasible separation. Feasible separation in distillation depends on the vapor-liquid equilibrium of the mixture to be separated. For ideal mixtures one can easily list all feasible separation sequences based on the pure component boiling points. However in practice, designers often have to deal with non-ideal mixtures.

The complex behavior of the non-ideal mixtures has extensively been studied. An attempt has already been made for the classification of homogeneous ternary non-ideal mixtures and has recently been applied again. However the classification of heterogeneous mixtures, especially that of the quaternary ones, is still not available. Because of the complex behavior of the different non-ideal mixtures, the synthesis step of their separation cannot always be generalized and there are practically no general guidelines for the synthesis as there are in the case of ideal mixtures. The non-ideal mixtures can be differentiated more because among the non-ideal mixtures it can happen that there is/ are azeotropes as well and azeotrope distillation is not successful for the separation, Szanyi (2004). The presence of azeotropic mixtures complicates the prediction of feasible separation processes. Schreinemakers (1902) showed a relatively simple analysis to determine the feasibility of separation processes which involves the residue curve maps (RCMs).

2.1 Residue curves

The least complicated of all distillation columns processes is the simple distillation, or open evaporation, of a mixture. The liquid is boiled and the vapors are removed from contact with the liquid as soon as they are formed. Thus, the composition of the liquid will change continuously with time, since the vapor is always richer in the more volatile components than the liquid from which they came from. The trajectory of the liquid compositions starting from some initial point is called a simple distillation residue curve or simply a residue curve. The collection of all such curves for a given mixture is called a residue curve map. These maps contains exactly the same information as the corresponding phase diagram for the mixture, but they represent it in a way that is much more useful for understanding and designing distillation systems. The concepts which we are about to develop for simple distillation serve as prototypes that can be extended to batch and continuous distillation columns. The pioneering work on simple distillation was published in the early 1900s by Schreinemakers et al (1902). He was the first to develop the general equations and analyze their properties, which was a remarkable achievement because he did this without the aid of the modern qualitative theory of nonlinear ordinary differential equations. The following properties are general rules governing the residue curve maps, Doherty et al (2001):

Property 1: The residue curve through any given liquid composition point is tangent to the vapor-liquid equilibrium tie-line through the same point.

Property 2: Residue curves do not cross each other, nor do they intersect themselves.

Property 3: The boiling temperature always increases along a residue curve (the only exception is at steady state where the boiling temperature remains constant because the composition remains constant).

Property 4: Steady state solution of the equations occur at all pure components and azeotropes.

Properties 5: Steady state solutions are limited to one of the following types: stable node, unstable node and the saddle point.

Property 6: Residue curves at nodes are tangent to a common direction. At pure component nodes this common direction must be one of the binary edges of the composition diagram.

2.2 Column Profiles

Residue curves closely approximate composition profiles in distillation columns for the total reflux situation, the curves can be used to derive the limits for operation at any finite reflux ratio. At finite reflux ratios, the occurrence of one or more pinch points limits the feasible separations. A pinch point curve occurs in a continuous distillation column when despite adding as many trays to a distillation column the composition does not change. Wahnschafft et al (1992) showed how pinch point curve can be used to access feasible separations. A pinch point curve can also be easily constructed graphically by finding a collection of tangent points on residue curves, whose tangent lines points back through the product. For the product pinch point curves, these points correspond to pinch points in the column where the vapor and liquid streams that pass each other are in equilibrium, and requires infinite number of trays to carry out a specific separation at the current reflux ratio. The reflux ratio must be increased in order to by pass the pinch point. Wahnschafft et al (1992) also identified regions of possible column profiles for both column sections, given product specifications. These regions of profiles contain all profiles that are attainable when a product is specified. Each column profile region is bounded by the total reflux curve and the product pinch point curve. For a continuous distillation column, there is a distillate and bottoms product resulting in distillate and bottoms product pinch point curves. If the rectifying and stripping column profile regions intersect in at least one point, then a tray by tray calculation can be performed from one specified product to the other resulting in a feasible column specification. If these

regions do not intersect, then there exists no tray by tray calculation between the specified products and the column is not feasible. The feed composition does not necessarily need to lie in any of the possible column profile regions for the column to be feasible, but the feed composition must lie on a mass balance line between the distillate and bottoms composition due to the overall balance constraint.

Traditionally distillation columns have been divided into the rectifying and the stripping sections as shown in Figure 2.1.

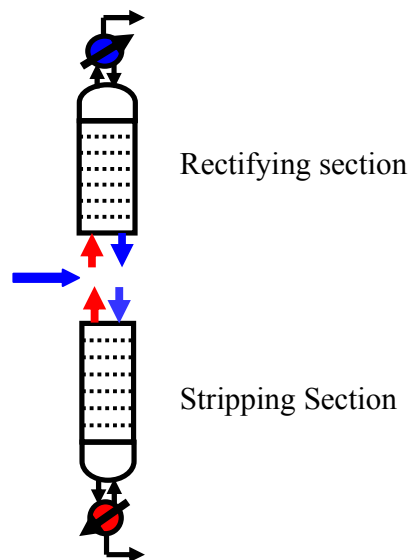


Figure 2.1 : The rectifying and stripping section of a continuous distillation column

These two sections can be defined by the following differential equations:

$$\text{Rectifying section equation} \quad \frac{dx}{dn} = \frac{V}{L}(x_i - y_i^*) + \frac{D}{L}(x_D - x_i) \quad 2.1$$

$$\text{Stripping section equation} \quad \frac{dx}{dn} = \frac{V}{L}(y_i^* - x_i) + \frac{B}{L}(x_B - x_i) \quad 2.2$$

Instead of viewing a distillation column in terms of only two sections, Tapp et al (2004) viewed a distillation column in terms of a number of column sections. These column sections are defined as sections with no feed additions or side stream withdrawal. In situations where constant molar overflow is assumed, this would also imply that the total vapour and liquid molar flowrates remained constant in a column section. Consequently it is clear that column sections are divided by areas of addition and removal of material. Mass balance over the column section, as shown in Figure 2.2, would give the following difference point equation:

$$\frac{dx}{dn} = \frac{V}{L}(x - y^*(x)) + \frac{\Delta}{L}(x_{\Delta} - x) \quad 2.3$$

Where $\Delta = V-L$, $X_{\Delta i} = X_D = X_B$

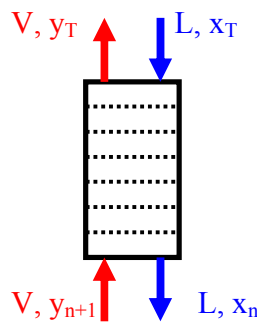


Figure 2.2: The column section of a continuous distillation column

The advantage of using this method is that, it gives the design engineer more degree of freedom. It is also important to notice that the top and bottoms of a column section does not necessarily have to be the distillate and bottoms composition of a continuous distillation column. This is due to the fact that the initial conditions simply represent the liquid and vapour at the top of the column section, as shown in Figure 2.2. In situations where constant molar overflow is assumed, this would mean that the vapor

and liquid flowrates would remain constant in a column section. The difference in composition between the vapour and liquid is called the difference vector for a column section. The difference is constant along the length of the column section. The term $\Delta = V-L$ can be considered to be the equivalent molar flow rate in a distillation column section. If Δ is negative, the net molar flow of material is downward, in the direction of the liquid flow. If Δ is positive, the net molar flow material is upwards in the direction of the vapour stream. The term $\Delta X_{\Delta i}$ is the net molar flowrate of component i in a column section. If the term is positive it means the net molar flow of component i is up the column in the direction of the vapour flow rate, and if the term is negative the net molar flow of the component i is down the column in the direction of the liquid flow rate. In the traditional rectifying section of a distillation column, Δ is positive as in $\Delta X_{\Delta i}$. The traditional stripping section of a distillation column, Δ is negative as in $\Delta X_{\Delta i}$. This means the difference point equation is a generalized differential equation describing the composition of the components along the length of a distillation. The rectifying and stripping section equations are special cases of the difference point equation. The column profiles of these sections can be measured using a semi-batch apparatus. In this thesis, semi-batch equipment, as shown in Figure 2.3, was used to measure column profiles of the rectifying section of a distillation column.

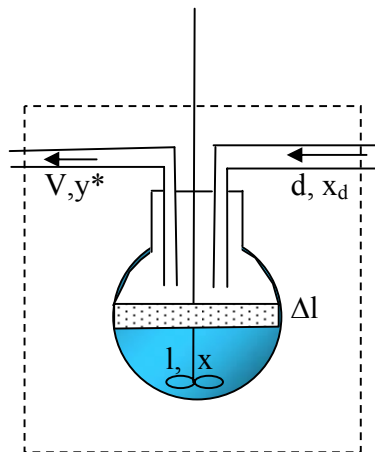


Figure 2.3: A semi-batch apparatus used to measure column profiles of the rectifying section.

Mulopo (2005) modified the above equipment, in order to measure column profiles of the stripping section, as shown in Figure 2.4 below.

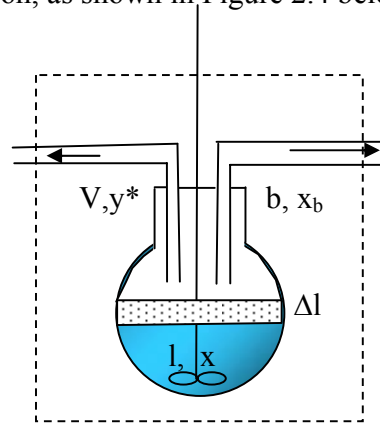


Figure 2.4: A semi-batch apparatus used to measure column profiles of the stripping section.

The separation term in equation 2.2 has a negative sign, compared to that of the rectifying section equation 2.1. The profiles represented by this equation should normally be simulated using a batch condensing apparatus as the “separation parts” in the two processes are equivalent. In fact simple condensation is a process where a vapour of quality V and composition y is condensed and the equilibrium liquid of composition x^* is removed. If one need to measure profiles of the stripping section, one need to remove material of composition x_b from the batch apparatus while retaining equilibrium boiling conditions. Mulopo et al. (2005) used both equations of the stripping and rectifying section, to derive a feed addition equation which measures profiles of the stripping section, since the combination of the separation vectors and mixing vectors are linear. These semi-batch apparatus are simple as compare to the traditional batch distillation column.

2.3 Batch Distillation column

Traditionally, the most popular kind of batch column is the so-called regular or rectifying column, which is made up of a large reboiler, to which all the feed is charged, and of a rectifying section from whose top cuts of different compositions are removed. Less frequently, an inverted or stripping batch column is preferred, for example when the amount of the light component in the feed charge is small and the products are recovered at high purity (Hilmen, 2000), in this column the feed is charged to the top vessel, and the products are withdrawn from the bottom, so that a smaller reboiler can be used. Yet a different configuration for a batch column can be considered, as was mentioned by Robinson and Gilliland back in 1950. Similarly to a continuous column, this kind of batch column is made up of the rectifying and stripping sections, with a feed tray in the middle. The liquid feed is charged to an intermediate vessel, and liquid stream is continuously recycled between the feed/withdrawal tray and the feed vessel. Liquid streams may be continuously withdrawn from the top and the middle vessel, a small reboiler can be used as compared to the one in a regular batch column.

2.3.1 Extractive distillation

Distillation of binary azeotrope and closed-boiling mixtures (AB) into pure components (light component A and heavy component B) requires the addition of a third component, the so-called entrainer (E), that enhances the separation. When the entrainer is heavy and is added continuously in the top section of the batch column, the process is called extractive distillation. For the realization of the extractive distillation in batch the most simple configuration is the rectifier though more sophisticated configurations such as a middle vessel column could also be used, Safrit and Westerberg (1997), Warter and Stichmair (1999), Cheong and Barton (1999 a, b, c). When the entrainer forms a homoazeotrope with at least one of the

original components and is added batchwise to the original mixture, the process is called homogeneous azeotropic or homoazeotropic batch distillation. When the entrainer forms a binary heteroazeotrope with at least one (and preferably with only one) of the original components or a ternary heteroazeotrope and is added batchwise to the original mixture, the process is called heterogeneous azeotropic or heteroazeotropic batch distillation. The studies in entrainer selection for heteroazeotropic batch distillation are limited, but valuable insight can be gained by the related literature for continuous columns. Pham and Doherty (1990a) studied the synthesis of continuous heteroazeotropic distillation and presented some general principles which could be used for distinguishing between feasible and infeasible entrainers for the process. An entrainer was considered to be feasible if the resulting residue curve map provided a feasible column sequence. Furzer et al (1994) screened entrainers for the process from a different point of view. The UNIFAC group contribution method was used for synthesizing efficient entrainers for the heterogeneous dehydration of ethanol. Simple heuristic rules were developed that could be used in a knowledge database of an expert system and limit the extensive search of molecules that could be used as entrainers.

Rodrique-Donis et al (2001) were the first to provide entrainer selection rules specifically for batch columns. They pointed out that the rules for continuous columns can be only used as a basis for batch columns as they do not cover all the possible cases. This is because heteroazeotropic batch distillation is more flexible than its continuous counterpart. They studied all possible residue curve maps of heteroazeotropic mixtures under the assumption of total reflux/ total reboil ratios and infinite number of stages. The classification of Matsuyama and Nishimura (1977) with its 113 classes, which was later extended to 125 classes by Foucher et al (1991), was adopted. The complete set of the feasible entrainers was tabulated in tables, Skouras et al (2005).

2.4 Nomenclature

B	: Bottoms flowrate (mol/time)
D	: Distillate flow rate (mol/time)
dx	: Change in liquid mole fraction
dn	: Change in number of stages
L	: Liquid flow rate (mol/time)
V	: Vapour flow rate (mol/time)
x	: Liquid mole fraction
x_B	: Bottoms liquid mole fraction
x_D	: Distillate liquid mole fraction
y	: Vapour mole fraction

2.5 Reference

1. Cheong, W., Barton, P.I., Azeotropic distillation in a middle vessel batch column. Part 1. Model formulation and linear separation boundaries, *Ind. Eng. Chem. Res.*, vol. 38, 1999, pg 1504-1530
2. Doherty M.F., Malone J.D., "Conceptual design of distillation column systems" 2001. McGraw-Hill, New York
3. Foucher, E.R., Doherty, M.F., Malone, M.F., Automatic screening of entrainers for homogeneous azeotropic distillation. *Ind. Eng. Chem. Res.*, vol. 30, 1991, pg 760
4. Furzer, I.A., Synthesis of etrainers in heteroazeotropic distillation systems. *The Canadian Journal of Chemical Engineering*, vol. 72, 1994, pg 358
5. Hilmen, E. Separation of Azeotropic Mixtures: Tools for analysis and studies on Batch distillation operations. (2000). Thesis, NTNU, Trondheim.
6. Matsuyama, H., Nishimura, H., Topological and thermodynamic classification of ternary vapor-liquid equilibria., *Journal of Chemical Engineering of Japan*, vol. 10, 1977, pg 181.
7. Mulopo, J. Hildebrandt, D. Glasser, D. Hausberger, B. Kauchali, S. "Experimental Simulation of distillation concentration profiles using batch apparatus: Column stripping section." *Chem. Eng. Sci.* 2005. 60.6815-6823.
8. Pham, H.N., Doherty, M.F., Design and synthesis of heterogeneous azeotropic distillation –III Column sequences, *Chem. Eng. Sci.*, vol. 45, 1990a, pg 1845
9. Robinson, C.S. and Gilliland, E.R. "Elements of Fractional Distillation" (1950). McGraw-Hill, New York.
10. Rodrigues-Donis, I., Gerbaud, V., Joulia, X., Heterogeneous entrainer selection for the separation of azeotropic and close boiling temperature mixtures by heterogeneous batch distillation. *Ind. Eng. Res.*, vol. 40, 2001, pg 4935.

11. Safrit, B.T., Westerberg, A.W., Improved operational policies for batch extractive distillation columns, *Ind. Eng. Chem. Res.*, vol. 36, 1997, pg 436-443.
12. Schreinemakers, F.A.H. *Z. Phys. Chem.*, 43, pp671-685, 1902
13. Skouras, S., Kiva, V., Skogestad, S., Feasible separations and entrainer selection rules for heteroazeotropic batch distillation., *Chem. Eng. Sci.*, vol. 60, 2005, pp 2895-2909
14. Szanyi, A.; Mizsey, P.; Fonyo, Z. "Optimization of Nonideal Separation Structures Based on Extractive Heterogeneous Azeotropic Distillation" *Ind. Eng. Chem. Res.*; 2004; 43(26); 8269-8274
15. Tapp, M., Holland, S.T., Hildebrandt, D and Glasser, D. "Column Profile Maps. 1. Derivation and Interpretation." *Ind. Eng. Chem.* (2004), 43 (2), 364-374
16. Wahnschafft, O.M., Keohler, J.W., Blass, E. and Westerberg, A.W. The product composition regions of single-feed azeotropic distillation columns, *Ind. Eng. Chem. Res.*, 31, 1992, pg 2345-2362
17. Warter, M., Stichmair, J., Batchwise extractive distillation in a column with middle vessel, *Comput. Chem. Eng. (Suppl.)*, 1999, pg 915-918

3 EXPERIMENTAL SIMULATION OF THE STABLE NODE REGION IN A DISTILLATION COLUMN PROFILE MAP USING A BATCH APPARATUS

This paper was submitted to the Industrial Engineering Chemistry Research Journal.

Abstract

Due to the large energy consumption of vapour liquid separations, particularly in the case of distillation columns, there is much interest in the optimisation of these systems. A simple theoretical method for the evaluation of the separation of mixtures using distillation columns, called column profile maps (CPMs), has been developed. We will experimentally confirm the predictions of this theory and experimentally demonstrate that CPMs at finite reflux are simply transforms of the residue curve maps.

The experimental technique uses a semi-batch apparatus and measures all liquid concentrations in the still as a function of time. The concentration profiles achieved in the semi-batch still have been shown to be essentially the same as those of a continuous distillation column section. The experimental technique involves the boiling of a known liquid composition in a still immersed in a bath. A feed is added at a controlled rate to the boiling liquid at regular intervals, and samples of the residue are taken periodically. The samples are analysed using gas chromatography. This technique for predicting the concentration profiles in a distillation column section is very economical, as it only uses a small quantity of material and is very simple and quick to use. The theory predicts, we can move a stable node into the mass balance triangle, and also predicts profiles enter the node in a specific direction. We experimentally confirm these predictions and find the position and type of node agrees with the theory and that the profiles do approach in a specific direction.

3.1 Introduction

The separation of mixtures using distillation processes can be complicated by the presence of azeotropes. Azeotropes can show up as the products of these distillations, possibly making the desired pure product difficult to produce. In this case, methods such as extractive distillation, changing the column's operational pressure or feed composition, or switching to non-distillation based separations methods are used to break the azeotropes. Azeotropes can also create distillation boundaries, which form distillation regions in which it is believed the types of feasible separations are limited. It is important that one knows what these distillation regions and boundaries are for a particular mixture when one is designing a separation system. Without the knowledge of these boundaries and regions, infeasible separation systems could be proposed and designed, wasting valuable time and resources. A tool for finding the distillation boundaries and regions is very important and helpful; this tool is called a residue curve maps (RCM).

Residue curve maps, or RCMs, were first defined and used by Schreinemakers et al (1902). They are constructed of residue curves (RCs), which can be defined through a simple experiment: a liquid mixture of known composition is placed in a single-stage batch still and is distilled without any reflux while continuously analysing the composition of the liquid remaining in the still (the residue liquid) over time, until the last drop is vaporized. We call the tracing of this change in residue liquid composition a residue curve provided the vapour being distilled off is in equilibrium with the liquid from which it is being produced, Gert-Jan et al (1994).

A useful place to begin describing the relationship between residue curve maps and distillation column configuration is to the separation of nonazeotropic mixtures. Most of the sequencing algorithms for distillation columns, in general, have focused on homogeneous, multicomponent, ideal mixtures to be separated into nearly pure products, Thompson and King (1972), Andrecovich and Westerberg (1985a,b),

Malone et al (1985). With ideal mixtures, there are no special difficulties in selecting the species that concentrate in the distillate and bottoms products. Nevertheless, these efforts have helped to resolve many conflicting heuristics that have been in common usage.

Unfortunately, ideal separations are rarely encountered in practice. Motivated by the desire to establish a nonheuristic procedure for the sequencing of column involving nonideal mixtures, Doherty and coworkers used residue-curve maps, first for homogeneous columns (Doherty and Caldarola, 1985), and later heterogeneous azeotropic columns, Pham and Doherty (1990c). As noted earlier, to establish the bounds between the distillation regions, distillation line maps should be used rather than residue curve maps, although often the distillation line and simple distillation boundaries do not differ appreciably. The basic difference between the design of sequences for ideal and non-ideal mixtures is that the product distribution for the latter depends upon the distillation region in which the feed composition lies. Furthermore, as the number of species increases, the product composition becomes more difficult to predict. However, when the maps of residue curves and distillation lines can be used, the feasible regions for the distillate and bottoms products compositions are well defined and the strategy for synthesizing the distillation sequence is simplified considerably, Wildagdo and Seider (1996).

3.2 Residue Curves

As shown by Doherty et al (1978) the composition pathway of a residue curve as a function of dimensionless time ζ is given by:

$$\frac{dx}{d\zeta} = x_i - y_i^* \quad 3.1$$

Where, for component i , the vapour composition, y_i^* , and the liquid composition, x_i , are in equilibrium with each other and ζ is a non-linear time dependent variable.

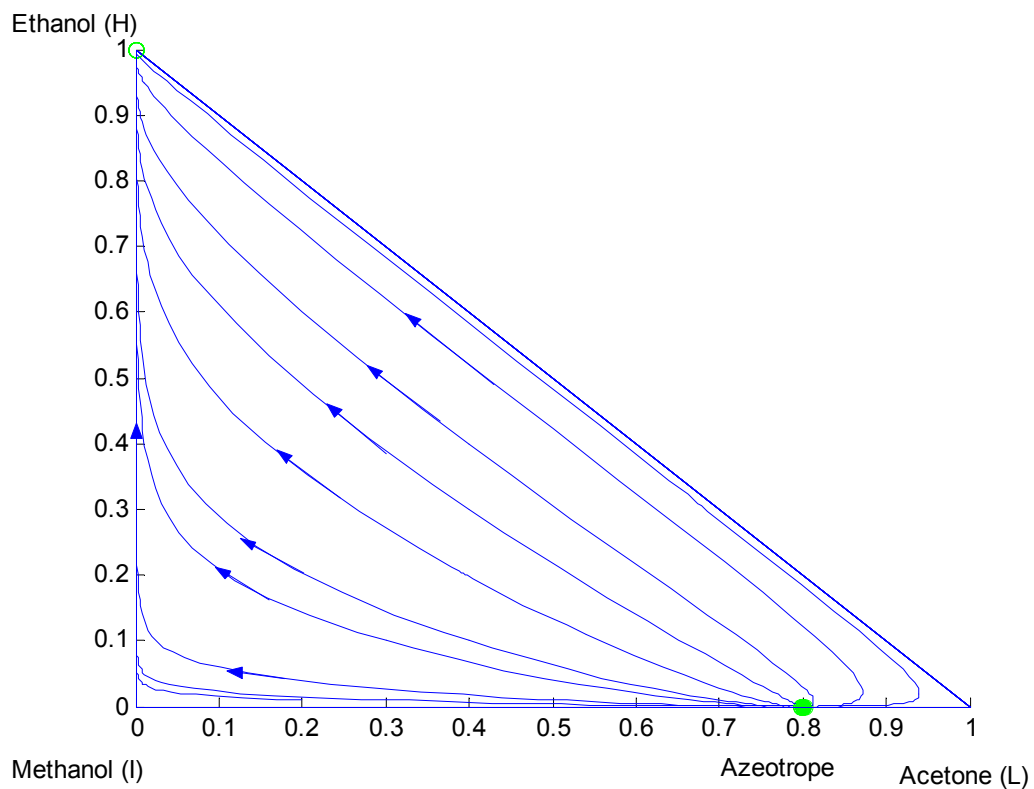


Figure 3.1: Residue curve map of Acetone, Ethanol, and Methanol system.

Integrating equation 3.1 with different starting points of x one can plot the residue curve map of a particular system. The above Figure 3.1 shows a residue curve map of the Acetone, Ethanol, and Methanol system. This system shows a binary azeotrope on

the methanol / Acetone axis. The number of singularities in the system correspond to the solution of the residue equation when the derivative is equal to zero.

$$\frac{dx}{d\xi} = 0 \Rightarrow x = y^* \quad 3.2$$

Singularities also referred to as nodes can be classified due to the behaviour of trajectories around them. The Acetone, Ethanol, and Methanol system for example contains four singularities inside or on the boundary of the mass balance triangle.

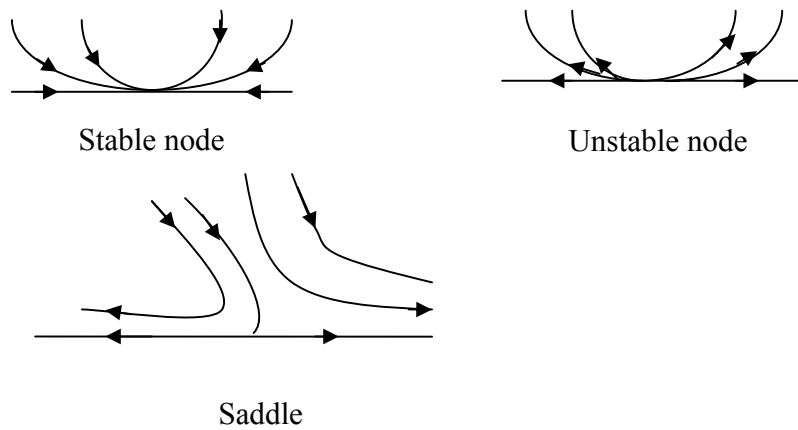


Figure 3.2: Types of nodes

A stable node is defined as a point where all the residue curves move towards the same point. A unstable node is defined as the opposite of the stable node as all the residue curve move away from a stationary point and a saddle point is defined as a point where some of the residue curve move towards this point and some residue curve move away from this point, this is shown in Figure 3.2. Looking at the Acetone, Ethanol, and Methanol system shown in Figure 3.3 we can see that the node corresponding to pure ethanol (B) is a stable node, the node corresponding to pure methanol (D) is a saddle and the node corresponding to pure acetone (F) is also a saddle node. The azeotrope (E) can be identified as an unstable node, Gert-Jan et al

(1994). All column profiles shown in this paper have been generated using the NRTL model at a system pressure of 0.83 bars. The NRTL model is defined by the following thermodynamic equation, see Sandler (1999) :

$$\gamma_i = \exp \left[\frac{\sum_{j=1} \tau_{ji} G_{ji} x_j}{\sum_{j=1} G_{ji} x_j} + \sum_{j=1} \frac{x_j G_{ij}}{\sum_{k=1} x_k G_{kj}} \left(\tau_{ij} - \frac{\sum_{k=1} x_k \tau_{kj} G_{kj}}{\sum_{k=1} x_k G_{kj}} \right) \right] \quad 3.3$$

Where $G_{ij} = \exp(-c_{ij} + d_{ij}(T - 273.15K)\tau_{ij})$ and $\tau_{ij} = a_{ij} + \frac{b_{ij}}{T} + e_{ij} \ln T + f_{ij}T$

The binary interaction parameters a_{ij} , b_{ij} , c_{ij} , d_{ij} , e_{ij} , f_{ij} for the NRTL model can be determined from the VLE and /or LLE data regression. Aspen plus ® 13.2 simulation program has a large number of built in binary parameters, this parameters were obtained form Aspen plus ® 13.2. Table 1.1 below has the binary parameters for the Methanol, Ethanol and Acetone system.

Table 3.1: The binary interaction parameters for the Methanol, Ethanol and Acetone system

Component i	Acetone	Acetone	Methanol
Component j	Methanol	Ethanol	Ethanol
A_{ij}	0	-0.3471	4.711
A_{ji}	0	-1.078	-2.31
B_{ij}	101.85	206.5	-1162.3
B_{ji}	114.13	479.1	483.84
C_{ij}	3	3	3

There are nodes that can be observed outside the mass balance triangle of the Acetone, Ethanol, and Methanol system. The outside space has been introduced by Holland et al. (2004a), the nodes show the same characteristics as the nodes inside the mass balance triangle (the saddle, stable and the unstable node). We will show the relevance of this later.

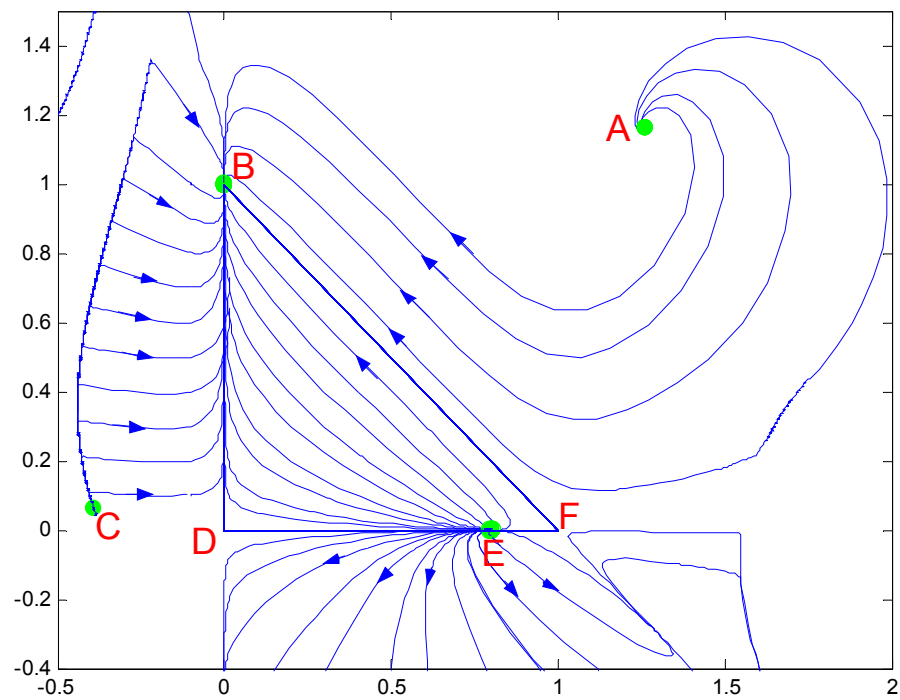


Figure 3.3: Identifying pinch points on RCM of methanol, ethanol, and acetone system.

3.3 Column profile map

3.3.1 Continuous distillation column

So far we have discussed columns operating at infinite reflux: what about realistic columns operating at finite reflux ratios?

Let us consider a mathematical model for the separation of a multi-component mixture in the rectifying section of a staged distillation column with a single feed and no side draws as shown in Figure 3.4.

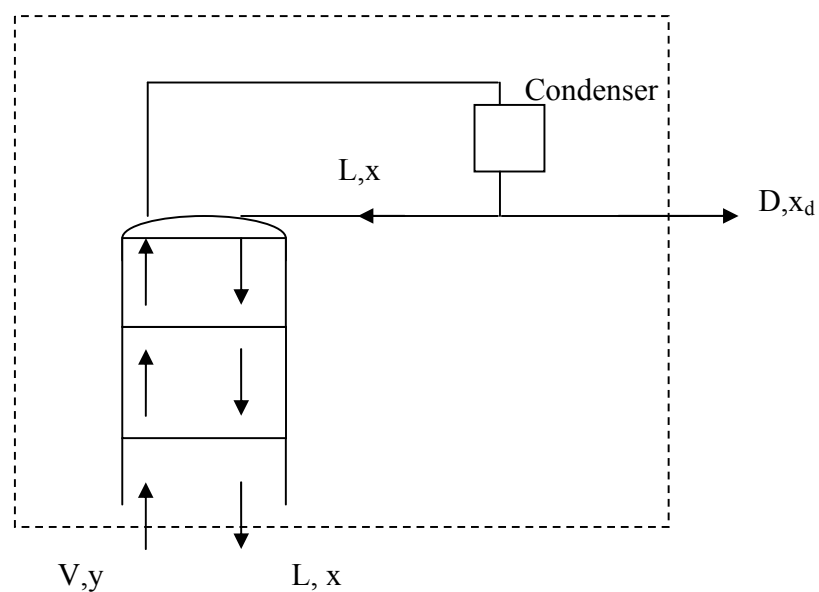


Figure 3.4: The rectifying section of a distillation column.

Taking a material balance around the rectifying section and assuming constant molar overflow gives:

$$Vy_{i, n+1} = Lx_{i, n} + Dx_{i, d} \quad 3.4$$

Assume that the reflux ratio is defined as: $r = L/D$ and as a result $V/L = (r+1)/r$.

Doherty and Perkins (1978) have shown that equation 3.4 can be approximated by a differential equation 3.5

$$\frac{dx_i}{dn} = \frac{r+1}{r}(x_i - y_i) + \frac{1}{r}(x_{i,d} - x_i) \quad 3.5$$

Equation 3.5 should approximate a packed distillation column or a staged column with many trays especially when dealing with difficult separations.

Multiplying the equation by r we obtain:

$$\frac{dx}{d\zeta} = (r+1)(x - y) + (x_d - x) \quad 3.6$$

Where, ζ is a non-linear time dependent variable, y , the vapour composition, x , the liquid composition, x_d , distillate composition and r the reflux ratio.

This equation is an approximate mathematical description for a rectifying section of a distillation column.

Similarly the differential equation of the stripping section can be modelled:

$$\frac{dx}{dn} = \frac{s}{s+1}(y - x) + \frac{1}{s+1}(x_b - x) \quad 3.7$$

Where s is the reboil ratio and x_b is the bottoms composition.

3.3.2 Batch distillation column

Let us now consider a batch system.

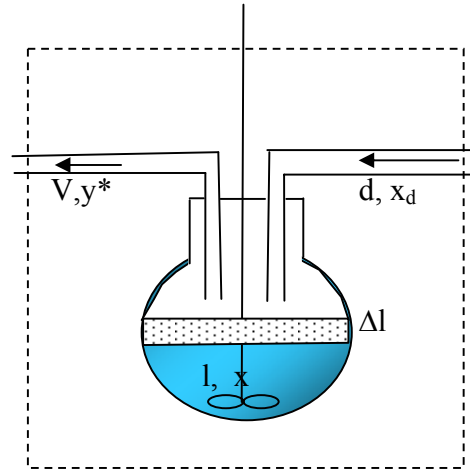


Figure 3.5 : A batch distillation column

Taking a material balance over time around the batch apparatus results in this equation 3.8, see Tapp et al (2003) for derivation.

$$\frac{dx_i}{dt} = \frac{v}{l}(x_i - y_i^*) + \frac{d}{l}(x_{i,d} - x_i) \quad 3.8$$

Where v is the vapour draw-off rate, d is the liquid feed-rate and l is the volume of the contents. By dividing equation 3.8 by d/l and letting $v/d = (r_f + 1)$ we get

$$\frac{dx_i}{d\zeta} = (r_f + 1)(x_i - y_i^*) + (x_{i,d} - x_i) \quad 3.9$$

Assuming that the liquid density is constant over the composition range, the ratios d/l and v/l can also be approximated from the corresponding volumetric flow rates.

It can be seen that the above batch equation 3.9 is mathematically equivalent to the derived equation 3.6 for a continuous distillation column; this implies that a batch system can be used to generate approximate distillation column profiles. In a recent

paper Tapp et al. (2004) have shown that one can derive a difference point equation 3.10 that is essentially the same as equation 3.5 for a column section.

$$\frac{dx}{dn} = \left[\frac{1}{R_\Delta} + 1 \right] (x - y^*) + \frac{1}{R_\Delta} (X_\Delta - x) \quad 3.10$$

Where
$$X_\Delta = \left[\frac{V.Y_T - L.X_T}{\Delta} \right]; R_\Delta = \frac{L}{\Delta} \text{ and } \Delta = (V - L) \neq 0$$

A column section is a section of counter current columns in which there is no addition or removal of material but where the end of the section has inputs that are not necessarily related to the outputs via equipment such as a reboiler and a condenser for stripping and rectifying sections respectively see Figure 3.6. It was shown in that paper how these equations were very powerful for designing complex separation systems.

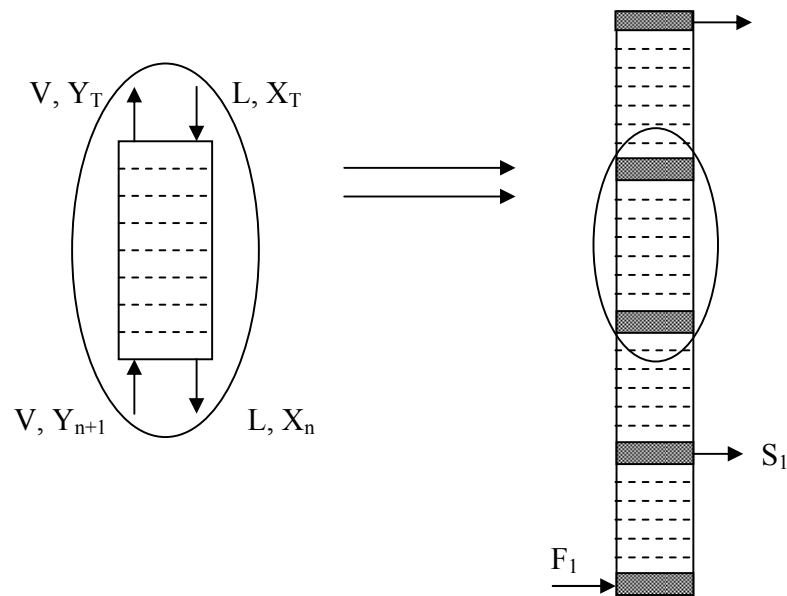


Figure 3.6: A distillation column consisting of four column sections

It would be useful to be able to measure such column section profiles. Looking at equation 3.8 one can deduce that for $V=L$ the rectifying section reduces to the residue curve equation, hence a residue curve is a column profile at infinite reflux. The advantage of using a column section lies in the fact that the composition on the top of the column section does not have to be x_d (the distillate composition) as no condenser or reboiler is used. This allows us to generate a complete set of profiles, and it is called a column profile map. An example of a column profile map is shown in Figure 3.7 for the Acetone, Ethanol, and Methanol system.

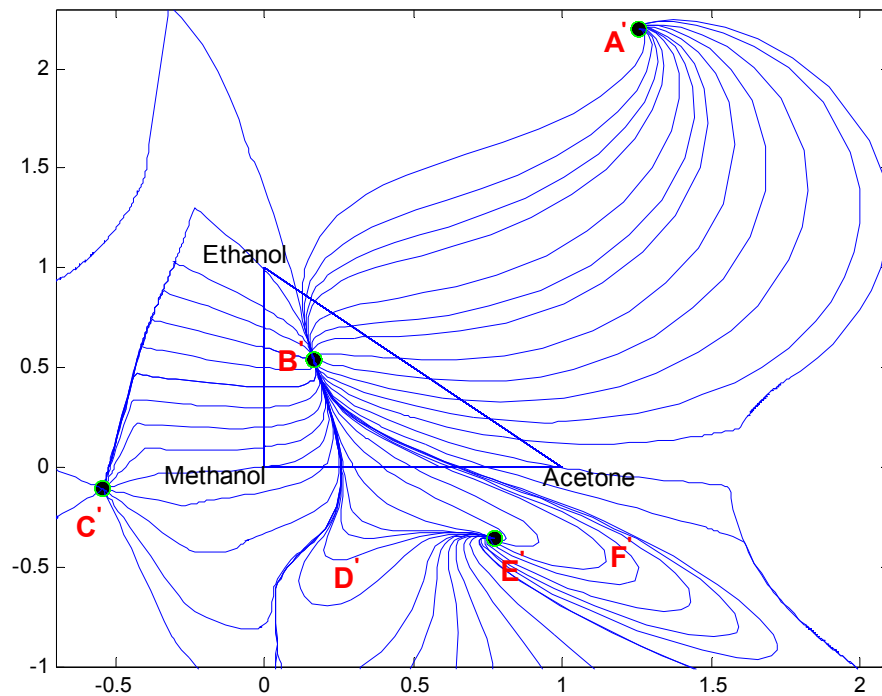


Figure 3.7: Column profile map, with a fixed reflux ratio of 1.

When the rectifying equation 3.8 is set equal to zero, the mixing vector is co-linear with the separation vector.

$$\frac{dx}{dt} = 0 \Rightarrow \frac{v}{l}(x - y) = -\frac{d}{l}(x_d - x) \quad 3.11$$

separation mixing

The x 's that satisfy this equation are known as stationary points on the column profile map. We can now examine the new mass balance triangle (MBT). The stable node (B) has been shifted into the MBT (stable node B'), the unstable node (F) and the saddle (D) points have moved outside the MBT which are now node F' and D' respectively. All the profiles have shifted downwards which shows that the CPM is simply the linear transformation of a residue curve map as shown in Figure 3.7. In a recent paper Holland et al. (2004a) has shown that column profile maps are just linear transformation of a residue curve map as shown in Figure 3.7.

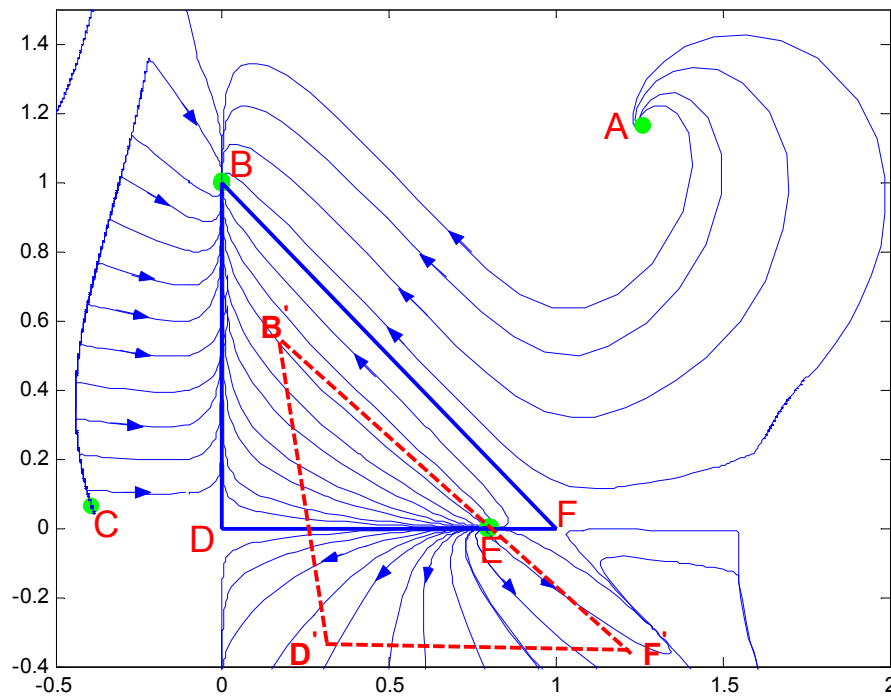


Figure 3.8: A residue curve map showing the transformed mass balance triangle of the column profile map.

The above Figure 3.8 shows the mass balance triangle of the column profile map, which has one positive co-ordinate and the other two co-ordinates are in the negative space. The shape of the mass balance triangle has change, due to the fact that the topology of the column profile map is slightly different from that of the residue curve map as illustrated in Figure 3.7. Under extreme conditions, the topology of the column profile map changes drastically, the nodes of the system merge and the transformed triangle collapses, see Tapp et al. (2004)

3.4 Experiment

In order to measure a column profile map of the rectifying section of the distillation column, an apparatus has been designed in such a way that the column profile composition could be measured during batch or simple boiling. The associated temperature and vapour curve in equilibrium with the liquid residue can also be obtained. This apparatus has been firstly introduced by Chronis et al. (1997) to measure residue curves and has been further developed by Tapp et al. (2003) to measure column profiles. The design of the apparatus is based on the fact that material and component balance over a still pot is mathematically identical to the differential equation derived by Doherty (see equation 3.5). For further details see appendix A.

3.4.1 Experimental setup

There are various components to the experimental set-up as shown in Figure 3.9, the still being the main component. The still was graduated in such a way that the level of the liquid inside the still can be measured and the volume calculated. There are four ports in the still. Two for the sampling and injection of the feed respectively. The other two were for the thermocouple probe and for keeping the pressure constant by releasing vapour below the oil in a bubbler. The bubbler was also used to measure the rate of vaporisation hence in turn measuring the rate of boiling. A condenser was attached to the other end of the bubbler to capture the vapour from the system. A

magnetic stirrer was used for the mixing of the liquid. Boiling stones were placed inside the still to assist nucleation. A HP6890 Hewlett Packard gas chromatograph was used for the analysis. The still was immersed in a water bath. The purpose of the bath was to maintain an even heat distribution and also to ensure that the liquid residue would be at its bubble point. In order to maintain the bubble point temperature, the water bath temperature must be increased continuously to maintain the temperature driving force (ΔT of 6°C) between the contents of the still and the water bath.

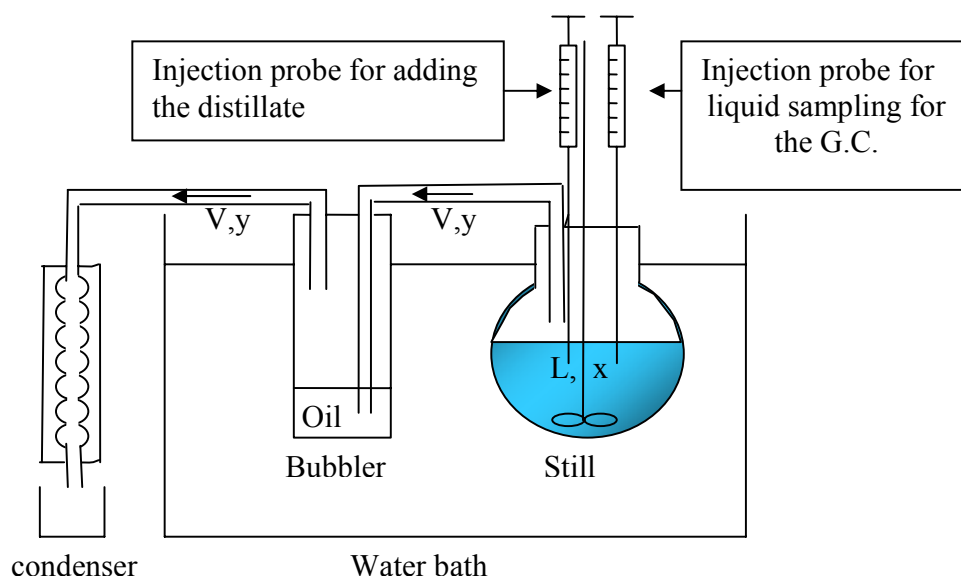


Figure 3.9: Experimental setup with still pot being the main component.

3.4.2 Experimental procedure

For this paper experiments were first performed to simulate the rectifying section of a distillation column that would separate methanol, ethanol and acetone. A bulk solution (about 200ml) of known composition of methanol, ethanol and acetone was prepared. A small quantity of this distillate was kept in a fridge to be used as a feed solution while the rest of the distillate was placed in the still. The still was placed inside a hot water bath. The level of liquid in the still was continuously recorded

during the experiment. It can be shown by material balance around the still that reflux ratio r and the distillate flow rate d can be determined as follows (see Appendix A for the derivation):

$$d = \frac{v}{r + 1} \quad 3.12$$

In order to approximate the desired reflux r , the distillate, d , is added over discrete time intervals. The vapour flow-rate was determined by the following mass balance equation:

$$v = d - \frac{dl}{dt} \quad 3.13$$

The feed addition rate was then determined by the ratio of the level in the still and the required reflux ratio, (see Appendix A for derivation).

$$d = -\frac{\frac{dl}{dt}}{r} \quad 3.14$$

In these experiments the feed material was added in discrete amounts rather than continuously. This was done in the following way: The liquid level was observed to change by an amount dl in a time interval dt . Using equation 3.14 one can say provided the value of dl is not too large that:

$$\Delta d = d * dt = -\frac{dl}{r} \quad 3.15$$

Where Δd is the amount to be added at the end of the time interval dt when the level has fallen by an amount dl . For our experiments we used a value of dl of 6.3 ml which happened in a time interval (dt) of 5 min, each experiment took about two hours. For the initial experiments a reflux ratio was chosen for each run and kept constant throughout the run; this made it possible to calculate the amount of distillate that must be added after each time interval. Liquid samples were drawn at regular intervals (the amount drawn from the still is negligible) and analysed using the gas chromatograph.

The runs were aborted when the liquid level in the still was below the 20 ml mark in the still, since it was found that after these inaccurate results were obtained.

For the experimental runs to produce the column profile maps the procedure was exactly the same as that described above except that the initial composition x_o of the material in the still could be different from that of the distillate composition x_d . If this was the case then a sample of solution of the required x_d was also prepared.

3.5 Results and Discussion

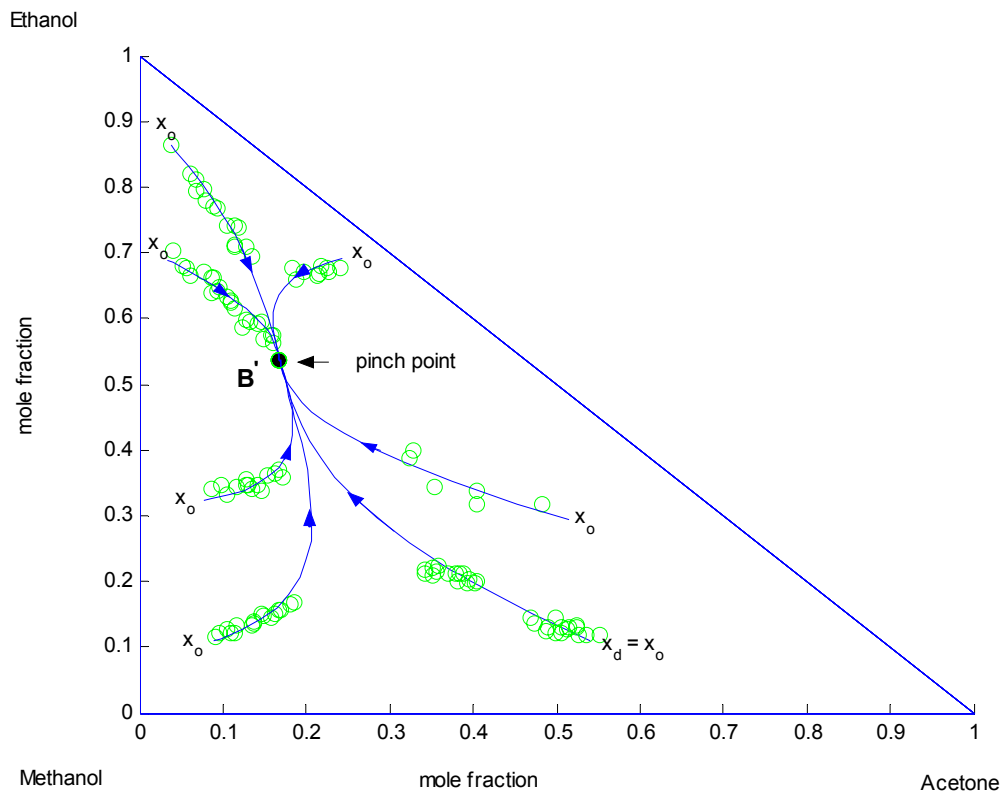


Figure 3.10: Column profiles with the reflux ratio equal to one, starting with different initial compositions x_o but with a fixed feed addition composition x_d . i.e. Column profile map.

Figure 3.10 represents the experimental results obtained for column profiles with the same reflux ratio, namely one, but starting with different initial compositions, x_o . The solid lines represent the theoretical column profiles. The thermodynamic data for the

NRTL model was used to generate theoretical profiles obtained from Aspen. The distillate composition, x_d , (Acetone 54 mol%, Ethanol 11 mol% and Methanol 35 mol%) was the same composition used to generate all the column profiles. The above Figure 3.10 shows that experimentally the stable node (B'), which was initially on the apex of the MBT has been shifted into the triangle. The unstable node (F'), saddle (D') and the azeotrope all have been shifted into the outside the MBT. This implies that the negative profiles have been moved into the positive space and the positive profiles have been moved into the negative space. The stable node moved in space, the same position as predicted hence claimed experimentally found B' . The experimental points on Figure 3.10 are scattered along the profile this could be attributed to inaccurate feed addition that may arise from the manual injection. Another possible reason for deviation from the theoretical curve could be due to superheating of the liquid mixture leading to deviation from equilibrium. It was noticed that at areas of high curvature, the experimental points appeared close to each other. This suggested that the profiles were moving slowly around these areas. A probable reason for this behaviour can be attributed to the vector properties of the differential equation 3.10. The phenomenon of distillation is a linear combination of the separation vector and the mixing vector. The separation vector is defined as the tangent to the residue curve and points in the opposite direction to that of the residue curve. The mixing vector is defined as the difference between the vector of distillate composite and the vector of points on the profile. Around the turning points the separation vector and the mixing vector align so that they are almost co-linear. There no other noticeable nodes inside the mass balance triangle.

The temperature profiles for these column profile map were quiet complicated as shown in Figure 3.11 below, these profiles were theoretically simulated. There are profiles which follow the same direction as those of residue curves i.e. they have an increasing temperature profile as shown by Figure 3.11 and there are those profiles which are moving in the opposite direction as the residue curves. These profiles have a decreasing temperature profile as shown in Figure 3.11. This implies that the

temperature inside the still kept on rising for profiles following the residue curve and the temperature kept on dropping for profiles moving in the opposite direction from the residue curve. There were also those profiles with decreasing or increasing temperatures, i.e. they had a maximum temperature along the profile.

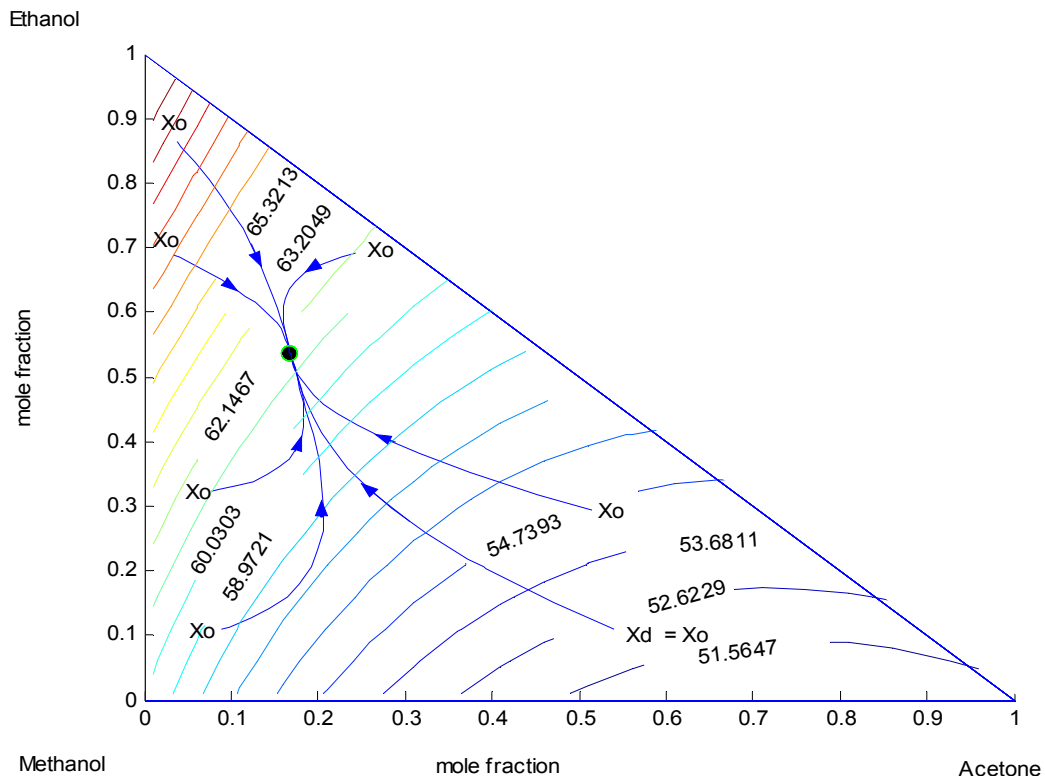


Figure 3.11: An isotherm plot with the column profile map of the reflux ratio $r = 1$ and a distillate composition $x_d = [0.54, 0.11, 0.35]$.

3.6 Conclusion

To confirm that the mass balance triangle has really shifted downwards, we showed that the pinch point (B') inside the original mass balance triangle is a stable node, as the other nodes moved into the negative space shown in Figure 3.10. Since we managed to simulate profiles starting from different initial points going towards the same pinch point it can be concluded that this stationary point is a stable node, which

in turn implies that the mass balance triangle can be moved. This experimental method can be used to identify the type of thermodynamic model which can be used. Most thermodynamic model predicts the same profile inside the mass balance triangle but predict different topology outside the mass balance triangle. This method of shifting profiles from outside to inside the mass balance triangle can be used to bring in some topology which is not predicted by other thermodynamic model and can be measured experimentally, see chapter 6 for comparison between different thermodynamic models.

3.7 Nomenclature

- d : Feed addition flow rate (mol/time)
- D : Distillate flow rate (mol/time)
- dx : Change in liquid mole fraction
- dn : Change in number of stages
- l : Amount of residue in the still (mol)
- L : Liquid flow rate (mol/time)
- n : Tray position
- P : System pressure (Pa)
- P_i^{sat} : Vapour pressure (Pa)
- r : Reflux ratio
- s : Reboil ratio
- t : Time variable
- v : Amount of vapour formed (mol/time)
- x : Liquid mole fraction
- x_b : Bottoms composition
- x_d : Distillate flow rate (mol/time)
- y : Vapour mole fraction
- γ : Liquid phase activity coefficient
- ζ : Time dependent variable

3.8 References

1. Andrecovich, M.J., Westerberg, A.W., Simple synthesis method based on utility bounding for heat integrated distillation sequence synthesis., *AIChE J.*, vol. 31, 1985a, pg 363
2. Andrecovich, M.J., Westerberg, A.W., A MILP formulation for heat intergrated distillation sequence synthesis., *AIChE J.*, vol. 31, 1985b, pg 1461
3. Chronis, T., Glasser, D., Hildebrandt, D., "A simple, reasonable accurate method for measuring residue curves and the associate VLE", *Distillation & Absorption*, 97 edition by R.Darton, *IchemE*, 1, pp187-196, 1997.
4. Chronis, T., "The simple measurement of residue curves and their associated vapour-liquid equilibrium", M.Sc. Thesis , University of Witwatersrand, 1996
5. Doherty, M.F., Calderola, G.A., Design and synthesis of homogeneous azeotropic distillation. III The sequence of column for azeotropic and extractive distillation., *Ind. Eng. Chem., Fundam.*, vol. 24, 1985, pg 474
6. Doherty, M.F., Perkins, J.D., "On the Dynamics of Distillation Processes, I-VII", *Chem. Eng. Sci.*, 34, 1978
7. Gert-Jan, Fien, A. F., Liu , Y.A., " Heuristic synthesis and shortcut design of separation processes using residue curve maps" *Ind.Eng.Chem.Res.*vol 33, pp2505-2522 ,1994
8. Holland, S., Tapp, M., Hildebrandt, D., Glasser, D., Novel separation system design using " Moving triangles", *Comp. and Chem. Eng.*, vol 29, pp 181-189, 2004a
9. Malone, M.F., Glinos, K., Marquez, F.E., Douglas, J.M., Simple, analytical criteria for the sequence of distillation columns. *AIChE J.*, vol. 31, 1985, pg 683
10. Mcgregor, C., Hausberger, B., Hildebrandt, D, Glasser, D., "Whats new in multi-component distillation? Residue curve maps: a new tool for distillation column design." *Chem Technology* ,pp 11-17,1998

11. Pham, H.N., Doherty, M.F., Design and synthesis of azeotropic distillation : III Column sequence., Chem. Eng. Sci., vol. 45, 1990c, pg 1845
12. Sandler, S.I., "Chemical Engineering Thermodynamics" 1999, John Wiley & Sons, New Jersey
13. Safrit, B., T., Westerberg, A.W., "Algorithm for generating the distillation regions for azeotropic multi-component mixtures", Ind. Eng. Res. Vol. 36, pp1827-1840, 1997
14. Stichlmair, J. G.,Herguijuela, J. R., "Separation regions and processes of zeotropic and azeotropic ternary distillation", AIChE Journal, vol. 38 ,pp1523-1535 ,1992
15. Schreinemakers, F.A.H. ,Z. Phys. Chem. ,43, pp671, 1902
16. Stanley I. Sandler, Chemical and Engineering Thermodynamics, Second Edition, pg 240, 1989
17. Tapp, M., Kauchali, S., Hausberger, B., Hildebrandt, D., Glasser, D., "An experimental simulation of distillation column concentration profiles using a batch apparatus", Chem. Eng. Sci., pg 479-486, 2003
18. Tapp, M., Holland, S., Hildebrandt, D., Glasser, D., " Theoretical simulation of concentration profiles in complex distillation columns." University of the Witwatersrand-PhD Thesis, 2004
19. Thompson, R.W., King, C.J., Syntematic synthesis of separation schemes., AIChE J., vol. 18, 1972, pg 941
20. Venimadhavan, G.,Buzad, G., Doherty, M.F., Malone, M.F., "Effect of kinetics on residue curve maps for reactive distillation", AIChE Journal, vol. 40,pp1814-1824 ,1994
21. Widagdo, S., Seider, W., Azeotropic Distillation., AIChE J., vol. 42, 1996, pg 96-130

4 CAN THE OPERATING LEAVES OF A DISTILLATION COLUMN REALLY BE EXPANDED?

This paper was published in the Industrial Engineering Chemistry Research Journal, 2005, vol. 44 (19), 7511-7519

Abstract

Residue curves and pinch point curves are used to determine the operation leaves and hence the feasible region for distillation columns operating at a specific distillate and bottoms composition for all possible constant reflux and reboil ratios. In this paper we will experimentally show that we can expand the operating leaves of the rectifying section beyond the pinch point curve by varying the reflux ratio within the distillation column and we will also show theoretically that this method can be used to cross the simple distillation boundaries.

Key words: Residue curves, pinch point curve, operating leaves, reflux ratio, distillation column, batch apparatus, distillation boundary, column profile.

4.1 Introduction

Batch distillation is becoming more important as a result of the recent increase in the production of high-value-added, low-volume specialty chemical and bio-chemicals. The flexibility in operation and the lower cost, for separating relatively pure components are the advantages offered by batch distillation over continuous

distillation. In many cases, the objective of the batch distillation is to recover the most volatile component of a feed mixture at a high degree of purity, leaving the relatively heavy components in the still.

Feasibility conditions for distillation are based on the two extreme operating conditions for a continuous distillation column process- minimum and total reflux. Neither condition is practical for operating a distillation column, because an infinite number of stages and intermediate condensers and reboilers are required for minimum reflux while no product is withdrawn at total reflux. However, these limiting conditions traditionally serve as bounds for distillation. Based on these extreme operation limits, graphical approaches have been developed to determine where in composition space a column can operate. These methods divide the column into sections (rectifying and stripping) in which column pressure is fixed and all stages are theoretical, it is assumed that constant molar overflow exists in each section, but this restriction can readily be lifted if heat effects are considered.

Using the extreme operating conditions, feasibility criteria have been developed for two different column-design approaches. The most common technique specifies the feed composition and determines all reachable products, Wahnschafft et al (1992), Fidkowski et al (1993). The other approach, which has received more attention lately, identifies all feed to a column section, Pollmann and Blass et al (1994), Castillo et al (1998).

These techniques will reliably determine column feasibility as long as all reachable compositions are contained between the minimum and total reflux bounds. However, it has been noted (Castillo et al 1998) that sectional profiles for columns can extend beyond these extreme operating limits in regions of composition space where the total reflux curves (distillation lines for a stage column and residue curves for a packed column) take on an S-shape, Hoffmaster et al (2002).

Wahnschafft et al (1992) showed a relatively simple analysis to determine the feasibility of separation processes, which involves residue and pinch point trajectories for the special case of separating ternary mixtures using distillation columns that produce two products. Based on this analysis, Castillo et al (1997) defined the operating leaves. Operation leaves define the region enclosed by the residue curve through a product composition and the respective pinch point curve for that product. This region comprises a whole range of possible column profiles for all constant reflux ratios with respect to the product composition. In a two-product column, leaves can be generated for the bottoms and the distillate composition. A distillation column is known to be feasible if these product leaves intersect.

In this paper we will experimentally show that we can expand the operating leaves for the rectifying section of a distillation column beyond the pinch point curve by varying the reflux ratio within the distillation column. By expanding the operation leaves we can design columns to do separations that were not previously considered possible.

4.2 Theoretical background

4.2.1 Operating leaf for constant reflux ratio

Doherty and Perkins et al (1978) have shown that equation 4.1 can be used to approximate the rectifying section of a distillation column.

$$\frac{dx}{dn} = \frac{r+1}{r}(x - y^*) + \frac{1}{r}(x_d - x) \quad 4.1$$

Where x_d is the distillate composition, r is the reflux ratio and y^* the vapour composition in equilibrium with the liquid composition x .

Different reflux ratios, for a specific value of x_d results in different column profiles as shown in Figure 4.1. The outer most profile being the residue curve as the reflux ratio tends to infinity.

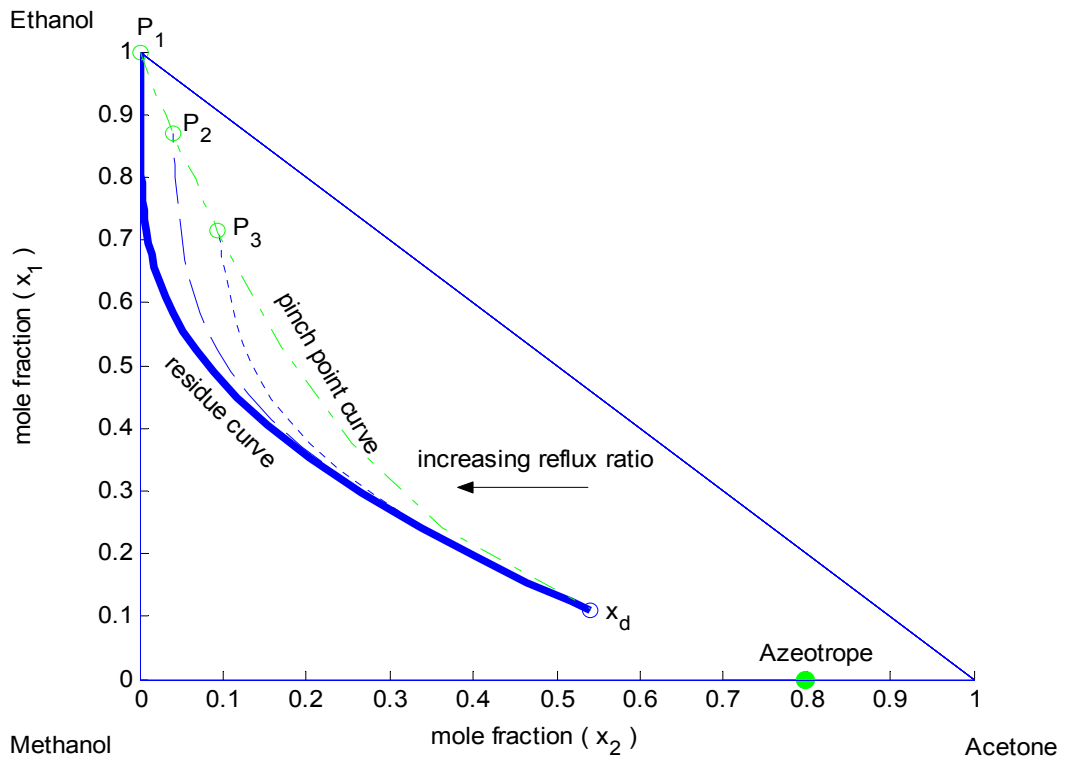


Figure 4.1: Column profiles for the Ethanol/ Methanol/ Acetone system using equation 4.1 for different reflux ratios and $x_d = [0.54, 0.11, 0.35]$ with the respective pinch point curve.

All column profiles shown in this paper have been generated using the NRTL model at a system pressure of 0.83 bar. In general column profiles start at distillate composition x_d and initially run along the residue curve. They then deviate from the residue curve depending on the reflux ratio and end at their respective pinch point. The locus of all pinch points from a specific distillate composition is called a pinch point curve, this is shown as the dash dotted line in Figure 4.1. The region that is enclosed by the residue curve through x_d and the pinch point curve is called the

operating leaf, Castillo et al (1997). This region represents the whole range of attainable profiles for all constant reflux ratios defined by the composition x_d . Pinch point curve can be determined mathematically by finding the solutions for equation 4.1 which are equal to zero.

$$\text{if } \frac{dx}{dn} = 0 \quad \text{then } (x - y^*) = -(x_d - x) \quad 4.2$$

separation
mixing

Setting equation 4.1 equal to zero gives us the above equation 4.2 which is the equation defining the pinch point. This equation has two vectors, namely the separation and the mixing vector. At the pinch point this two vectors are co-linear as shown in Figure 4.2.

From equation 4.2 it can be seen that the pinch point curve is only a function of the distillate composition x_d and not of the reflux ratio r . In other words only the different compositions of x_d result in different paths of the pinch point curve. The pinch curve can also be easily constructed graphically by finding the points on the residue curves with their tangents passing through the composition x_d . This makes it a quick and easy tool to find the attainable region for a certain x_d .

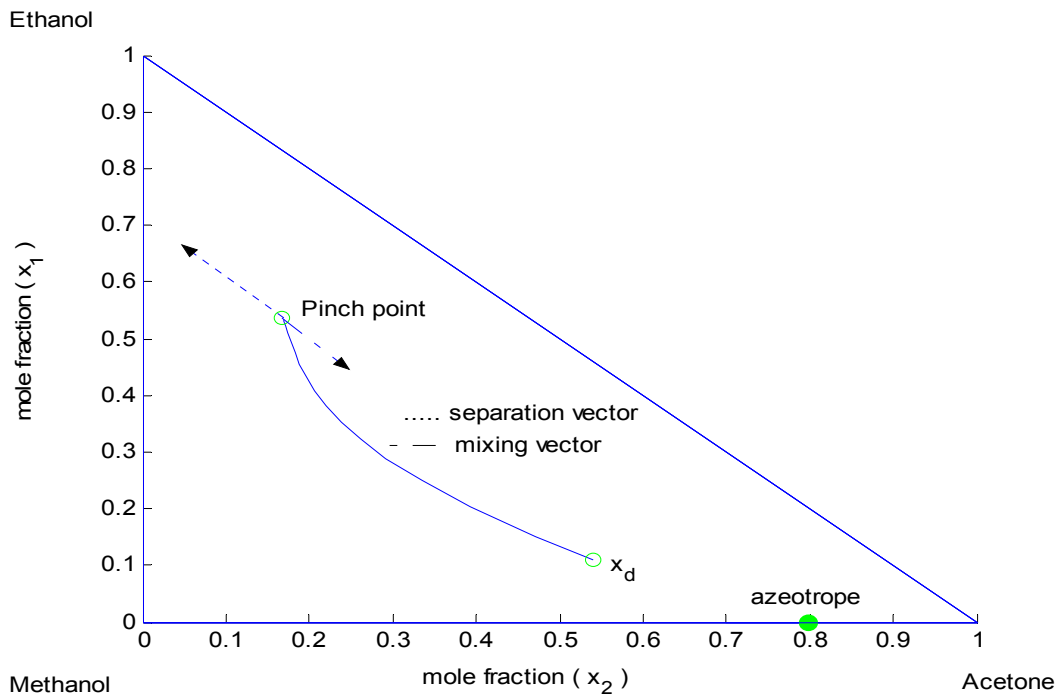


Figure 4.2: A column profile with its respective pinch point showing the co-linearity of separation and mixing vector. $x_d = [0.54, 0.11, 0.35]$

4.2.2 Operating leaf for non-constant reflux ratio

The reflux ratio does not necessarily need to be constant throughout the column. It can be changed by using side condensers, reboilers or by adding or removing feed or side streams.

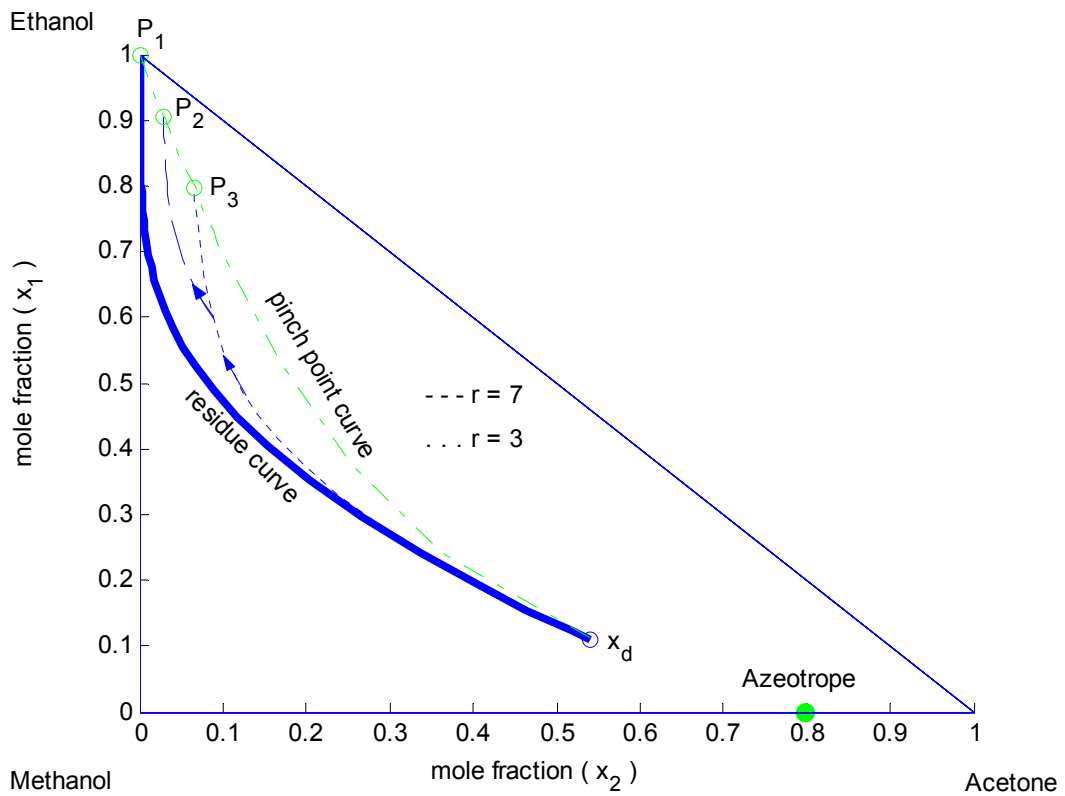


Figure 4.3: Increasing the reflux ratio along a column profile, $x_d = [0.54, 0.11, 0.35]$

Increasing the reflux ratio along the column profile causes the column profile to run closer to the residue curve, this column profile pinch closer to the pinch point P_1 of the residue curve. This implies that the column profile will always be inside the operating leaf when the reflux ratio is increased along the column profile as shown in Figure 4.3, Tapp et al. (2003).

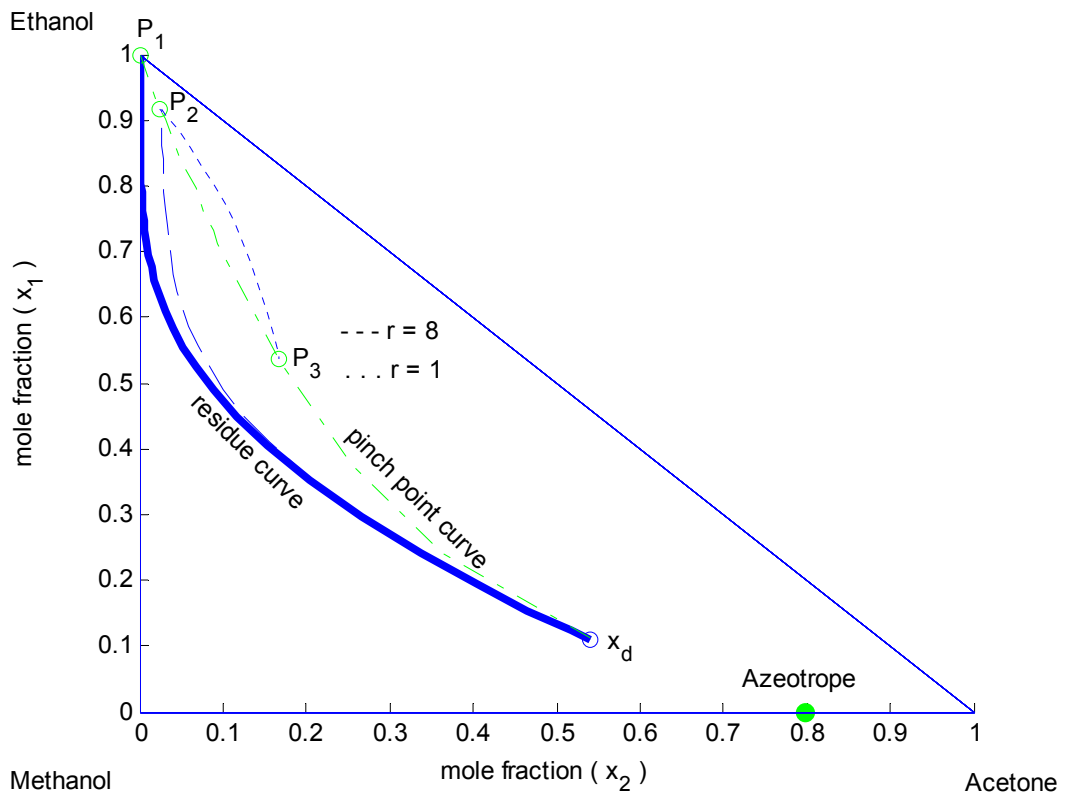


Figure 4.4: Decreasing the reflux ratio along the column profile with an $x_d = [0.54, 0.11, 0.35]$

Decreasing the reflux ratio along the column profile can cause the profile to turn back to its new pinch point P_3 which is closer to x_d . The profile crosses the pinch point curve, and expands the operating leaf as illustrated in the above Figure 4.4, Tapp et al. (2003). In other words, compositions outside the operating leaf can be achieved. This behavior can be explained by looking at the net flow within the column. In a rectifying section: $V - L = D > 0$ and all composition x_i are greater than zero. This means there is a net flow up the column. By varying the reflux ratio all x_i are still

greater than zero, but $V - L \neq D$ rather $V - L = \Delta$ see Tapp et al (2004) with $\Delta =$ net flow rate in a column section and can be negative. A negative Δ would result in a net flow down the column, in other words the profiles runs in the opposite direction. The greatest extension of the operating leaf, can be achieved by following the residue curve until its respective pinch point and then reducing the reflux ratio to the lowest reflux ratio possible as shown in Figure 4.5 below.

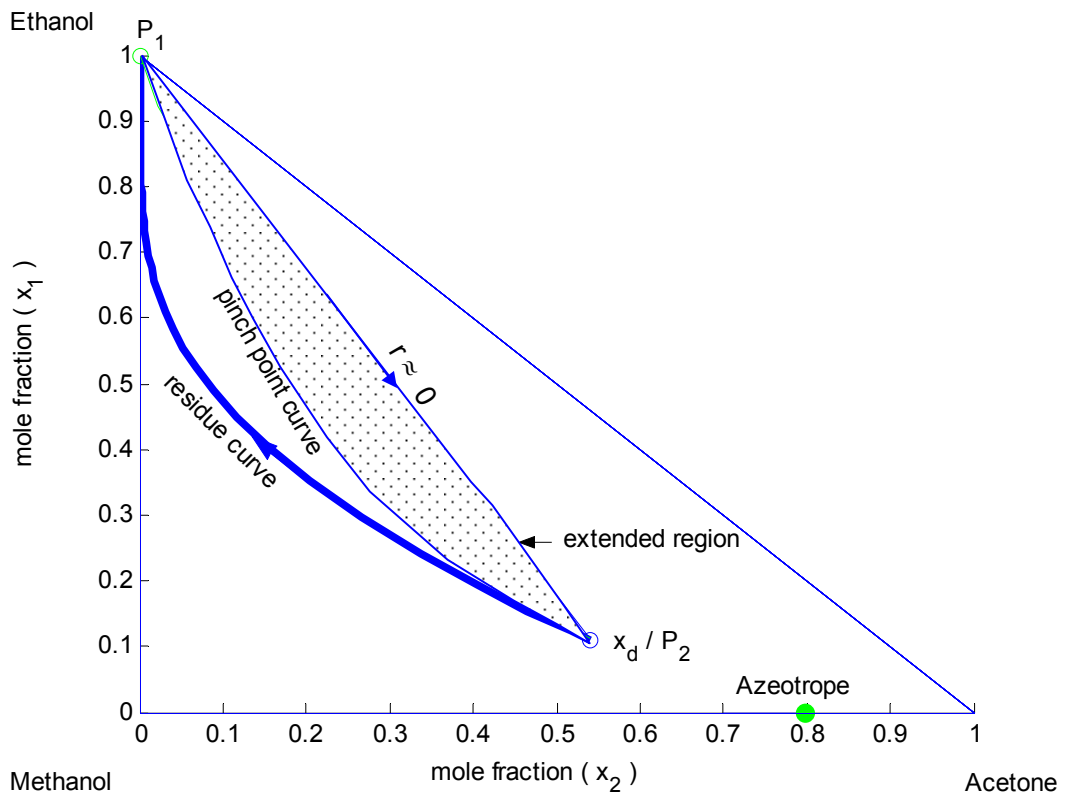


Figure 4.5: The greatest extension of the operating leaf with an $x_d = [0.54, 0.11, 0.35]$

This method of expanding the operating leaf can be very useful as it expands the region of operation in a distillation column as well as can be used to cross the distillation boundaries.

4.2.3 Crossing simple distillation boundaries

The chloroform, benzene and acetone system is used as an example to illustrate the crossing of a simple distillation boundary by expanding the operating leaf as illustrated in Figure 4.6. The acetone/ benzene/ chloroform system has one simple distillation boundary that divides the residue curve map into two distillation regions as shown in Figure 4.6. Fixing the distillate composition $x_d = [0.132, 0.2, 0.668]$ results in a column profile. The greatest extension of the operating leaf can be achieved by following the residue curve until its respective pinch point and then reducing the reflux ratio to the lowest reflux ratio possible. Applying this technique, an operating leaf can be achieved that lies in both distillation regions. In other words profiles can be generated that starts in one distillation region (at x_d) and crossing over the simple distillation boundary to its respective pinch point.

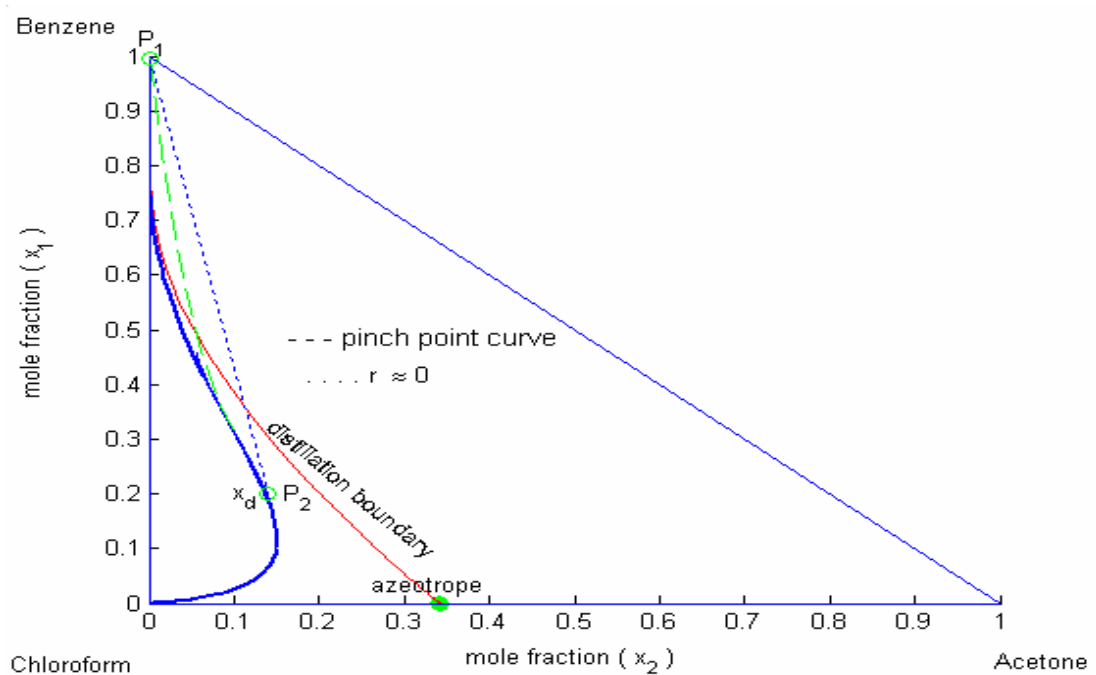


Figure 4.6: Acetone, Benzene and Chloroform system showing the crossing of a simple distillation boundary with an $x_d = [0.132, 0.2, 0.668]$

4.3 Experiment

In order to measure a column profile that expands the rectifying leaf an apparatus has been designed in such a way that the column profile composition could be measured during batch or simple boiling. The associated temperature and vapour curve in equilibrium with the liquid residue can also be obtained. This apparatus has been firstly introduced by Chronis et al (1997) to measure residue curves and has been further developed by Tapp et al (2003) to measure column profiles. The design of the apparatus is based on the fact that material and component balance over a still pot is mathematically identical to the differential equation derived by Doherty (see equation 4.1). For further details see Appendix A.

4.3.1 Experimental setup

There are various components to the experimental set-up as shown in Figure 4.7, the still being the main component. The still was graduated in such a way that the level of the liquid inside the still can be measured and the volume calculated. There are four ports in the still. Two of the ports are used for the sampling and injection of material respectively. The other two were for the thermocouple probe and for keeping the pressure constant by releasing vapour below the oil in a bubbler. The bubbler was also used to measure the rate of vaporisation hence in turn measuring the rate of boiling. A condenser was attached to the bubbler to capture the vapour from the system. A magnetic stirrer was used for the mixing of the liquid. Boiling stones were placed inside the still to assist nucleation. A HP6890 Hewlett Packard gas chromatograph was used for the analysis. The still was immersed in a water bath. The purpose of the bath was to maintain an even heat distribution and also to ensure that the liquid residue would be at its bubble point. In order to maintain the bubble point temperature, the water bath temperature must be increased continuously to maintain the temperature driving force (ΔT of 6°C) between contents of the still and the water bath.

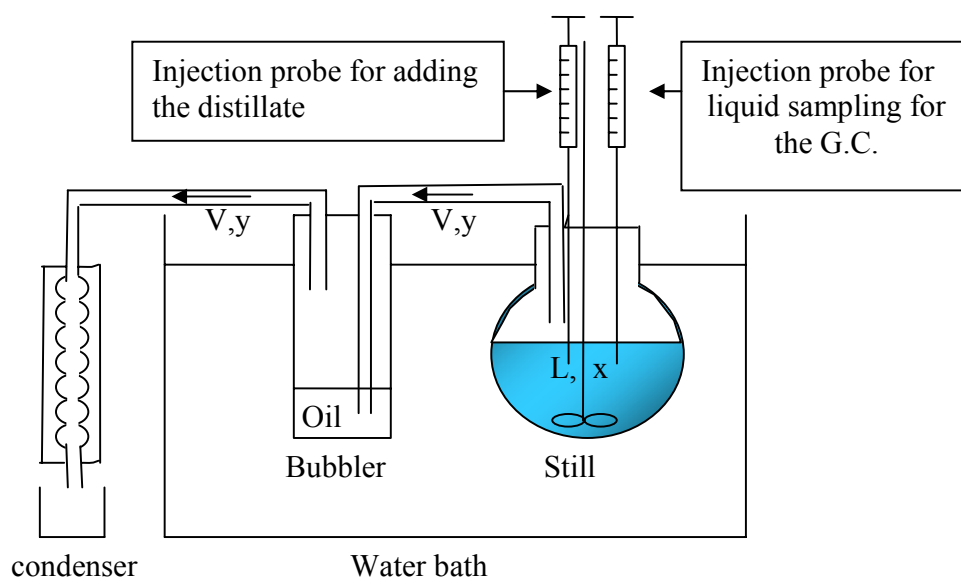


Figure 4.7: Experimental set-up with the still being the main component

4.3.2 Experimental procedure

For this paper experiments were first performed to simulate the rectifying section of a distillation column that would separate methanol, ethanol and acetone. A bulk solution (about 200ml) of known composition of methanol, ethanol and acetone was prepared. A small quantity of this distillate was kept in a fridge to be used as a feed solution while the rest of the distillate was placed in the still. The still was placed inside the hot water bath. The temperature of the bath was then adjusted to ensure that the liquid in the still was at its bubble point at all times. The varying level of liquid in the still was continuously recorded during the experiment. It can be shown by

material balance around the still that the reflux ratio r , the vapour flow rate v and the distillate flow rate d can be related as follows (see Appendix A for the derivation):

$$d = \frac{v}{r + 1} \quad 4.3$$

The vapour flow-rate was determined by the following mass balance equation:

$$v = d - \frac{dl}{dt} \quad 4.4$$

Where $\frac{dl}{dt}$ is the change of liquid level in the still per change in time. Combining equation 4.3 and 4.4 allows the determination of the distillate flow rate d .

$$d = -\frac{\frac{dl}{dt}}{r} \quad 4.5$$

In these experiments d was added in discrete amounts rather than continuously. This was done in the following way: The liquid level was observed to change by an amount dl in a time interval dt . Using equation 4.5 one can say provided the value of dl is not too large that:

$$\Delta d = d * dt = -\frac{dl}{r} \quad 4.6$$

Where Δd is the amount to be added at the end of the time interval dt when the level has fallen by an amount dl . For our experiments we used a value of dl of 6.3 ml which happened in a time interval (dt) of 5 min. For the initial experiments a reflux ratio was chosen for each run and kept constant throughout the run; this made it possible to calculate the amount of d that must be added after each time interval. Liquid samples were drawn at regular intervals and analysed using the gas

chromatograph .The runs were aborted when the liquid level in the still was below the 20 ml mark in the still, since it was discovered that after this inaccurate results were obtained. For the experimental runs to produce the extended part of the operating leaf, the procedure was exactly the same as that described above except that as we approach the pinch point the reflux ratio was changed to a lower reflux, according to the addition rate equation 4.6, as we change the reflux ratio to a lower value, the distillate addition flow rate will become higher. This implies that more distillate was added when working with a lower reflux ratio as compared to working at a higher reflux, which made it possible for the profile to move in the opposite direction from that of the residue curve. The bubble point temperature, after changing the reflux ratio also changes to a lower temperature as shown in Figure 4.8. The liquid inside the still continued boiling; this is because the distillate composition x_d was richer in acetone which is the most volatile component.

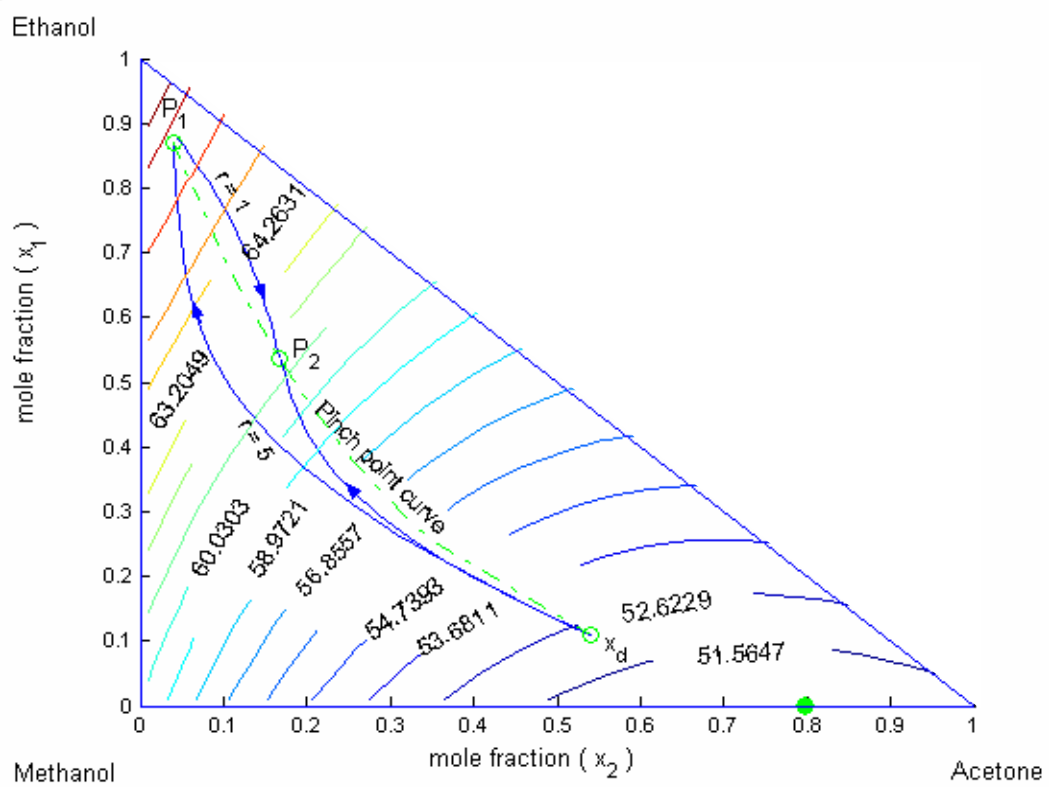


Figure 4.8: An isotherm plot showing column profile with a reflux of 5, reflux of 1 and their respective pinch point P_1 and P_2 , $x_d = [0.54, 0.11, 0.35]$

Figure 4.8 shows a plot of the isotherms in the Ethanol/ Methanol /Acetone system. The isotherms depend only on the thermodynamic data. Isotherms are not affected by the reflux ratio or the distillate composition x_d . That makes the isotherm plot a nice visual tool to understand the temperature change inside the distillation column. The profile with a reflux ratio of 5 in Figure 4.8 has an increasing temperature until its respective pinch point P_1 , at the pinch point P_1 the reflux ratio is the changed to 1.

The profile with a reflux ratio of 1 has a decreasing temperature profile as shown in the above Figure 4.8. Figure 4.8 shows the changes in temperature profiles for column profiles. This is an important result as profiles can be made to run from high to low temperature, hence the temperature along a profile does not need to be monotonically increasing.

4.4 Results

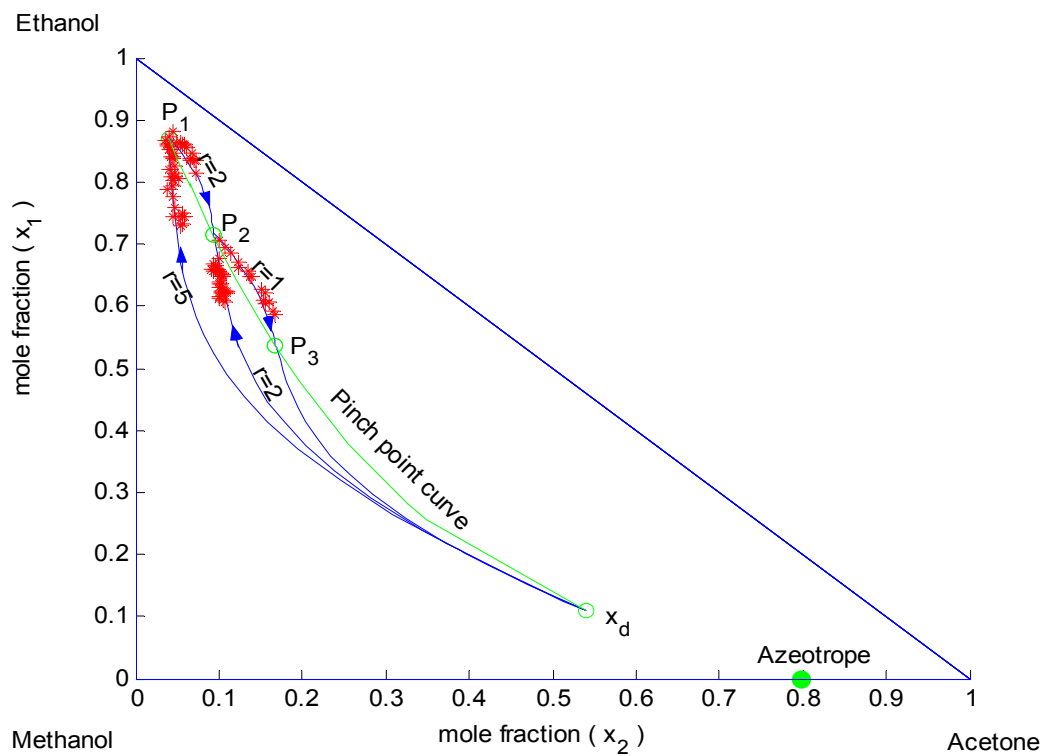


Figure 4.9: Experimental results of an extended region of an operating leaf with distillate composition x_d of [0.54,0.11,0.35].

The stars and circles in Figures 4.9 and 4.10 represent experimental results. The above Figure 4.9 shows two experimental runs with different distillate adding policies because of the different reflux ratios used, but the same distillate composition $x_d = [$

0.54, 0.11, 0.35]. The first run started with the reflux ratio of 5, after approaching the pinch point P_1 the reflux ratio was changed to a reflux of 2. The second set of experimental data point were obtained by starting with a reflux ratio of 2 approaching pinch point P_2 , then the reflux ratio was the changed to 1. It is also interesting to note that the two profiles with a reflux ratio of two approaches the pinch point P_2 from different directions (along the direction of the eigenvector of the pinch point) see Figure 4.9. The experimental points follow the predicted path well. They cross the pinch point curve and expand the operating leaf.

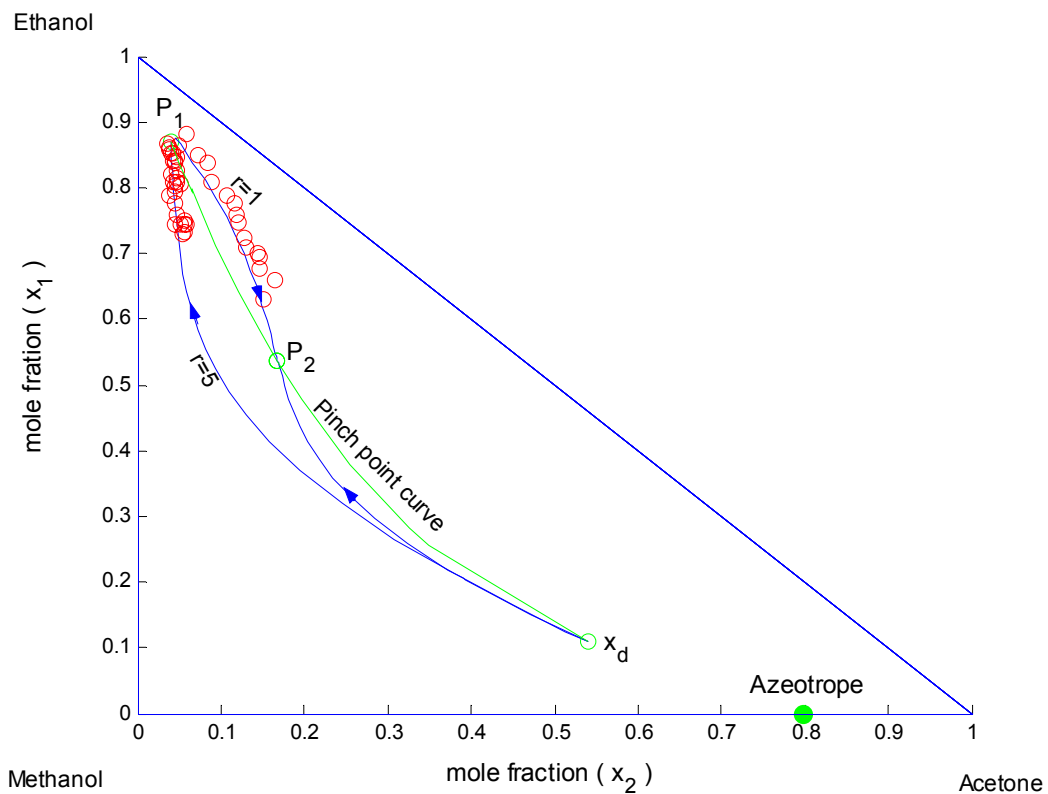


Figure 4.10: Experimental results showing the great extension of the operating leaf with the distillate composition x_d of [0.54, 0.11, 0.35].

The experimental results with a reflux ratio of 5 follow the theoretically simulated results and then reduced to a reflux ratio of 1 as shown in Figure 4.10 above. The experimental results with a reflux ratio of 1 clearly show that the pinch point curve can be crossed and in turn extending the operating leaf, some of the experimental results of Figures 4.9 and 4.10 are tabulated in Appendix C.

4.5 Discussion

It has previously been shown that column profile curves approach pinch curves along the direction of the eigenvector with the smallest eigenvalues. When one operates a column from a fixed feed with different but constant reflux values, this will always approach the pinch point from the same side. However if one effectively goes past the pinch for a low reflux ratio, using a higher reflux ratio then reducing the reflux ratio, one must approach the pinch value along the same eigenvector. The only way to achieve this is approach the pinch point in this direction from the outside. This means approaching the pinch point from outside the operating leaf. It has been shown experimentally using a batch analogue of a column profile that this effect is real and that one can extend the operating leaf in this way.

4.6 Conclusion

We have shown that by having a variable reflux ratio in a column (in particularly going from a high value to a lower value) one can extend the operating leaf. The experimental results revealed that the pinch point curve can be crossed hence expanding the operating leaf. The greatest extension will result by reducing the reflux ratio from a very large reflux to the smallest possible reflux ratio. This would result in the greatest extension of the operating leaf, it was shown theoretically that the extended region can be used to cross the simple distillation boundary. It is also important to mention that column profiles show a different behavior as residue curves. Residue curves move always from low to high temperatures whereas column profiles can be made to run from high to low temperature as well. This might change the way on how to synthesis distillation column sections, as it adds more degree of freedom for the design of distillation columns.

4.7 Nomenclature

- d : Feed addition flow rate (mol/time)
- D : Feed addition flow rate in a continuous distillation column (mol/time)
- dl : Change in liquid level
- dt : Change in time
- dn : Change in number of stages
- dx : Change in liquid composition
- l : Amount of residue in the still (mol/time)
- L : Amount of liquid flow rate in a continuous distillation column (mol/time)
- P_i : Pinch point
- r : Reflux ratio
- t : Time variable
- v : Amount of vapour formed in the still (mol/time)
- V : Amount of vapour formed in a continuous distillation column (mol/time)
- x : Liquid mole fraction
- x_d : Distillate mole fraction
- y* : Vapour mole fraction

4.8 References

1. Castillo, F.J.L. Towler, G.P., Synthesis of homogeneous azeotropic distillation sequences. A thesis submitted to University of Manchester, Institute of Science and Technology, 1997
2. Castillo, F., Thong, D., Tower, G., Homogeneous azeotropic distillation: 1. Design procedure for single-feed column at non- total reflux., *Int. Eng. Chem. Res.*, vol. 37, 1998, pp 987.
3. Chronis, T., "The simple measurement of residue curves and their associated vapour-liquid equilibrium", M.Sc. Thesis , University of Witwatersrand, 1996
4. Chronis, T., Glasser, D., Hildebrandt, D. A simple, reasonable accurate method for measuring residue curves and the associate VLE, *Distillation & Absorption*, 97 edition by R.Darton, *IchemE*, 1, 1997, pp187-196.
5. Doherty, M.F., Perkins, J.D., "On the Dynamics of Distillation Processes, I-VII", *Chem. Eng. Sci.*, 34, 1978
6. Fidkowski, Z., Doherty, M., Malone, M., Feasibility of separation for distillation of non-ideal ternary mixtures, *AIChE Journal*, vol. 39, 1993, pp 1303
7. Hoffmaster, W.R., Hauan, S., "Sectional and overall reachability for systems with s-shaped distillation lines." *AIChE Journal*, vol. 48, 2002, pp 2545-2556,
8. McGregor, C., Hausberger, B., Hildebrandt, D, Glasser, D., "Whats new in multi-component distillation? Residue curve maps: a new tool for distillation column design." *Chem Technology* , 1998, pp 11-17

9. Pollmann, P., Blass, E., Best product of homogeneous azeotropic distillation, Gas. Sep. Purif., vol. 8, 1994, pp 194
10. Safrit, B., T., Westerberg, A.W., “Algorithm for generating the distillation regions for azeotropic multi-component mixtures”, Ind. Eng. Res. Vol. 36, 1997, pp1827-1840.
11. Stanley I. Sandler, Chemical and Engineering Thermodynamics, Second Edition, 1989, pg 240.
12. Stichlmair, J. G.,Herguijuela, J. R., “Separation regions and processes of zeotropic and azeotropic ternary distillation”, AIChE Journal, vol. 38, 1992, pp1523-1535.
13. Tapp, M., Holland, S.T., Hildebrandt, D., Glasser, D., Expanding the operating leaves in distillation column sections by distributed feed addition and sidestream withdrawal.,Accepted for publication in the proceedings of the PSE conference 2004, Kuming, China, (2003).
14. Tapp, M., Kauchali, S., Hausberger, B., Hildebrandt, D., Glasser, D., “An experimental simulation of distillation column concentration profiles using a batch apparatus”, Chem. Eng. Sci., 2003, pg 479-486.
22. Tapp, M., Holland, S., Hildebrandt, D., Glasser, D., Column Profile Maps Part 1.Derivation and Interpretation. Ind.Eng.Chem.Res. Vol. 43, pp364-374, 2004.
23. Venimadhavan, G.,Buzad, G., Doherty, M.F., Malone, M.F., “Effect of kinetics on residue curve maps for reactive distillation”, AIChE Journal, vol. 40, 1994, pp1814-1824 ,

15. Wahnschafft, O.M., Keohler, J.W., Blass, E. and Westerberg, A.W. The product composition regions of single-feed azeotropic distillation columns, *Ind. Eng. Chem. Res.*, 31, 1992, pg 2345-2362,

5 EXPERIMENTAL MEASUREMENT OF THE SADDLE NODE REGION IN A DISTILLATION COLUMN PROFILE MAP BY USING A BATCH APPARATUS.

This paper was published in the Chemical Engineering Research and Design Journal.

Abstract

A simple theoretical method for the evaluation of the separation of mixtures using distillation columns operating at finite reflux, called column profile maps (CPMs), has been developed, Tapp et al (2004). These CPMs are simply transforms of the residue curve maps (RCMs) and are used for sequencing and synthesis of distillation columns. Thus for example the Methanol, Diethyl ether and Benzene system has a low boiling azeotrope between Methanol and Benzene which appears as a saddle point in the RCM. As a result the RCM has two stable nodes and hence two distillation regions divided by a simple distillation boundary. It can be theoretically shown that the transformation of the CPM moves the saddle point that was on the boundary of the mass balance triangle in the RCM into the mass balance triangle of the CPM. Similarly the two stable nodes, corresponding to pure component nodes, in the RCM move out of the mass balance triangle of the CPM.

The CPM of this system was experimentally evaluated to verify that a saddle point node does indeed occur inside the mass balance triangle. The experimental technique uses a semi-batch apparatus and measures the boiling liquid concentration in the still as a function of time, Modise et al (2005). The importance of this is that concentration profiles achieved in the semi-batch still are essentially the same as those of a continuous distillation column section. The experimental measurements showed that there is indeed a saddle point in the CPM.

Key words: Distillation boundary, pinch point curve, column profiles, distillate, azeotropes

5.1 Introduction

Distillation is a proven, versatile and intensively investigated unit operation and plays a major role in many chemical processes. This situation is unlikely to change even in the long term, because alternative unit operations are often neither technically feasible nor commercially competitive. The most important issue in designing a chemical process is feasibility. A design is usually performed by solving a mathematical model of the process which is normally subject to constraints such as nonnegative flow rates and mole fractions, bounds on temperature because of thermal degradation, pressure or on the cost of the design. The worst scenario is that after extensive and lengthy simulation one discovers that the desired specification cannot be met, and significant changes must be made to the flowsheet structure to achieve the process goals, Koehler et al (1995).

In the distillation of non-ideal multicomponent mixtures, there are phenomena that do not occur in ideal distillation, e.g., that finite ratios sometimes lead to a better separation than total reflux. A common practice has been to determine feasible product composition based on the extreme operating conditions of an infinite reflux ratio (Doherty and Calderola, 1985) thus missing out potential opportunities. Examples of exceptions are the work of Petlyuk et al (1978), who not only observed that total reflux boundaries can be crossed but analyzed an example of a highly non ideal mixture to estimate the location of the absolute distillation boundaries. However, the objective of work also seems to have been to show that these boundaries can be reasonably well approximated by residue curve boundaries, and he did not develop a general procedure to establish the range of potential products composition. Nikolaev et al (1979) demonstrated that the location of product composition boundaries for continuous distillation is a function of the reflux ratio. For the determination of product compositions feasible at total reflux one should in principle use so-called distillation line diagram. It turns out that the absolute product composition region is often larger than the region reachable at total reflux and should

be determined using residue curve maps which provide the necessary information on the vapor liquid equilibrium behavior of ternary mixtures. Even in ideal distillation, there are always product compositions that can be obtained from columns operated at finite reflux ratios but not at total reflux. However, the difference between the product compositions attainable at high and at lower reflux is most relevant to azeotropic system with total reflux boundaries that exhibit significant curvature. In such cases, distillation column sequences can be devised which are feasible only due to the possibility of crossing such a boundary in one column operated at finite reflux ratios. The curvature of the residue curve, simply reflects the selectivity with which components modify each others volatilities. Only in the case that total reflux boundaries are straight lines is there no selectivity at all.

In this paper we will show that experimental simulations of distillation column profile maps by using a semi-batch apparatus may also be desirable in the preliminary design of a distillation column.

5.2 Operation Leaves

Feasible conditions for distillation columns are often based on the two extreme operating conditions for a continuous distillation process, minimum and total reflux. Neither condition is practical for operating a distillation column, because an infinite number of stages and intermediate condensers and reboilers are required for minimum reflux while no product is withdrawn at total reflux. However, these limiting conditions traditionally serve as bounds for distillation. Based on these extreme operation limits, graphical approaches can be shown to determine where in composition space a column can operate (King 1980). The composition pathway of a residue curve as a function of dimensionless time (ζ) is given by equation 5.1:

$$\frac{dx}{d\zeta} = x_i - y_i^* \quad 5.1$$

Where, for component i , the vapour composition, y_i^* , and the liquid composition, x_i , are in equilibrium with each other and ζ is the non-linear time dependent variable.

The two bounding operational conditions may be equally impractical, but they are useful in setting bounds or limits on the separation. For a specific separation, operation at total reflux requires the least number of separation stages, but no overhead or bottom product is withdrawn from the column and no feed is introduced into the column as shown in Figure 5.1, see Castillo et al (1998).

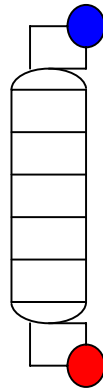


Figure 5.1: Distillation column with no bottoms or distillate withdrawn and no feed

At minimum reflux, the separation is performed using the minimum possible energy at the expense of the number of separation stages, which approaches infinity. Minimum reflux operation is characterized by the existence of a zone in the column of constant composition for all the components King et al (1980). This zone is known as the column pinch. A pinch occurs in a distillation column when, despite adding more stages to the column, the composition profile does not change. This situation corresponds to the solution of the residue equation when the derivative is set equal to zero at any point in the column, i.e

$$\frac{dx}{d\zeta} = 0 \Rightarrow x_i = y_i^* \quad 5.2$$

Distillation columns have been divided into rectifying and stripping sections. Doherty et al (1978) introduced the concept of differential equations as a shortcut design tool to determine the composition profiles along the length of the rectifying and stripping sections in a distillation column. Each section has a differential equation that describes the change of liquid composition along the column section. Let's consider the rectifying section of a distillation column as shown in Figure 5.2.

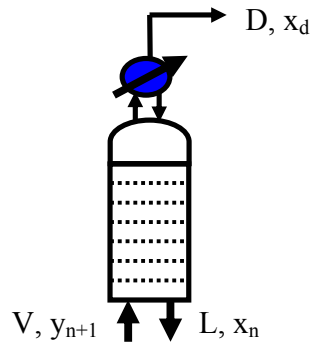


Figure 5.2: The rectifying section of a distillation column

The differential equation describing the rectifying section is:

$$\frac{dx}{dn} = \frac{V}{L} (x_i - y_i^*) + \frac{D}{L} (x_d - x_i) \quad 5.3$$

Where V is the vapor flowrate, L is the liquid flowrate and D is the distillate flowrate.

The stripping section is defined by the following equation:

$$\frac{dx}{dn} = -\frac{V}{L} (x - y^*) - \frac{B}{L} (x_b - x) \quad 5.4$$

Where V is the vapor flowrate, L is the liquid flowrate and B is the bottoms flowrate.

5.2.1 Closed leaves

Wahnschafft et al (1992) showed graphically that the point, where the straight line passing through the product composition is tangential to the residue curve is called a pinch point, see Figure 5.3. The set of pinch points forms a curve that we call the pinch point curve. Pinch point curves describe the minimum reflux condition. The region bounded by the pinch point curve and residue curve is called the operating leaf, see Figure 5.3, a closed leaf in this case Castillo et al (1998).

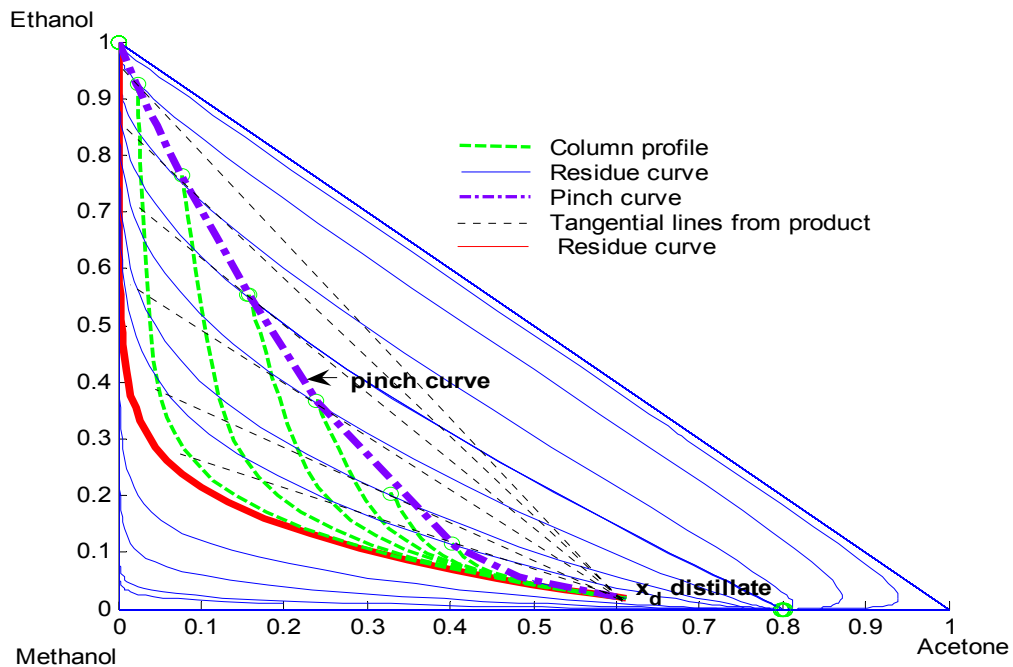


Figure 5.3: Residue curve map with tangential lines from product showing pinch points.

This procedure is based on the principle of finding all feed compositions that will produce a specified product in a column section. Once the operating leaves for the rectifying and stripping section are constructed, separation can quickly be deemed feasible if the regions of both sections overlap one another.

5.2.2 Open leaves

There are however cases where the pinch point curve becomes more complex as shown in Figure 5.4. In this case the pinch point curve consists of two branches. The dark dashed line is tangential to two different residue curves, unlike other lines which are tangential to only one residue curve.

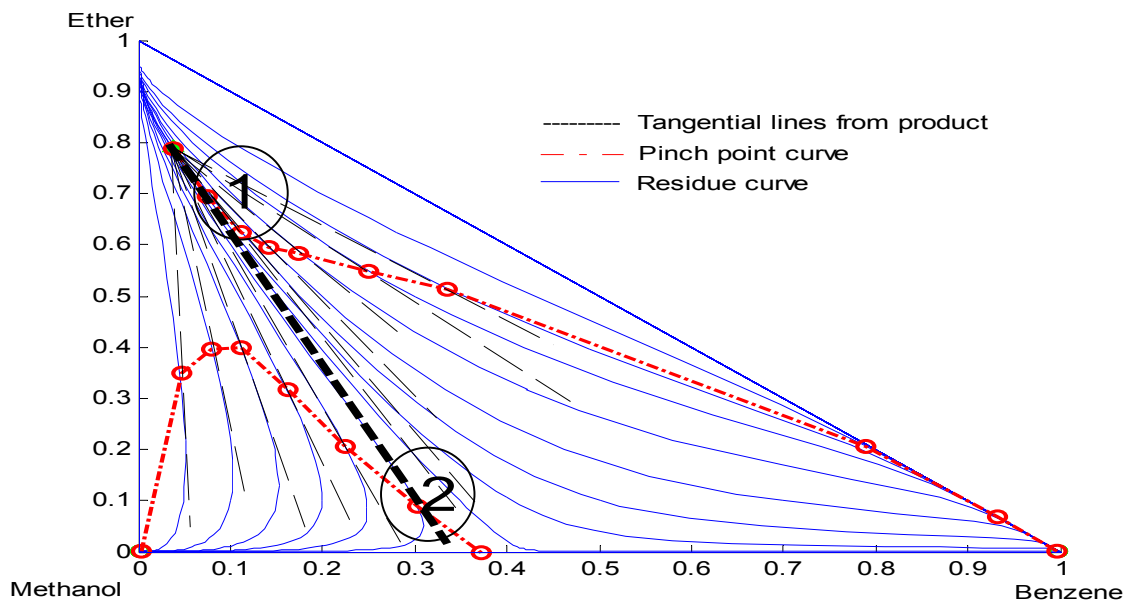


Figure 5.4: A branched pinch point curve.

This line is tangential to a residue curve (at point 1) which is a branch that ends at the pure benzene node and also tangential to a residue curve (at point 2) which is on a branch that ends at pure methanol node as shown in Figure 5.4. This type of behavior was discovered by Castillo et al (1998), who said there exists operating leaves with pinch curves on different sides of a distillation boundary. This type of operation leaf is called an open leaf. The curvature of the distillation boundary is very significant, since the more the distillation boundary is s-shaped the more possibilities of having lines tangential to more than one residue curves. The area in which the distillate x_d product is positioned is also very important, a very small change in the composition might change the direction of the profile. In the case of the open leaf one can get

situations where small changes in parameters can have dramatic effects on the column profile. Thus in Figure 5.5 we can see that for a given distillate value x_d a small change in the reflux ratio can have a dramatic effect on the column profile. The area which is close to the distillation boundary is very sensitive to this because the tangential lines from the product might be tangential to one or two residue curves. Figure 5.6 show profiles with small changes in the initial compositions which result in profiles moving in different directions.

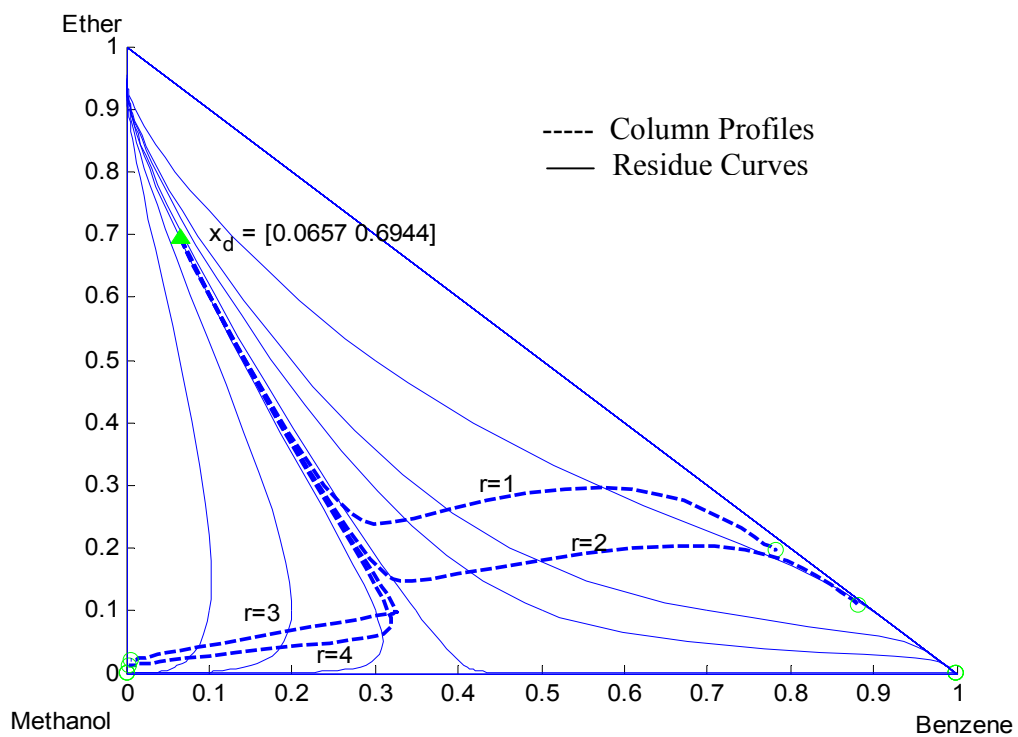


Figure 5.5: An open leaf, showing the column profiles pinching at different distillation regions.

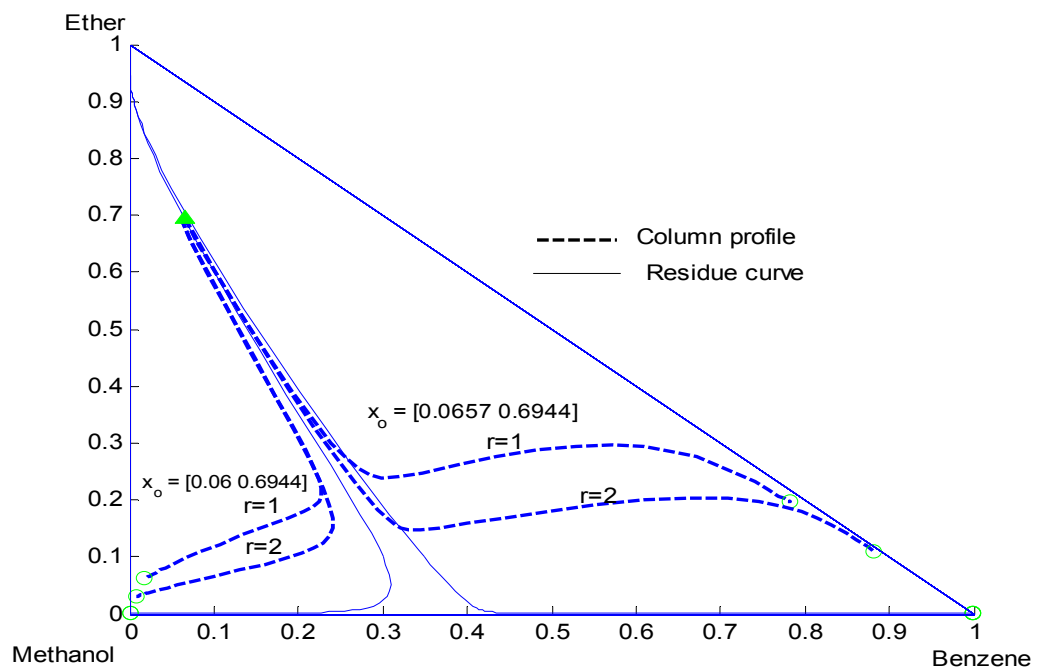


Figure 5.6: A slight change in the composition changes the direction of the column profile.

This could be very important because one may end up with unstable column behavior. The two profiles with the same reflux ratio, same distillate but slightly different initial composition clearly shows this. However it is not very easy to see this unstable behavior in real columns using the residue curve maps (R.C.M.). Nor is it very easy to understand why this should happen from these pictures. A much more instructive way to view this is using the column profile map (C.P.M) Tapp et al (2003). Tapp showed C.P.M. are useful in distillation analysis and synthesis. The liquid profiles correspond to the liquid composition in a section of a continuous distillation column. For this paper we will be looking at the top half of the continuous distillation column, the rectifying section, which is described by the following equation 5.5:

$$\frac{dx_i}{dn} = \frac{r+1}{r}(x_i-y_i) + \frac{1}{r}(x_{i,d}-x_i) \quad 5.5$$

Where, n is number of stages, y , the vapour composition, x , the liquid composition, x_d , distillate composition and r the reflux ratio. These profiles can also be shown to correspond to the liquid composition as it changes with time in a semi-batch apparatus.

Suppose we draw the C.P.M for the Diethyl ether, Methanol and Benzene system using a reflux ratio of 3 and a distillate composition of 6,6 % Benzene, 69,57% Diethyl ether and 23,96% Methanol, as shown in Figure 5.7. We can immediately see that the problem is that we appear to have introduced a saddle point into the space or alternatively we can topologically regard the C.P.M as being a transformed R.C.M in which the stationary point (azeotrope) that was on the mass balance triangle (M.B.T) boundary has been moved into the space.

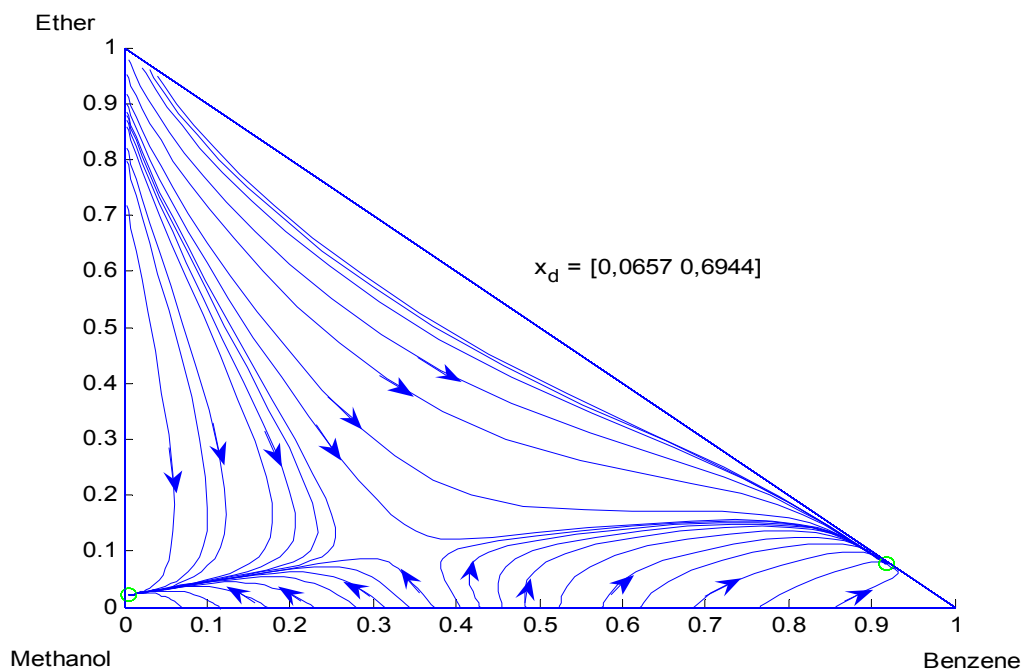


Figure 5.7: Column profile map of Methanol, Diethyl ether and Benzene using a reflux ratio of three ($r=3$) for a rectifying section of distillation column.

It can also be noticed that the whole topology has been shifted, the pure methanol and benzene nodes have also been shifted. The profiles no longer converge at the pure di-ethyl ether node, it seems that they are converging outside the mass balance triangle. This topological interpretation is a very useful way of viewing the C.P.M namely as a movement of the stationary points as the parameters of the system change (in this case the reflux ratio).

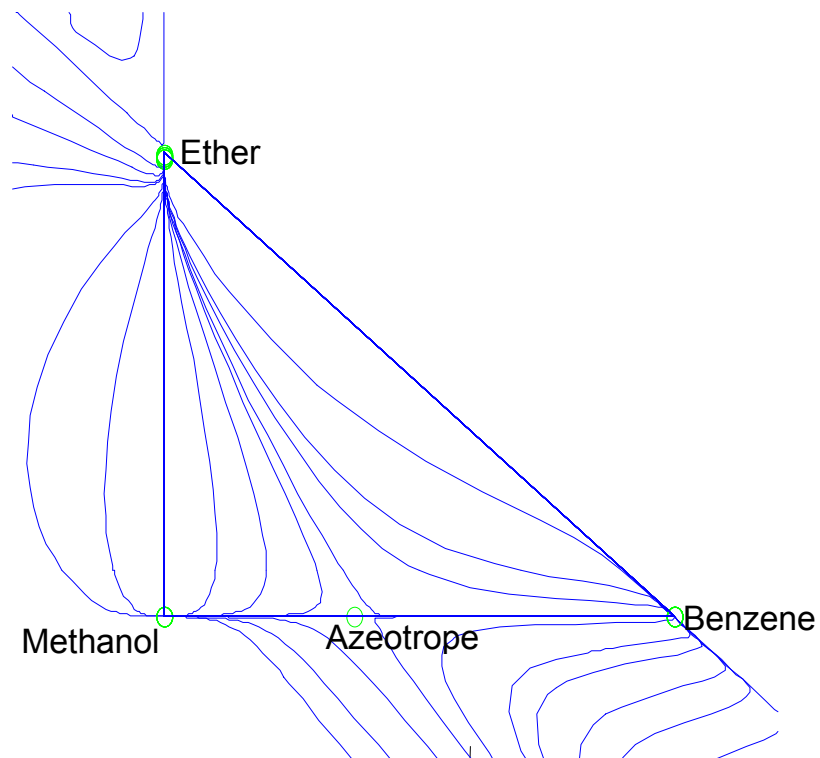


Figure 5.8: The residue curve map of Di-ethyl ether, Methanol and Benzene in full space.

In order to understand the C.P.M, one needs to draw the R.C.M's in the negative space as well, as shown in Figure 5.8. It is clear from Figure 5.8 that the profiles introduced in Figure 5.7 can be viewed as coming from the negative space. One might then reasonably ask the question; how good were the thermodynamic models in the negative space? We of course have no direct method of checking this but if in the system of interest, our predictions of how in the C.P.M's, the stationary points move

related to those in the R.C.M's, are borne out in practice, we will be reasonably happy that we are on the right track. Let us therefore see if we can reproduce the saddle point behavior in Figure 5.7.

5.3 Experiment

In order to measure a column profile map of the rectifying section of the distillation column, an apparatus has been designed in such a way that the column profile composition could be measured during batch or simple boiling. The associated temperature and vapour curve in equilibrium with the liquid residue can also be obtained. This apparatus was first introduced by Chronis et al (1997) to measure residue curves and has been further developed by Tapp et al (2003) to measure column profile maps. The design of the apparatus is based on the fact that material and component balance over a still pot is mathematically identical to the differential equation derived by Doherty (see equation 5.3). For further details see Modise et al (2005).

5.3.1 Experimental setup

There are various components to the experimental set-up as shown in Figure 5.9, the still being the main component. The still was graduated in such a way that the level of the liquid inside the still can be measured and the volume calculated. There are four ports in the still. Two are for the sampling and injection of the feed respectively. The other two were for the thermocouple probe and for keeping the pressure constant by releasing vapour below the oil in a bubbler. The bubbler was also used to measure the rate of vaporisation hence in turn measuring the rate of boiling. A condenser was attached to the other end of the bubbler to capture the vapour from the system. A magnetic stirrer was used for the mixing of the liquid. Boiling stones were placed inside the still to assist nucleation. A HP6890 Hewlett Packard gas chromatograph

was used for the analysis. The still was immersed in a water bath. The purpose of the bath was to maintain an even heat distribution and also to ensure that the liquid residue would be at its bubble point. In order to maintain the bubble point temperature, the water bath temperature must be increase continuously to maintain the temperature driving force (ΔT of 6°C) between the contents of the still and the water bath.

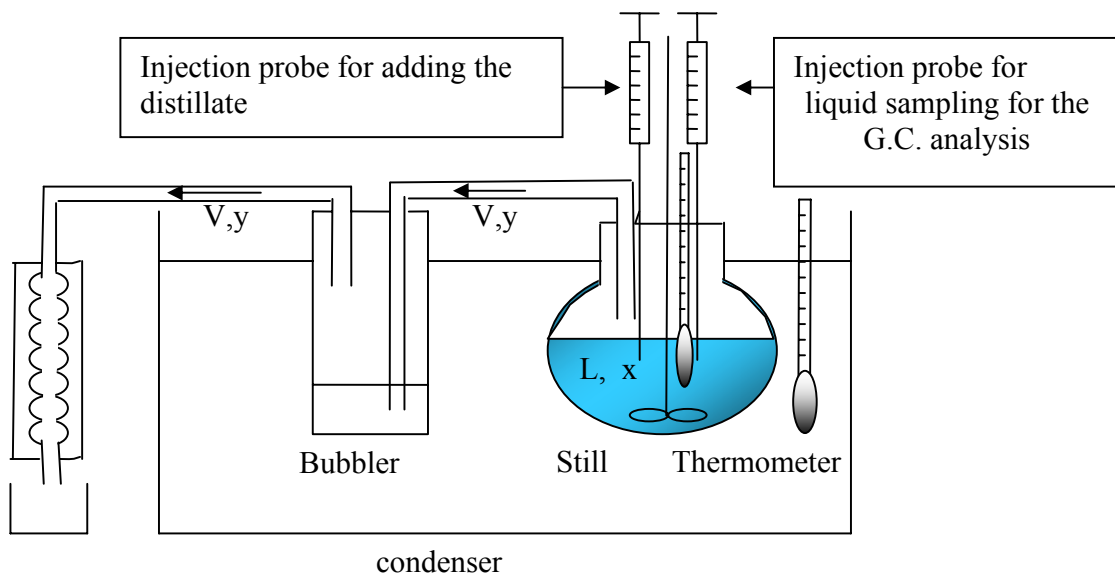


Figure 5.9: Experimental setup with still pot being the main component.

5.3.2 Experimental procedure

Numerical experiments were first performed to simulate the rectifying section of a distillation column that would separate Methanol, Diethyl ether and Benzene. A bulk solution (about 200ml) of known composition of Methanol, Diethyl ether and Benzene was prepared. A small quantity of this distillate was kept in a fridge to be used as a feed solution while the rest of the distillate was placed in the still. The still was placed inside a hot water bath. The level of liquid in the still was continuously recorded during the experiment. It can be shown by material balance around the still

that reflux ratio r and the distillate flow rate d can be determined as follows, see Modise et al (2005) for the derivation:

$$d = \frac{v}{r + 1} \quad 5.6$$

For convenience the distillate, d , is added over discrete time intervals. The vapour flow-rate was determined by the following mass balance equation:

$$v = d - \frac{dl}{dt} \quad 5.7$$

The feed addition rate was then determined by the ratio of the level in the still and the required reflux ratio.

$$d = -\frac{dl}{r \cdot dt} \quad 5.8$$

As described above in these experiments the feed material was added in discrete amounts rather than continuously. This was done in the following way: The liquid level was observed to change by an amount dl in a time interval dt . Using equation 5.8 one can say provided the value of dl is not too large that:

$$\Delta d = d \cdot dt = -\frac{dl}{r} \quad 5.9$$

Where Δd is the amount to be added at the end of the time interval dt when the level has fallen by an amount dl . For our experiments we used a value of dl of 6.3 ml which happened in a time interval (dt) of about 5 min. For the initial experiments a reflux ratio was chosen for each run and kept constant throughout the run; this made it possible to calculate the amount of distillate that must be added after each time interval. Liquid samples were drawn at regular intervals and analyzed using the gas chromatograph.

The runs were aborted when the liquid level in the still was below the 20 ml mark in the still, since it was found that after this inaccurate results were obtained.

For the experimental runs to produce the column profile maps the procedure was exactly the same as that described above except that the initial composition x_0 of the

material in the still could be different from that of the distillate composition x_d . If this was the case then a sample of solution of the required x_d was also prepared.

5.4 Results

Once we have obtained the results we can plot concentration versus time graphs.

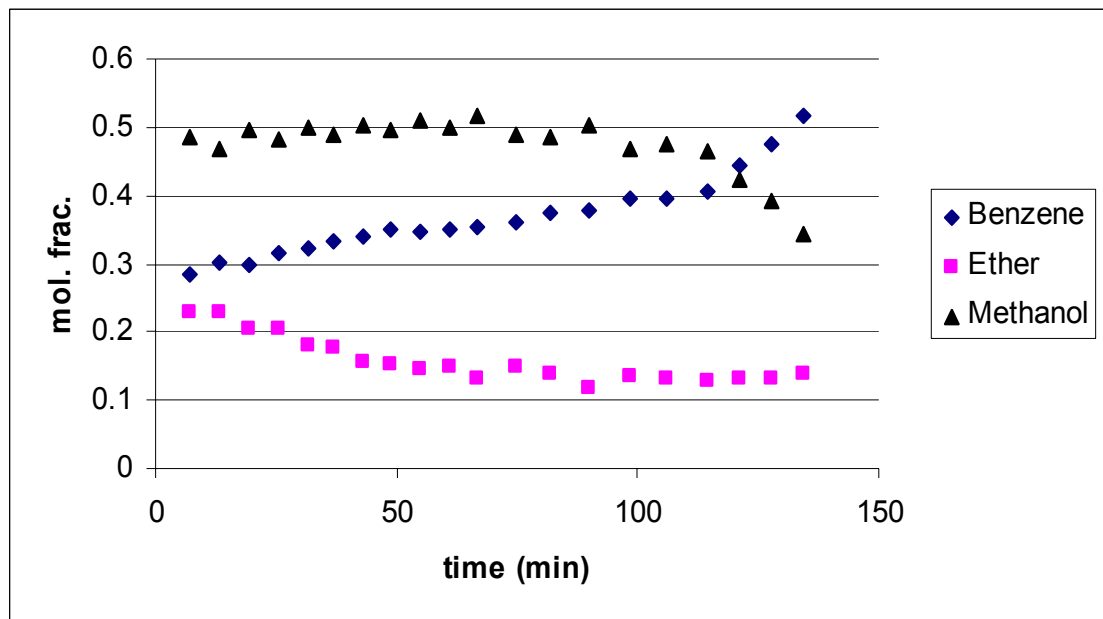


Figure 5.10: Measured experimental profile. Profile 1 in Figure 5.13, at 0.83 bars

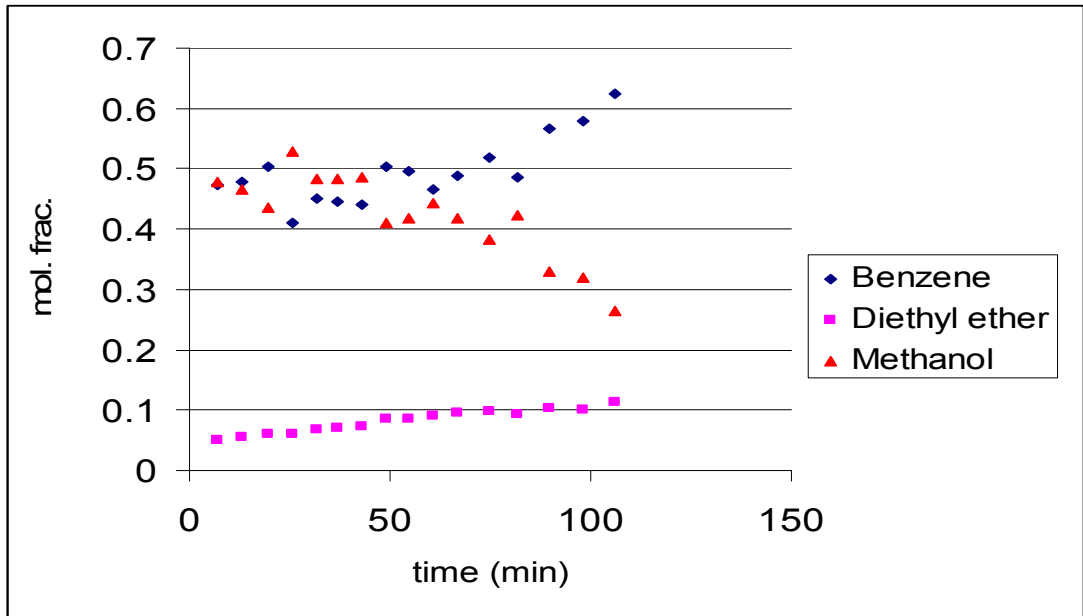


Figure 5.11: Measured experimental profile. Profile 2 in Figure 5.13, at 0.83 bars

We can see that in both profiles in Figure 5.10 and 5.11 concentration remains fairly constant for some time and suddenly deviate near the end. Furthermore particularly in Figure 5.11 one sees that the apparent accuracy of the benzene and methanol analysis is very poor while this is not the case in Figure 5.10. From these figures it is not easy to understand why this is the case. The only thing to note is that the profile of these two components is fairly constant (pinching) over this time period. We will examine the reason for this later. The other point to note is that the time variable in the batch still is related to the number of stages in a continuous column so that our remark above about pinching is consistent with normal column operation.

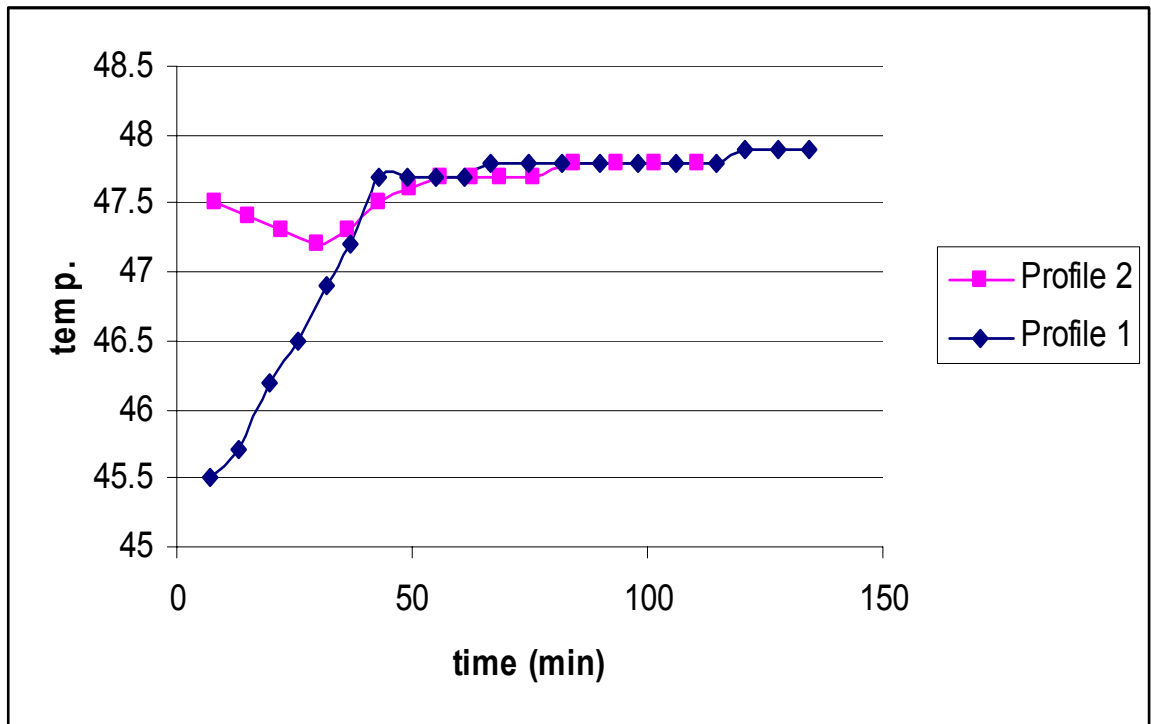


Figure 5.12: The temperature profile of Profiles 1 and 2 versus time, at 0.83 bars

Figure 5.12 shows that the temperature profiles in column profile maps can also be quite complicated, as compared to those of residue curves. For profile 1, the temperature of the profile is always increasing while the temperature profile of profile 2 start at a higher temperature and decreases to a minimum temperature and then increases again to a maximum. Again we need to note that these curves are equivalent to what we get in a real column profile and thus while residue curves have monotonic temperature profiles this is not necessary in column profiles. Let us rather plot these profiles on a ternary diagram, this is done in Figure 5.13.

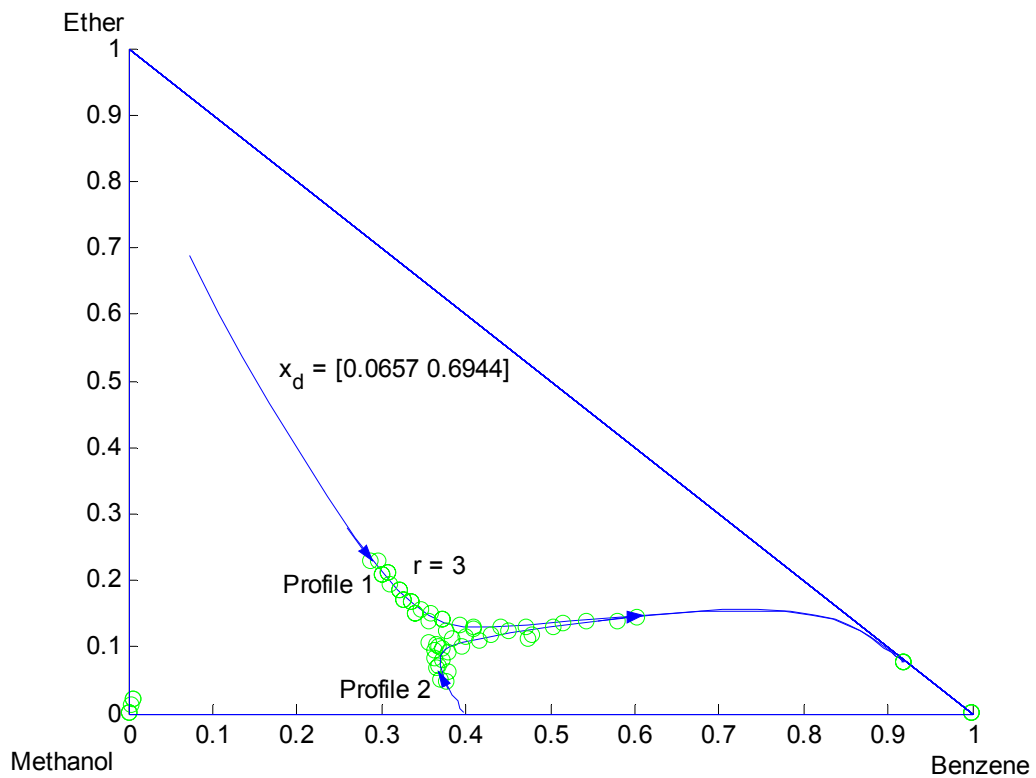


Figure 5.13: Column profiles with the reflux of 3 with the distillate composition of 0.0657 benzene and 0.6944 of Diethyl ether.

Figure 5.13 shows two column profiles starting at different initial points and terminating virtually at the same pinch point. Both profiles were also simulated at the reflux ratio of 3. Profile 1 has reasonably smooth curvature around the saddle point region as compared to profile 2 which has a sharp curvature around the saddle point region. We can speculate that the large scatter in the results in Figure 5.11 is because of the sharp curvature in the column profile curve for Profile 2. Many more results were taken and are shown in Figure 5.14. This was done to more accurately, experimentally delineate the saddle point.

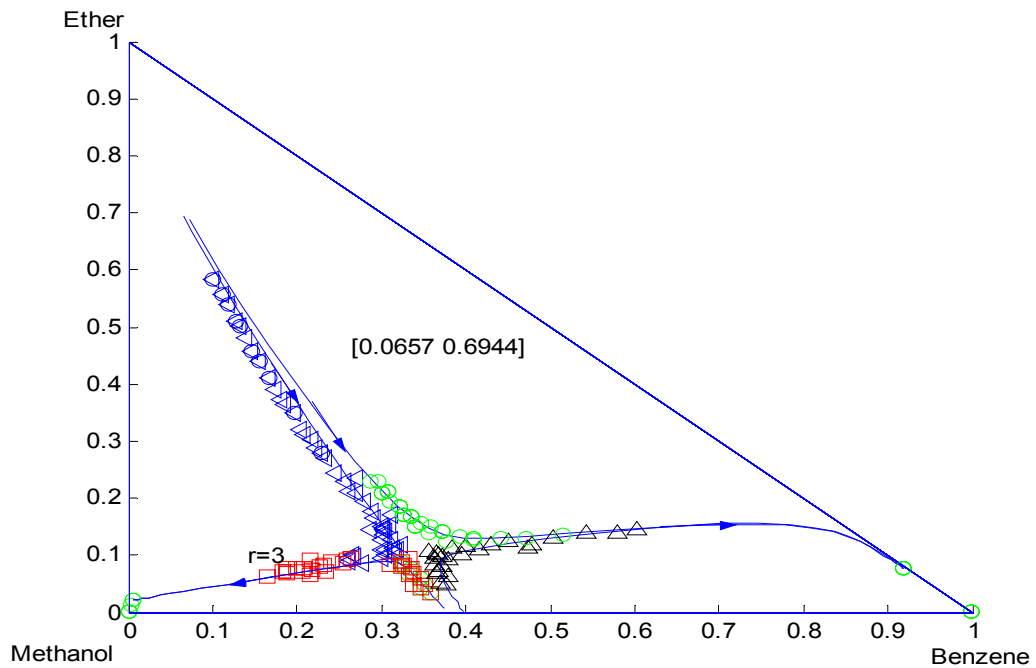


Figure 5.14: Column profile map with a reflux ratio of three, starting with different initial points with a fixed distillate composition $x_d = [0.0657 \ 0.6944]$

Figure 5.14 represents experimental results obtained for a column profile map with a reflux ratio of three, but different initial points. The solid lines represent the theoretical results while the points represent the experimental results. The NRTL model, see Sandler et al (1999), was used to simulate the theoretical results. The parameters of the NRTL model were obtained from Aspen plus[®] 13.2 and they are tabulated below, table 5.1.

Table 5.5.1: NRTL parameters for the Ethyl Ether, Methanol and benzene system.

Component i	Ether	Ether	Methanol
Component j	Methanol	Benzene	Benzene
Temperature units	K	K	K
Source	VLE-IG	VLE-IG	VLE-IG
A _{ij}	-5.2556	0.0576	-1.7086
A _{ji}	7.0779	-0.4759	11.5801
B _{ij}	1893.486	94.4718	892.2404
B _{ji}	-1999.4722	27.468	-3282.554
C _{ij}	0.3	0.3	0.4

It can be clearly seen that relative to the RCM the CPM has the saddle point in the MBT. Its presence could cause major problems in the design and operation of a distillation column that has column profiles in this region.

5.5 Conclusion

The experimental results in Figure 5.14 clearly show that one can effectively map the saddle point in C.P.M space. Furthermore they also clearly show the sensitivity of the results to the initial value, as one would expect close to a saddle point. It was also noticed that the curvature of the distillation boundary play a major role in the determination which side of the distillation region, the column profile will pinch. These results are also very interesting from a more fundamental point of view. Because the results are so sensitive to the position of the saddle point, these measurements are an extremely good test of the underlying thermodynamics close to the saddle point. Because in the batch apparatus we can effectively change the position of the saddle point by changing the effective reflux ratio we are in a position to test the underlying thermodynamics at different points in the space. This could prove a useful tool to discriminate among different thermodynamic models and the parameters used in these models. This result shows the value of looking at the residue curve in negative space, in that one could then predict that the saddle point would be moved into the real space (positive mole fractions) and so we could predict the likely

unstable behavior from the residue curve map alone. Furthermore because time variable is related to the number of stages in a continuous column we also get information about pinch regions in our columns.

5.6 Nomenclature

A_{ij}	:	Interaction parameters
B	:	Bottoms flow rate
B_{ij}	:	Interaction parameters
C_{ij}	:	Interaction parameters
d	:	Feed addition flow rate (mol/time)
D	:	Distillate flow rate (mol/time)
dx	:	Change in composition
dt	:	Change in time
dl	:	Change in liquid level
dn	:	Change in number of stages
l	:	Amount of residue in the still (mol)
L	:	Vapour flow rate (mol/time)
n	:	Tray position
P	:	System pressure (Pa)
P_i^{sat}	:	Vapour pressure (Pa)
r	:	Reflux ratio
s	:	Reboil ratio
t	:	Time variable
v	:	Amount of vapour formed (mol/time)
x	:	Liquid mole fraction
x_b	:	Bottoms composition
x_d	:	Distillate flow rate (mol/time)
y	:	Vapour mole fraction
γ	:	Liquid phase activity coefficient
ζ	:	Time dependent variable

5.7 References

1. Castillo, F., Thong, Y., Towler, G., "Homogeneous azeotropic distillation. 1. Design procedure for single-feed columns at nontotal reflux." *Ind. Eng. Chem. Res.*, 1998, vol. 37, Pg 987-997
2. Chronis, T., Glasser, D., Hildebrandt, D., "A simple, reasonable accurate method for measuring residue curves and the associate VLE", *Distillation & Absorption*, 97 edition by R.Darton, IChemE, 1, pp187-196, 1997
3. Doherty, M.F.; Calderola, G.A., "Design and Synthesis of Homogeneous Azeotropic Distillation. 3. The Sequence of Columns for Azeotropic and Extractive Distillation." *Ind. Eng. Chem. Fundam.*, 1985, vol. 24, pg 474-485.
4. Doherty, M.F., Perkins, J.D., "On the Dynamics of Distillation Processes, I-VII", *Chem. Eng. Sci.*, 34, 1978
5. King, C., *Separation processes*, 2nd ed., McGraw-Hill Inc., New York, 1980
6. Koehler, J., Poellmann, P., Blass, E., "A review on minimum energy calculations for ideal and non ideal distillation." *Ind. Eng. Chem. Res.*, 1995, vol. 34, 1003
7. Modise, T., Tapp, M., Hildebrandt, D., Glasser, D., "Can the operating leaves of a distillation column really be expanded?" Submitted to *Ind. Eng. Chem. Res.*, 2005, vol. 44, Pg 7511-7519
8. Nikolaev, N.S.; Kiva, V.N.; Mozzhukhin, A., S., Serafimov, L.A.; Goloborodkin, S.I., "Utilization of functional operation for determining the region of continuous rectification." *Theor.Found. Chem. Eng.*, 1979, vol. 13, pg 418-423
9. Tapp, M., Kauchali, S., Hausberger, B., Hildebrandt, D., Glasser, D., "An experimental simulation of distillation column concentration profiles using a batch apparatus", *Chem. Eng. Sci.*, 2003, vol. 58, pg 479-486,
10. Tapp, M., Simon T. Holland, Hildebrandt, D., Glasser, D., "Column profile maps. 1. Derivation and Interpretation", *Ind. Eng. Chem. Res.*, 2004, vol. 43, pg 364-374.

11. Sandler, S.I., "Chemical Engineering Thermodynamics" 1999, John Wiley & Sons, New Jersey
12. Petlyuk, F. B.; "Rectification of Zeotropic, Azeotropic , and Continuous Mixtures in Simple and Complex Infinite Columns with Finite reflux." Theor. Found. Chem. Eng., 1978, vol.12, pg. 671-678
13. Wahnschafft, O., Koehler, J., Blass, E., Westerberg, A., "The product composition regions of single-feed azeotropic distillation columns" Ind. Eng. Chem. Res., 1992, vol. 31, Pg 2345-2361

6 USING DISTILLATION COLUMN PROFILE MAPS TO IDENTIFY SUITABLE THERMODYNAMIC MODEL FOR COMPLEX SYSTEMS.

This paper was presented at the annual AIChE conference, San Francisco, California, Nov. 12-17, 2006.

Abstract

Proper selection of thermodynamic models is absolutely necessary as a starting point for accurate process simulation. A process that is otherwise fully optimized in terms of equipment selection, configuration, and operation can be rendered essentially worthless if the simulation is based on inaccurate thermodynamic models. Column Profile Maps (CPMs) are linear transforms of the residue curve maps. In this paper we will show how Column Profile Maps (CPMS) can be used to discriminate between thermodynamic models for complex systems by considering a ternary example. The ethanol, water and ethyl acetate system is a very complicated system because it has a ternary azeotrope and liquid-liquid equilibrium envelope. The composition of the ternary azeotrope is very difficult to predict or measure since it is very close to the liquid-liquid envelope. Furzer et al (2001) required new UNIFAC vapour-liquid equilibrium parameters because with the known parameters, he failed to calculate the composition of the ternary azeotrope correctly.

In this paper we will show the discrepancy between two thermodynamic models, namely UNIQUAC and NRTL, which predict different compositions for the ternary azeotrope even though the predicted residue curve maps are very similar. It would therefore be very difficult to use VLE data measured at compositions other than the ternary azeotrope to discriminate between the two models.

We will show that the predicted topology of the column profiles are quite different for the two thermodynamic models. We have developed an experimental apparatus

and method to measure CPMs (Tapp et al, 2004). We were able to measure a CPM for this system and then use the experimentally measured CPM to identify which one of the two thermodynamic models agrees with the experimental simulation. In this way we are able to test thermodynamic models and discriminate between them more quickly and easily than using conventional methods.

6.1 Introduction

The Ethyl Acetate, Ethanol and Water system is not a well known system. This system has been studied by several researchers in order to find suitable interaction parameters for different thermodynamic models. Furzer et al (2001) used a single-stage, multicomponent flash program using the UNIFAC Vapor-liquid equilibrium interaction parameters, he failed to find the ternary azeotrope. Thus the homogeneous ternary azeotrope in the ethyl acetate, ethanol and water system could not be predicted by the use of the UNIFAC VLE interaction parameters. Furthermore when the total reflux distillation program was run with the UNIFAC VLE parameters, discrete distillation lines were generated which do not terminate at the ternary homogeneous azeotrope. The generation of additional discrete distillation lines using UNIFAC VLE interaction parameters could be expected to generate low-quality process simulation results, which would be unsatisfactory for chemical engineering design. Furzer collected a wide range of experimental VLE data on the ethyl acetate, ethanol and water system to determine a new set of UNIFAC VLE interaction parameters. A single-stage, multicomponent flash program converged accurately of the ternary homogeneous azeotrope with the new UNIFAC VLE interaction parameters.

Naveed Aslam et al (2006) examined the sensitivity of activity coefficient parameters and system variables on the prediction of azeotropes in multicomponent mixtures. The approach provides a systematic basis to adjust the parameters, which were based

on binary phase equilibrium information in such a way that error associated with extrapolating the parameters based upon binary information to predict the ternary and higher order azeotropic points is minimized if not eliminated.

For highly non-ideal liquid phase behaviour, particularly with the formation of azeotropes and multiple azeotropes, there is a need to use a predictive model for the liquid phase activity coefficient. Typical models which have been widely used in literature include NRTL, UNIQUAC and the UNIFAC models. The variation in product predicted composition is very important in designing multicomponent distillation columns.

6.2 Ideal Systems

The simplest model for systems involving two or more components is the ideal mixture in which the chemical potential of every component is a linear function of the logarithm of its mole fraction according to the following equation:

$$\mu_i(T, P, x) = \mu_i^0(T, P) + RT \ln x_i \quad 6.1$$

where μ_i^0 is the chemical potential of pure component i at temperature T and pressure P of the mixture. The equilibrium relation between an ideal liquid and a perfect gas mixture is given by the following equation:

$$\mu_i^{0L} + RT \ln x_i = \mu_i^{PG} + RT \ln \frac{P}{P^*} + RT \ln y_i \quad 6.2$$

Where μ_i^{0L} is the Gibbs energy per mole of pure liquid i at temperature and pressure of the mixture, and μ_i^{PG} depends only on the temperature. Rearranging equation 6.2 to:

$$\frac{Py_i}{x_i} = P^* \exp \frac{\mu_i^{0L} - \mu_i^{PG}}{RT} \quad 6.3$$

In general the exponential on the right-hand side is strongly dependent on the temperature and weakly dependent on the pressure. If we neglect the weak pressure dependence and let $x_i, y_i \rightarrow 1$ at constant temperature, the pressure P must change and approach the saturated vapor pressure of pure component i , $P_i^{sat}(T)$ for all compositions, which leads to the equilibrium relation or Raoult's law:

$$y_i = \frac{P_i^{sat}(T)}{P} x_i \quad 6.4$$

The Raoult's law enables us to calculate the phase equilibrium behavior of certain mixtures using only pure component physical properties. The pure component saturated vapor pressure is calculated from the Antoine equation 6.5:

$$\ln P_i^{vap} = A - \frac{B}{T + C} \quad 6.5$$

Where A, B, C are the Antoine coefficients and T is the temperature.

6.3 Non-ideal system

Very few mixtures are ideal mixtures, most mixtures are non-ideal. The chemical potential of non-ideal mixtures are more complex than those of ideal mixtures. The chemical potential of each component in a real mixture is given by the following equation 6.6:

$$\mu_i^L(T, P, x) = \mu_i^0(T, P) + RT \ln x_i \gamma_i \quad 6.6$$

where μ_i^{0L} is again the chemical potential of pure liquid i at the temperature and pressure of the mixture and γ_i is a correction factor, called the activity coefficient of component i, which depends on temperature, pressure and composition of the liquid. The equilibrium relation for a non-ideal liquid mixture is given by the following equation 6.7:

$$y_i(x) = \frac{\gamma_i x_i P_i^{vap}}{P_{tot}} \quad 6.7$$

Where x_i is the liquid composition, γ_i is the activity coefficient, P_{tot} is the total pressure of the system; P_i^{vap} is the vapor pressure for each component. It is clear that the activity coefficient for ideal mixture is one; the activity coefficient for non-ideal mixtures can be calculated using thermodynamic models. For this paper we will discuss the NRTL and UNIQUAC models, Sandler et al (1999).

6.3.1 The NRTL model

In order for us to calculate the activity coefficient γ_i we need to use the thermodynamic models, the NRTL and UNIQUAC models. The activity coefficient γ_i for the NRTL model is defined by the following equation 6.8:

$$\gamma_i = \exp \left[\frac{\sum_{j=1} \tau_{ji} G_{ji} x_j}{\sum_{j=1} G_{ji} x_j} + \sum_{j=1} \frac{x_j G_{ij}}{\sum_{k=1} x_k G_{kj}} \left(\tau_{ij} - \frac{\sum_{k=1} x_k \tau_{kj} G_{kj}}{\sum_{k=1} x_k G_{kj}} \right) \right] \quad 6.8$$

The important feature of this equation is that all the parameters that appear can be determined from activity coefficient data for binary mixtures. That is, by correlating

activity coefficient data for the species 1-species 2 mixture using the NRTL model, the 1-2 parameters can be determined. Similarly, from data for species 2-species 3 and species 1-species 3 binary mixtures, the 2-3 and 1-3 parameters can be found. One should keep in mind that this ability to predict multicomponent behavior from data on binary mixtures is not an exact result, but rather arises from the assumptions made or the models used.

6.3.2 The Uniquac model

We will now consider the UNIQUAC activity coefficient equation, the model of Abrams and Prausnitz (Sandler, 1999). This model, based on statistical mechanical theory, allows local composition to result from both the size and energy differences between the molecules in the mixture. The result is the expression

$$\frac{G^{ex}}{RT} = \frac{G^{ex}(combinatorial)}{RT} + \frac{G^{ex}(residual)}{RT} \quad 6.9$$

Where the first term accounts for molecular size and shape differences, and the second term accounts largely for energy differences. These terms, in multicomponent form, are given by:

$$\frac{G^{ex}(combinatorial)}{RT} = \sum_i x_i \ln \frac{\phi_i}{x_i} + \frac{z}{2} \sum_i x_i q_i \ln \frac{\theta_i}{\phi_i} \quad 6.10$$

$$\frac{G^{ex}(residual)}{RT} = - \sum_i q_i x_i \ln \left(\sum_j \theta_j \tau_{ji} \right) \quad 6.11$$

Where q_i is the surface area parameter for species i , θ_i is the fractional area for species i , ϕ_i is the segment or volume fraction of the species and

$$\tau_{ij} = \exp\left[-\frac{(A_{ij} - A_{jj})}{RT}\right] \quad 6.12$$

With A_{ij} being the average interaction energy for a species i-species j interaction and z being the average coordination number, usually taken to be 10. Combining all the equations 6.9 to 6.11 to give the following equations:

$$\ln \gamma_i = \ln \gamma_i(\text{combinatorial}) + \ln \gamma_i(\text{residual}) \quad 6.13$$

$$\ln \gamma_i(\text{combinatorial}) = \ln \frac{\phi_i}{x_i} + \frac{z}{2} q_i \ln \frac{\theta_i}{\phi_i} + l_i - \frac{\phi_i}{x_i} \sum_j x_j l_j \quad 6.14$$

$$\ln \gamma_i(\text{residual}) = q_i \left[1 - \ln \left(\sum_j \theta_j \tau_{ji} \right) - \sum_j \frac{\theta_j \tau_{ij}}{\sum_k \theta_k \tau_{kj}} \right] \quad 6.15$$

With $l_i = \frac{z(r_i - q_i)}{2} - (r_i - 1)$. Since the size and surface are parameters r_i and q_i can be evaluated from molecular structure information, the UNIQUAC equation contains only two adjustable parameters, τ_{12} and τ_{21} (or, equivalently, $A_{12} - A_{22}$ and $A_{21} - A_{11}$) for each binary pair. Thus, the likes of the NRTL equation, it is a two-parameter activity coefficient model. It does have a better theoretical basis than the other model, and it is somewhat more complicated. The UNIQUAC model requires only two adjustable parameters per binary. This differs from NRTL model which utilizes a third parameter (α) to account for non-randomness. The disadvantage of these method is that binary pair interaction are required, making the parameters for a mixture of more than three or more components difficult to obtain. This problem is removed by the contribution approach because the molecules are broken into groups, and these groups are assigned the interaction parameters. The advantage of this is that a large

number of components can be represented by relatively few groups. The system under study in this paper, Water, Ethanol and Ethyl Acetate, is a highly non-ideal liquid system which provides three binary azeotropes and a ternary low boiling azeotrope, Cairns et al (1988).

6.4 Binary Vapor-Liquid Equilibrium

For this paper we will be looking at the Ethyl acetate, Ethanol and Water system. The first binary VLE diagram is between Ethanol and Water as illustrated in Figure 6.1 below. The total pressure used for the system was taken as 0.83 bars for all the calculations in this paper.

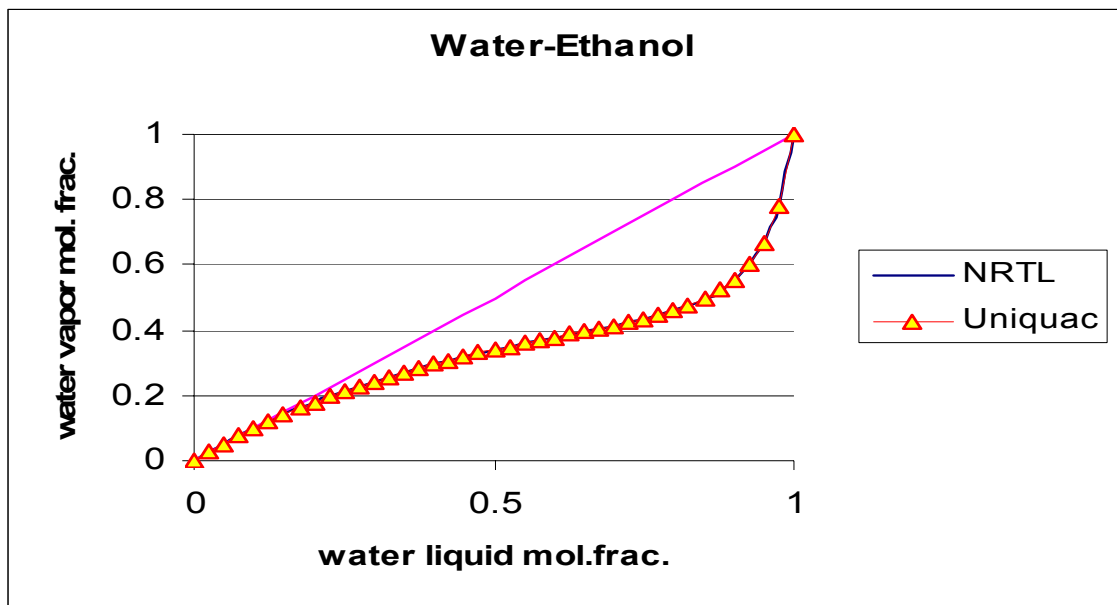


Figure 6.1: Comparison of predicted binary VLE for Water-Ethanol system using the UNIQUAC and NRTL models at a total Pressure of 0,83 bars.

Figure 6.1 shows the binary VLE diagram between the Ethanol-Water system. The VLE has been predicted using both the NRTL and UNIQUAC models and it can be seen that there is not much of a difference between the predictions of the two models..

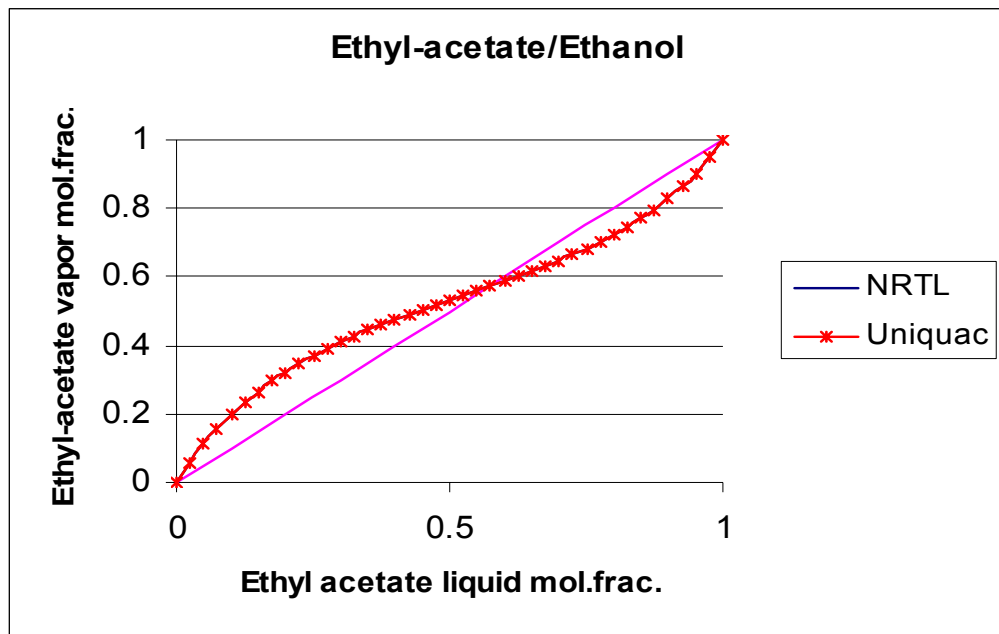


Figure 6.2: Comparison of predicted binary VLE diagram for Ethyl-acetate-Ethanol system using the UNIQUAC and NRTL models at a total Pressure of 0,83 bars.

Similarly we see in Figure 6.2 that the VLE predictions of the two models also agree for the Ethyl-acetate–Ethanol system.

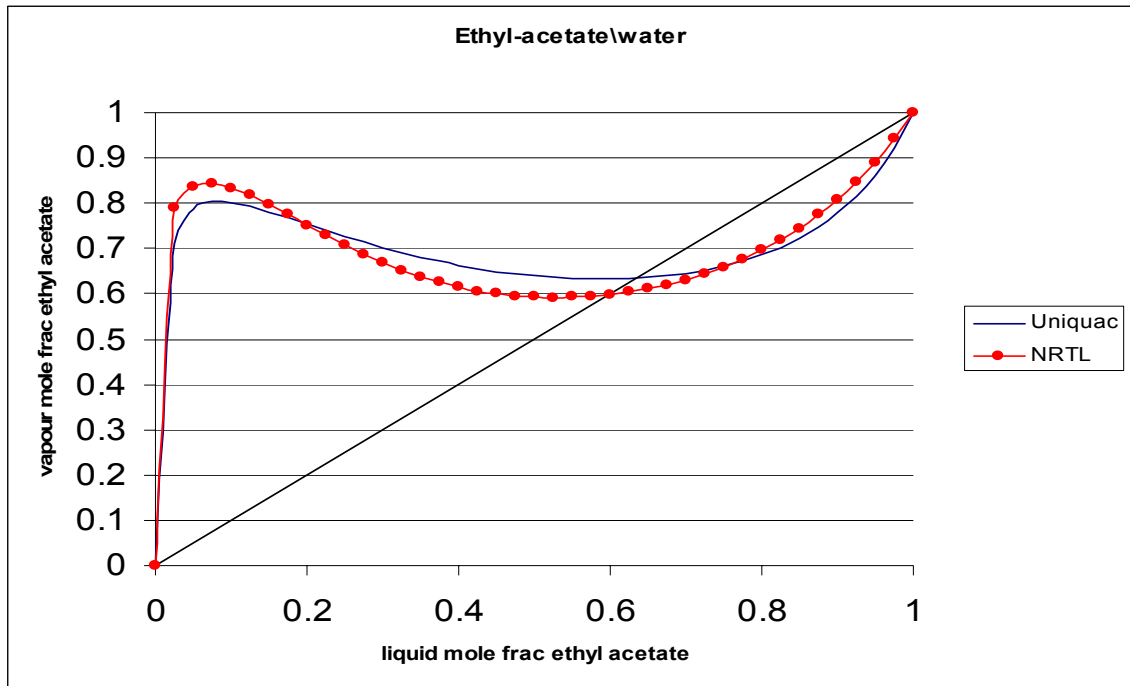


Figure 6.3: Comparison of prediction binary VLE for Water-Ethyl acetate system using the UNIQUAC and NRTL models at a total Pressure of 0,83 bars.

Figure 6.3 compares the predicted VLE for the water-ethyl acetate system. The predictions of the two thermodynamic models, i.e. the NRTL and UNIQUAC models, do not in this agree, and in particular the predicted composition of the binary azeotrope is different. Between about 21% and 78% of ethyl acetate a liquid-liquid equilibrium is predicted and the ternary azeotrope lies in this region.

All the above profiles have been simulated using Aspen plus ® 13.2 simulation program. The binary interaction parameters used for the two models have been tabulated in Table 6.1 and Table 6.2, these parameters were obtained from Aspen plus ® 13.2 .

Table 6.1: Binary interaction parameters for NRTL model

Component i	Ethyl Acetate	Ethyl Acetate	Water
Component j	Water	Ethanol	Ethanol
A _{ij}	-3.7198	0	0
A _{ji}	9.4632	0	0
B _{ij}	1286.1383	95.0457	670.4442
B _{ji}	-1705.683	216.3048	-55.1698
C _{ij}	0.2	0.3	0.3031

Table 6.2: Binary interaction parameter for UNIQUAC model

Component i	Water	Water	Ethyl Acetate
Component j	Ethyl Acetate	Ethanol	Ethanol
A _{ij}	0	0	0
A _{ji}	0	0	0
B _{ij}	-79.477	-116.7512	-195.6135
B _{ji}	-405.68	-25.6061	37.2172

We have looked at the binary VLE diagrams for the Ethyl Acetate, Water and Ethanol system. We now look at the residue curve map of this system.

6.5 Residue Curves

Virtually every chemical plant has a separation unit to recover products, by-products, and unreacted raw materials. Although many new separation techniques are being developed, distillation remains the method of choice, especially for the large-scale separation of non-ideal mixtures Van Dongen et al (1985). For well behaved non azeotropic mixtures, the boiling point of the pure component is enough to establish what splits are feasible, that is, to determine the top and bottom products of a

distillation column. Because the volatility order of the component does not change with composition, it is always possible to design a column that performs the split, provided that enough trays and reflux are used. If the mixture forms azeotropes, then the volatility order changes with composition. Under these circumstances, which components will be in the top product and which will be in the bottom product depend on the feed composition.

Establishing the feasibility of a proposed multicomponent separation becomes difficult, Castillo et al (1998). An efficient conceptual design step requires efficient and reliable tools that require minimum information. One of the most widely used conceptual tools is Residue Curve Maps that are used for conceptual design of non-ideal distillation separation sequences. Residue curves are the most mature concept process design tool and are part of almost all the available design packages. Reliability of residue curves, as a conceptual design tool, depends of the accuracy of the model representing the phase equilibrium and algorithm used for prediction of thermodynamic landmarks, such as azeotropes, Aslam et al (2006).

Through the separation of the residue curve map, many years later, several Russian scientist analyzed the composition profiles in multicomponent distillation columns in the vicinity of azeotropes and pure species. Bushmakina and Kish et al (1957) studied ternary mixture, while Zharov et al (1967) extended their analysis to quaternary mixtures and multicomponent systems, in general. In the 1985, Van Dongen and Doherty introduced the concept of nonlinear autonomous ordinary differential equations as a shortcut design tool to determine the composition profile along the length of a distillation column. The differential approximation models the liquid phase composition profile in both the rectifying and the stripping sections of the column. (Widagdo and Seider, 1996). The set of differential equations describing the simple distillation process is identical to the one for the concentration profiles of packed columns operated at infinite reflux when the mass transfer coefficient is unity. Van Dongen and Doherty et al (1985) also demonstrated that the results yielded by a

differential column model and by stage by stage calculations are essentially the same. A vapour liquid residue curve is constructed by tracing the composition of a simple distillation in time, which is described by equation 6.16:

$$\frac{dx}{dt} = x - y^* \quad 6.16$$

where x , is the liquid composition, y^* , is the vapour composition in equilibrium with the liquid composition.

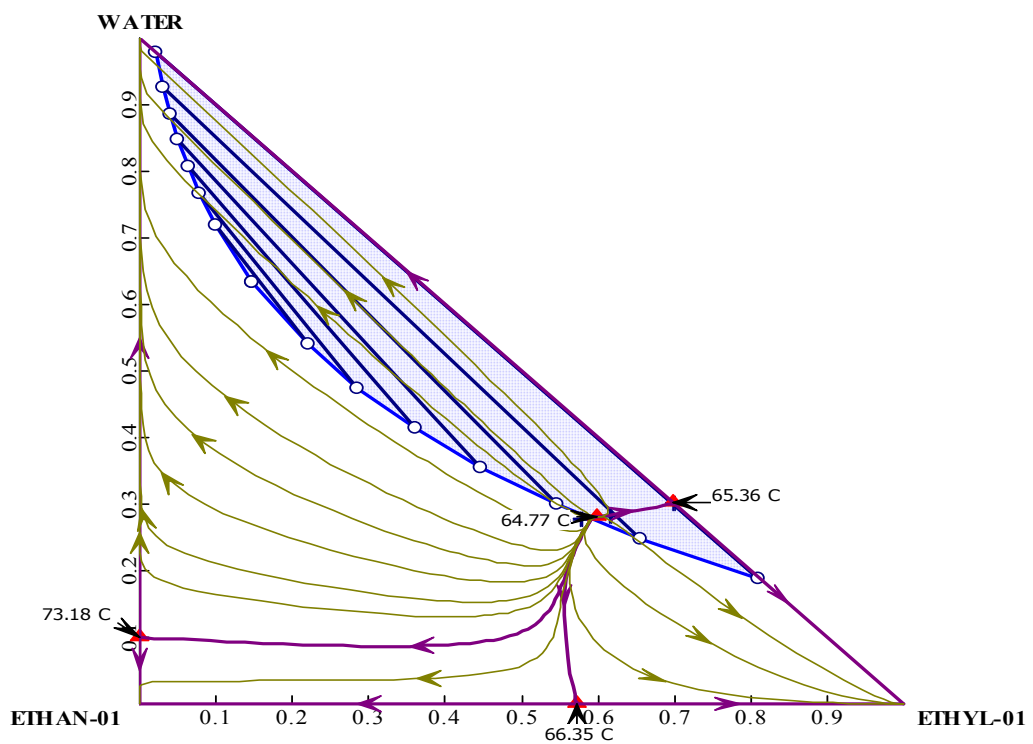


Figure 6.4: Predicted RCM for the ethyl acetate-ethanol-water system using UNIQUAC at the total pressure of 0.83 bar.

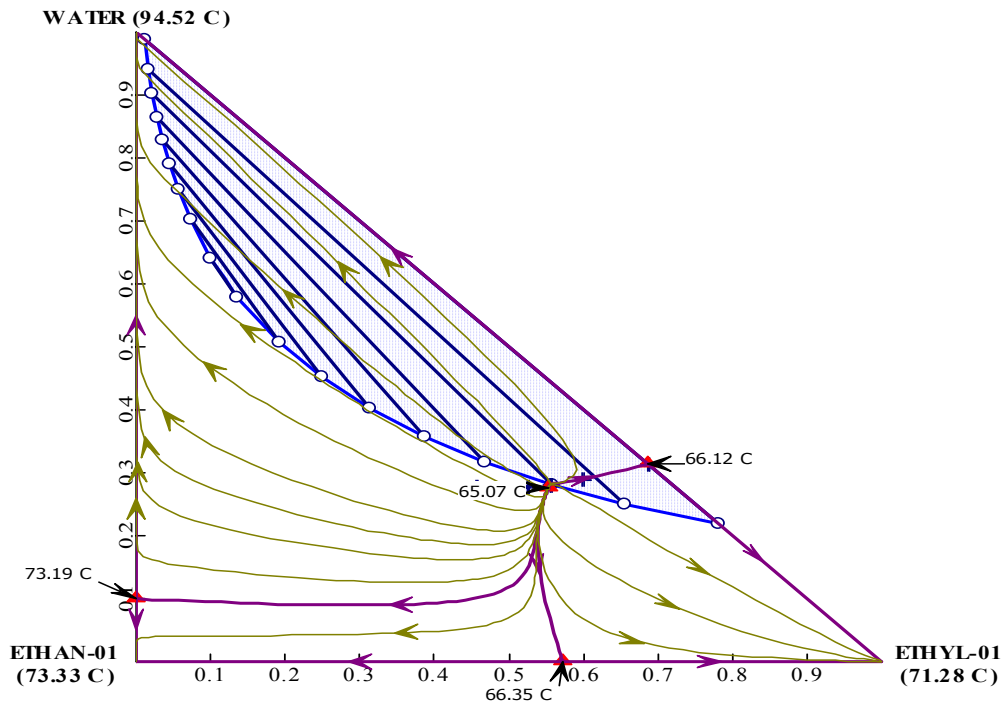


Figure 6.5: Predicted RCM for the ethyl acetate-ethanol-water system using NRTL at a total pressure of 0.83 bar.

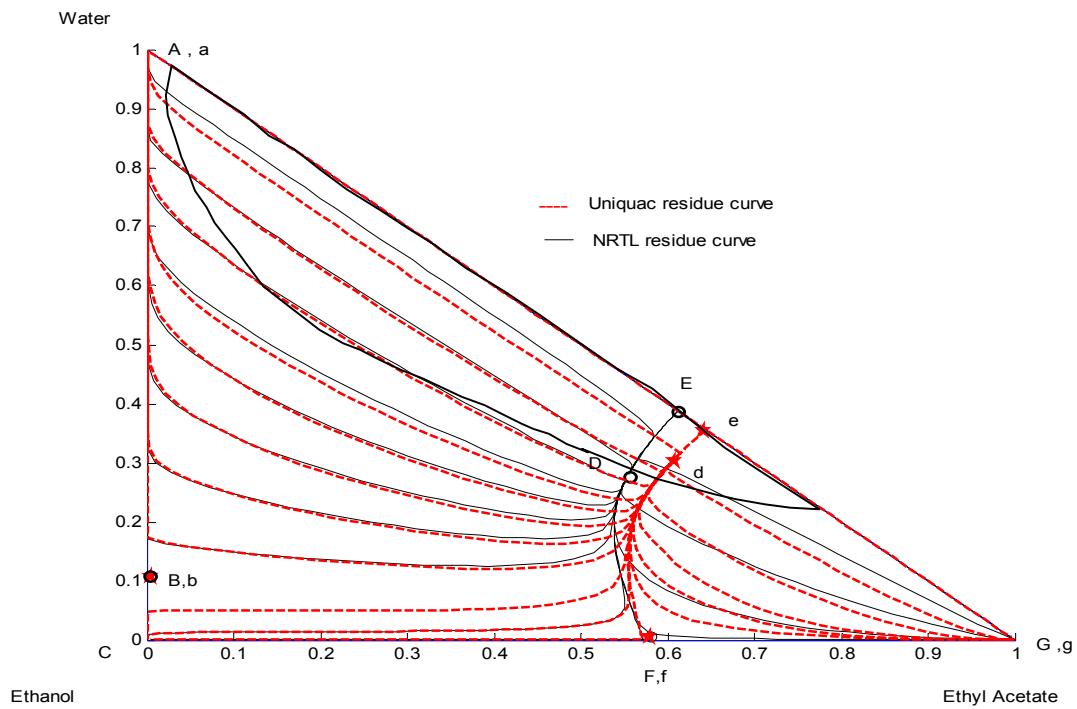


Figure 6.6: Comparison of the predicted RCMs for the ethyl acetate-ethanol-water system using the two thermodynamic models, UNIQUAC and NRTL at the total pressure of 0.83 bar.

We can see from Figures 6.4 and 6.5, that the NRTL and UNIQUAC models both predict RCMs with a ternary azeotrope and an LLE region. As the position between the binary azeotrope in the water-ethyl acetate system is predicted differently, the position of the ternary azeotrope is also predicted differently by the two models. The ternary azeotrope predicted by the UNIQUAC model is enclosed by LLE envelope while the other model, NRTL, predicts the ternary azeotrope just outside the LLE envelope. This discrepancy between the two thermodynamic models causes relatively small changes in the curvature of the residue curves in the vicinity of the ternary azeotrope. The water-ethyl acetate binary azeotrope as well as the ternary azeotrope are quite close to or are enclosed by the LLE envelope which makes it difficult for researcher to both accurately measure as well as predict these azeotropes. The residue curve map has shown us that there is a discrepancy between the two models but it is very difficult to obtain VLE data that can discriminate between the two models. We ask the question: *What about using CPMs, which are linear transforms of residue curve maps, for discriminating between thermodynamic models?*

6.6 Column Profile Map

Franklin et al (1988) examined the Underwood equation more extensively and discovered that this equation could be used to generate a family of liquid profiles with a common compositional offset from their respective vapour profiles in ternary and quaternary systems. He suggested that these maps of profiles could be used to model counter-current vapour-liquid equilibrium including not only distillation, but also absorption or stripping columns. Tapp et al. (2004) showed that similar three component maps, which they called Column Profile Maps (CPMs), could be produced using the difference point equation, equation 6.17, to model individual column sections. Tapp et al. (2004) defined a column section (CS) as a length of column between points of addition or removal of material or energy.

$$\frac{dx}{dn} = \left[\frac{1}{R_{\Delta}} + 1 \right] (x - y^*) + \frac{1}{R_{\Delta}} (X_{\Delta} - x) \quad 6.17$$

A reflux, R_{Δ} , and a difference point, X_{Δ} , must be defined for a CPM. This is equivalent to setting a scaled net molar flow for a column section. An initial point is chosen in the mass balance triangle and the above equation is integrated in both directions, i.e. both as $n \rightarrow \infty$ and $n \rightarrow -\infty$. Using this technique the entire ternary space can be populated with column profile trajectories with common net molar flow. Tapp et al (2004) showed that the CPMs at finite reflux are simply transforms of the residue curve maps. The transform shifts the fixed points of the system in the space, maintaining (in constant relative volatility system) the shape of the boundaries initially defined by the mass balance triangle, i.e. the profiles connecting the fixed points are straight. All the original singularities are present but have been shifted in the composition space. This has resulted in the phenomenon being referred to as “moving triangles”, Holland et al (2004). Figure 6.7 below shows a CPM of the ethyl acetate-ethanol-water system, calculated using the NRTL thermodynamic model. A reflux ratio of one and distillate composition (difference point) of 80% ethyl acetate, 10% ethanol and 10% water are used. We notice **two stationary points** on this column profile map, namely the saddle point \bar{B} and the stable node \bar{A} , both of which lie in near the LLE envelope. Examining the topology allows us to identify that node \bar{B} is the shifted ternary azeotrope node in the RCM while node \bar{A} is the shifted pure water node in the RCM.

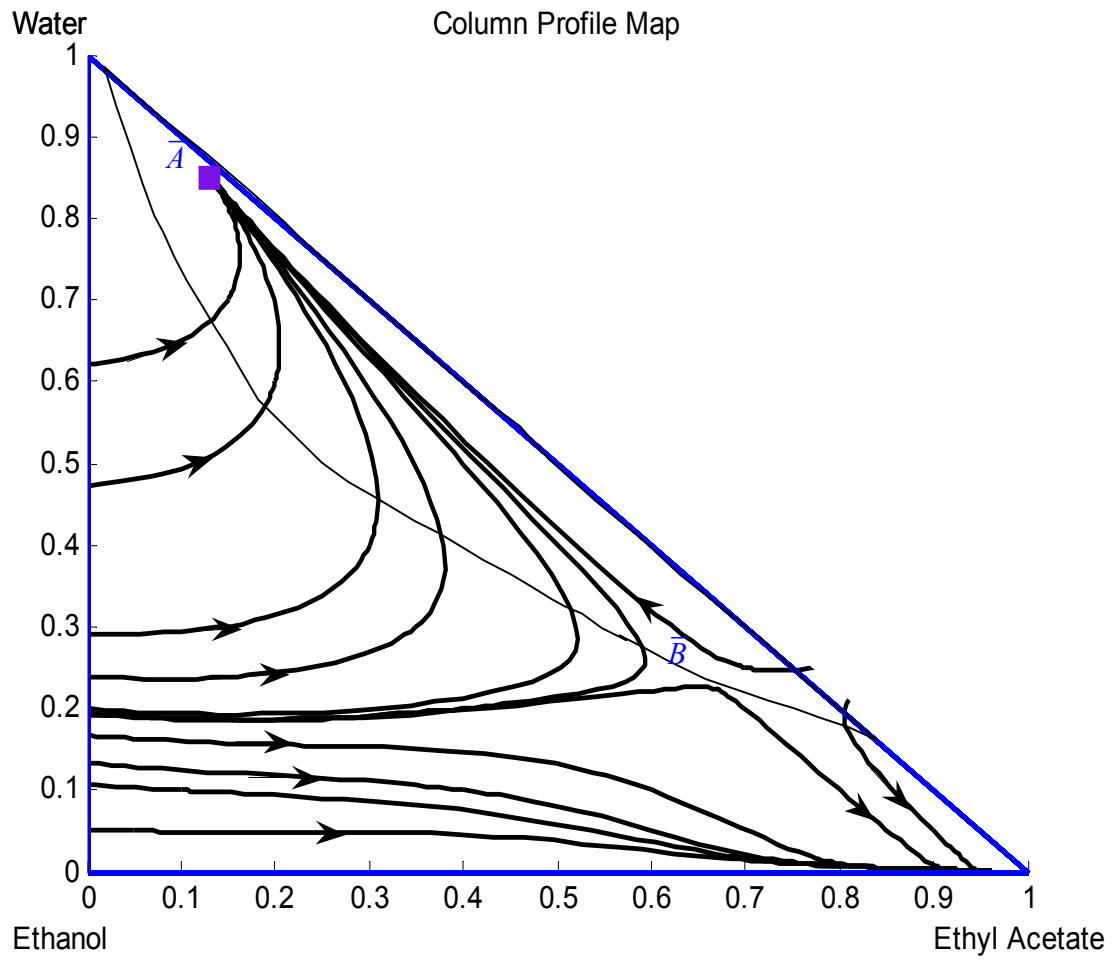


Figure 6.7: Predicted CPM for a reflux ratio of 1 and distillate composition of 80% ethyl acetate, 10 % ethanol and 10% water. Thermodynamics predicted using the NRTL model at the total pressure of 0.83 bar.

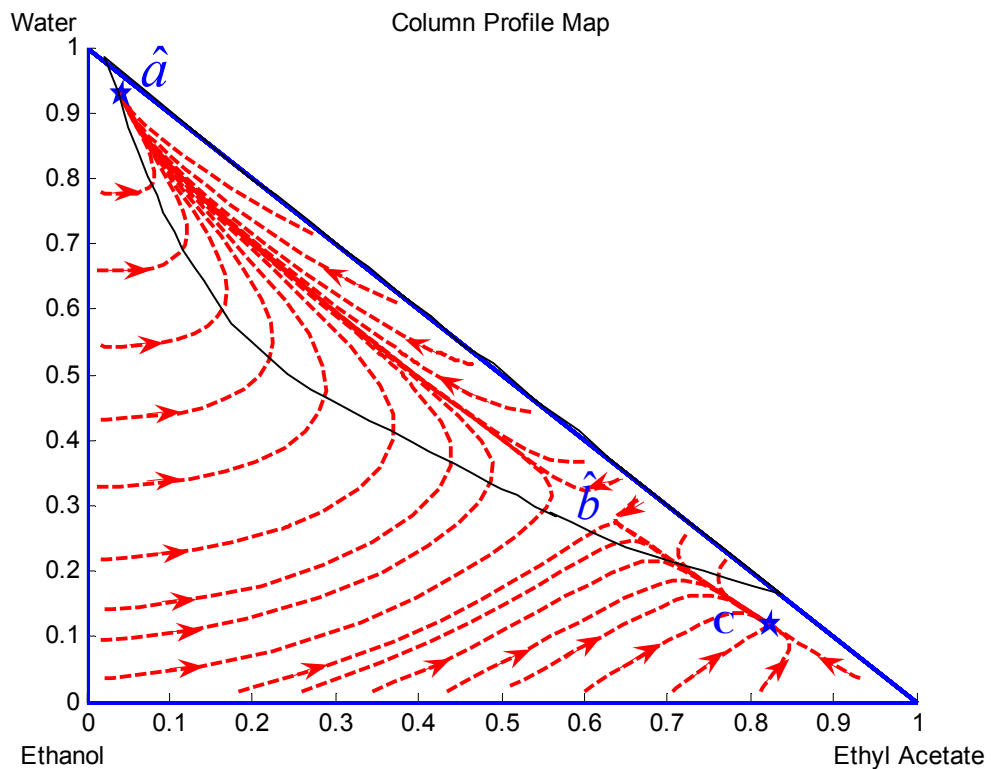


Figure 6.8: Predicted CPM for a the reflux ratio of 1 and distillate composition of 80% ethyl acetate, 10 % ethanol and 10 % water. Thermodynamics predicted using the UNIQUAC model at a total pressure of 0.83 bar.

Figure 6.8 shows the predicted CPM of the ethyl acetate, ethanol and water system, when using the UNIQUAC thermodynamic model. A reflux ratio of one and distillate composition of 80% ethyl acetate, 10% ethanol and 10% water was used. The most obvious difference between this CPM and the previous one predicted using the NRTL model is that there are **three stationary points** in this CPM, namely the stable node \hat{a} , the saddle point \hat{b} and the stable node C. Nodes \hat{a} and \hat{b} lie in the LLE region and are similar in position to the two nodes \bar{B} and \bar{A} in Figure 6.7 predicted by the NRTL model. Node C however only appears in the CPM predicted using the UNIQUAC model.

It must be noted the two column profile maps of Figure 6.7 and Figure 6.8 were made under the same conditions, i.e. the reflux ratio of one, and same distillate composition. The only difference between the two column profile maps is that different thermodynamic model used to simulate these maps. These differences were also not apparent in the RCM's predicted using the two thermodynamic models.

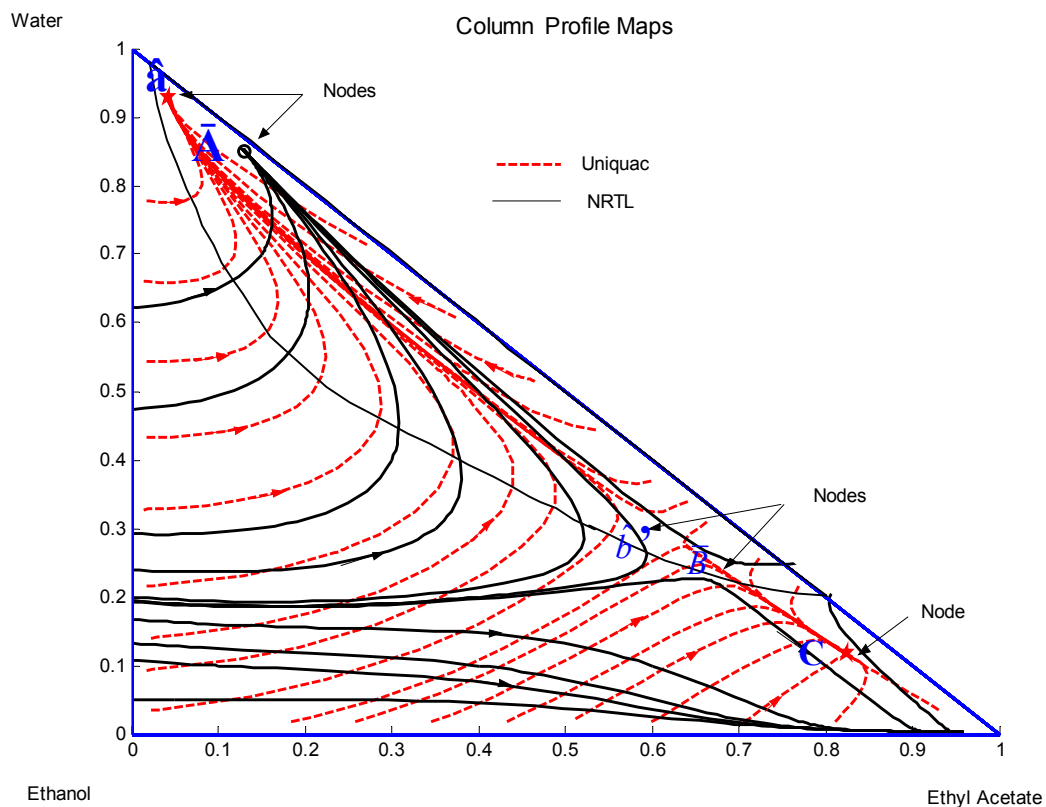


Figure 6.9: Comparison of the predicted CPMs for the NRTL and UNIQUAC models at a total pressure of 0.83 bar. A reflux ratio of 1 and distillate composition of 80% ethyl acetate, 10 % ethanol and 10 % water is used for both maps.

The above Figure 6.9 shows the two column profile maps superimposed on each other. It is quite clear that, the two maps, predict different compositions of the stationary nodes. The stable node \hat{a} predicted by the UNIQUAC model is not the

same composition as the stable node \bar{A} predicted by the NRTL model. Similarly the saddle point \hat{b} of the UNIQUAC model and the saddle point \bar{B} of the NRTL model are at different compositions. In all cases these nodes lie in the LLE region and hence could be difficult to verify experimentally. The UNIQUAC model predicts a stable node C, which is not being predicted by the NRTL thermodynamic model and this node lies outside of the LLE region. As a result of this node, the curvature of the profile in the two CPMs is quite different at low water concentrations. We therefore propose that we experimentally measured column profiles and verify or disprove the existence of node C. We can also compare the curvature of the CPM's and thereby discriminate between the two thermodynamic models. Let us now consider the how we experimental measurement column profiles.

6.7 Experiment

In order to measure a CPM of the rectifying section of the distillation column, an apparatus has been designed in such a way that the column profile composition can be measured during batch or simple boiling. The associated temperature and vapour in equilibrium with the liquid residue can also be obtained. This apparatus was first introduced by Chronis et al (1996) to measure residue curves and has been further developed by Tapp et al (2004) to measure rectifying column profiles. The design of the apparatus is based on the concept that the material and component balance over a batch still is mathematically identical to the differential equation 6.17

6.7.1 Experimental Setup

There are various components to the experimental set-up as shown in Figure 6.10, the still being the main component. The still is graduated in such a way that the level of the liquid inside the still can be measured and the volume of liquid remaining in the still calculated. There are four ports in the still. One port is used for sampling the

liquid and one for injection of the feed. The other two are used for the thermocouple probe and for keeping the pressure constant by releasing vapour below the oil in a bubbler. The bubbler is also used to measure the rate of vaporisation hence the rate of boiling. A condenser is attached to the other end of the bubbler to capture the vapour from the system. A magnetic stirrer is used for the mixing of the liquid. Boiling stones were placed inside the still to assist nucleation. A HP1890 Hewlett Packard gas chromatograph was used for the analysis. The still is immersed in a water bath. The purpose of the bath is to maintain an even heat distribution and also to ensure that the liquid residue is at its bubble point. In order to maintain the bubble point temperature, the water bath temperature must be increased continuously to maintain the temperature driving force between the contents of the still and the water bath; in these experiments the temperature driving force was set at 5 °C. Some of the experiments were run into the predicted LLE Envelope, we did not however observe two, distinct liquid phases during the experiments.

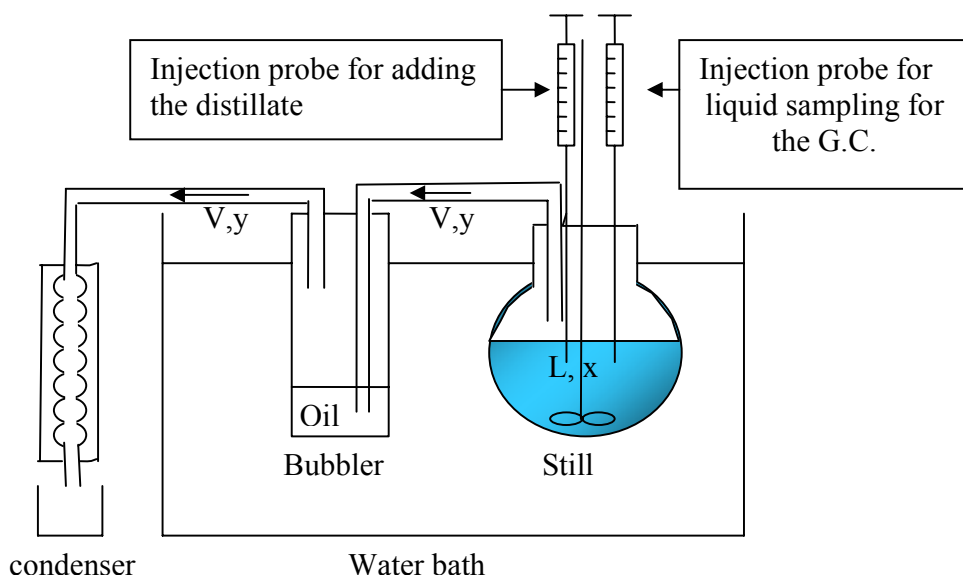


Figure 6.10: Experimental setup with still pot being the main component.

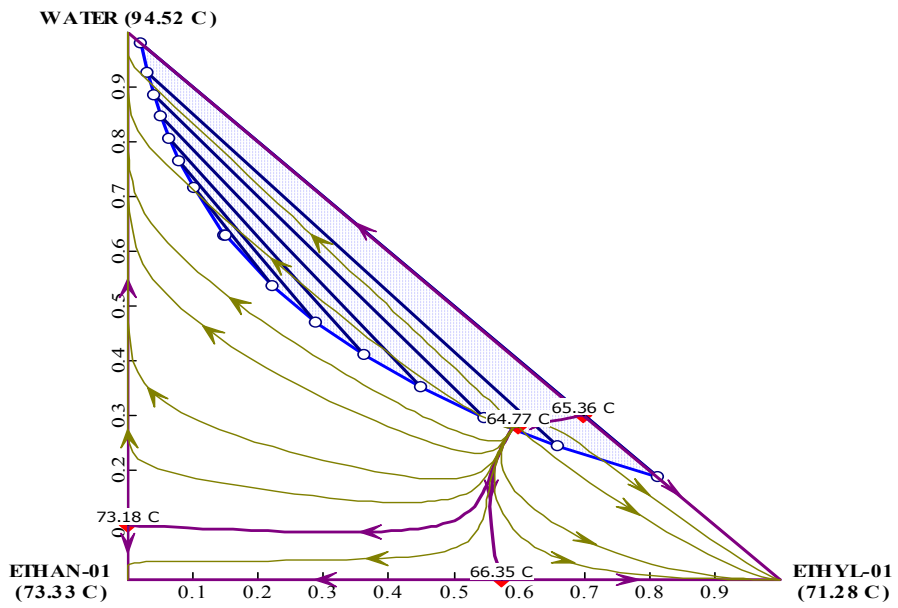


Figure 6.11 Predicted RCM for the ethyl acetate, ethanol and water system with the Liquid-Liquid Envelope at 63 °C, at a total Pressure of 0,83 bars.

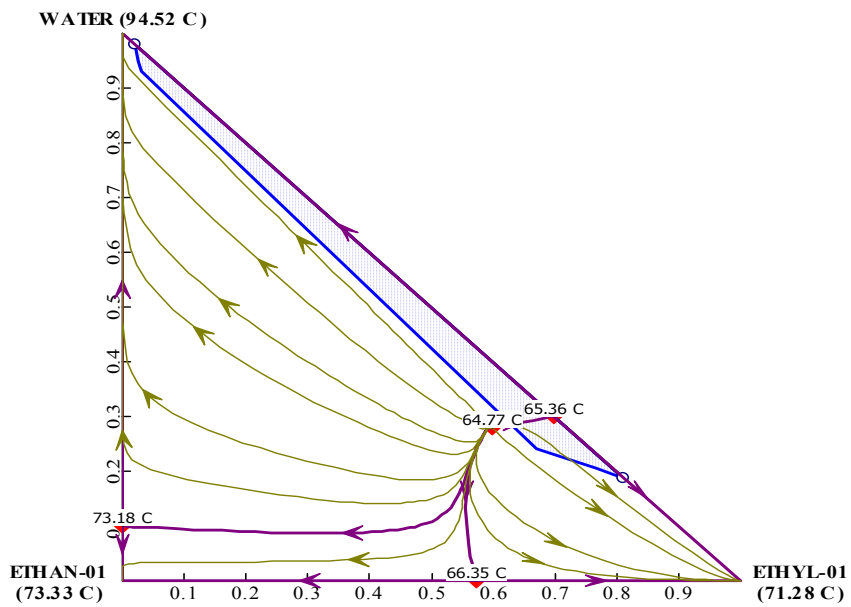


Figure 6.12: RCM for the ethyl acetate, ethanol and water system with the LLE envelope at 64.8°C. The total pressure is 0.83 bar.

Figure 6.11 and 6.12 shows the predicted LLE at two different temperatures. The LLE envelopes are superimposed on the RCM. It can be seen that the solubility

depends very strongly on temperature and that the size of the LLE region is very sensitive to temperature. Thus during the boiling experiments, as the temperature in the still increases, the liquid-liquid envelope become smaller and this makes it possible for experiments to be conducted in the apparent liquid-liquid region.

6.7.2 Experimental Procedure

Experiments were first performed to simulate the **rectifying section** of a distillation column that would separate ethyl acetate, ethanol and water. In these experiments the initial composition of the still was the same as that used for the feed addition during the batch experiments. A bulk solution (about 200ml) of known composition of ethyl acetate, ethanol and water was prepared. A small quantity of this distillate was kept in a fridge to be used as a feed solution while the rest of the distillate was placed in the still. The still was placed inside a hot water bath. The level of liquid in the still was continuously recorded during the experiment. It can be shown by material balance around the still that reflux ratio r and the distillate flow rate d can be determined as follows (see Appendix A for the derivation):

$$d = \frac{v}{r + 1} \quad 6.18$$

In order to approximate the desired reflux r , the distillate, d , is added over discrete time intervals. The vapour flow-rate was determined by the following mass balance equation:

$$v = d - \frac{dl}{dt} \quad 6.19$$

The feed addition rate was then determined by the ratio of the level in the still and the required reflux ratio, (see Appendix A for derivation).

$$d = -\frac{\frac{dl}{dt}}{r} \quad 6.20$$

In these experiments the feed material was added in discrete amounts rather than continuously. This was done in the following way: The liquid level was observed to change by an amount dl in a time interval dt . Using equation 6.12 one can say provided the value of dl is not too large that:

$$\Delta d = d * dt = - \frac{dl}{r} \quad 6.21$$

Where Δd is the amount to be added at the end of the time interval dt when the level has fallen by an amount dl . For our experiments we used a value of dl of 1.3 ml which happened in a time interval (dt) of about 5 min. For the initial experiments a reflux ratio was chosen for each run and kept constant throughout the run; this made it possible to calculate the amount of distillate that must be added after each time interval. Liquid samples were drawn at regular intervals and analysed using the gas chromatograph. The runs were aborted when the liquid level in the still was below the 20 ml mark in the still, since it was found that after these inaccurate results were obtained.

The second sets of experimental runs were done to produce the CPMs. The experimental procedure was exactly the same as that described above except that the initial composition x_o of the material in the still could be different from that of the distillate composition x_d . If this was the case then a sample of solution of the required composition x_d was also prepared.

6.8 Results and Discussion

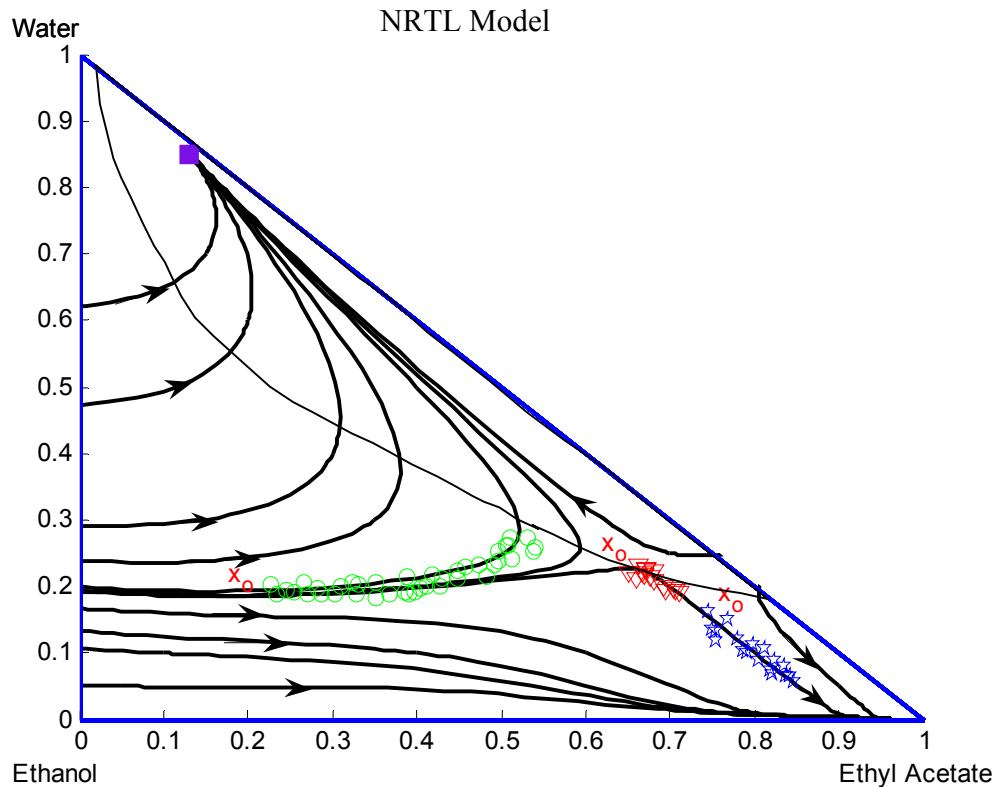


Figure 6.13: Comparison of the measured and predicted CPM for the ethyl acetate, water and ethanol system using the NRTL thermodynamic model. The total pressure is 0.83 bar.

Figure 6.13 compares the experimental results obtained using the reflux of one, the distillate composition of 80% ethyl acetate, 10% ethanol and 10% water to the CPM predicted using the NRTL thermodynamic model. It can be seen that the experimental results follow the theoretically simulated profiles fairly closely. Starting the experiments from different initial compositions x_0 , the results follow the profiles of the theoretically predicted profiles. In particular, the column profiles do not pinch at any point in the ethyl acetate rich region

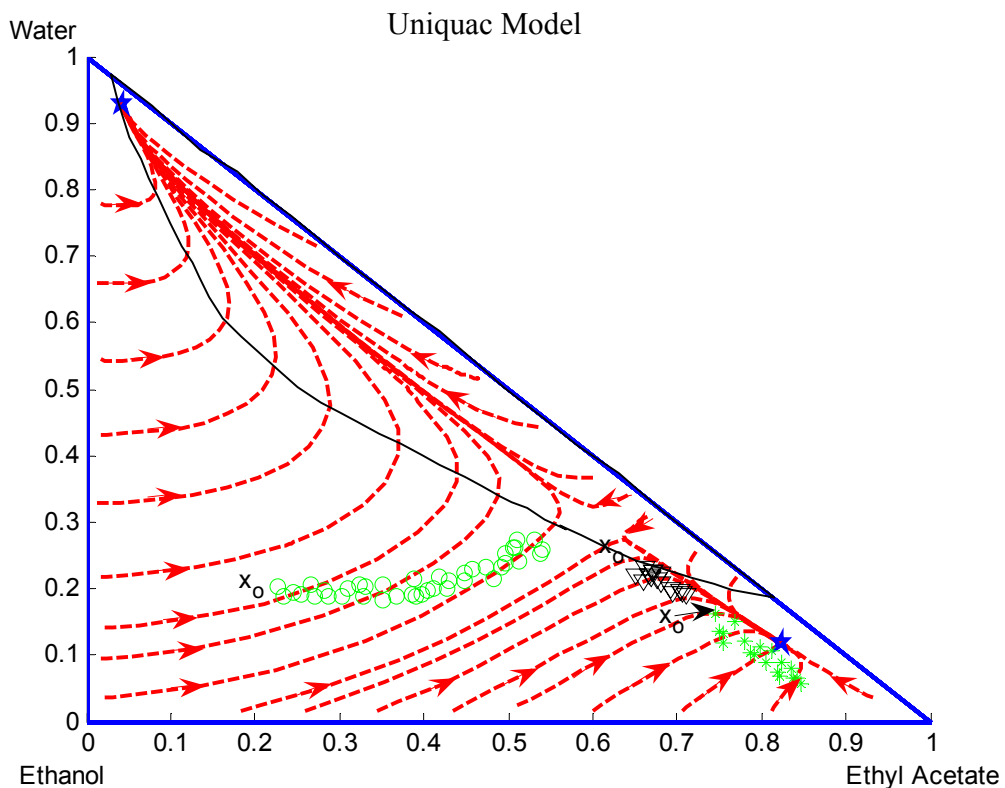


Figure 6.14: Comparison of the measured and predicted CPM for the ethyl acetate, water and ethanol system using the UNIQUAC thermodynamic model. The total pressure is 0.83 bar.

Figure 6.14 shows the same experimentally measured column profiles superimposed on the CPM predicted by the UNIQUAC thermodynamic model. The reflux ratio was again set at one and a distillate composition of 80% ethyl acetate, 10% ethanol and 10% water was used. The initial compositions x_0 were varied. *The experimentally measured column profiles do not follow the profiles predicted by the UNIQUAC thermodynamic model.* In particular,

- the experimental results represented by the green circles shown in Figure 6.14, cross the theoretically predicted profiles.
- The experimental results which were measured close to the stable node predicted by the UNIQUAC thermodynamic model, represented by the green

stars, passes through the stable node which is not supposed to happen if there really is a stable node in this region.

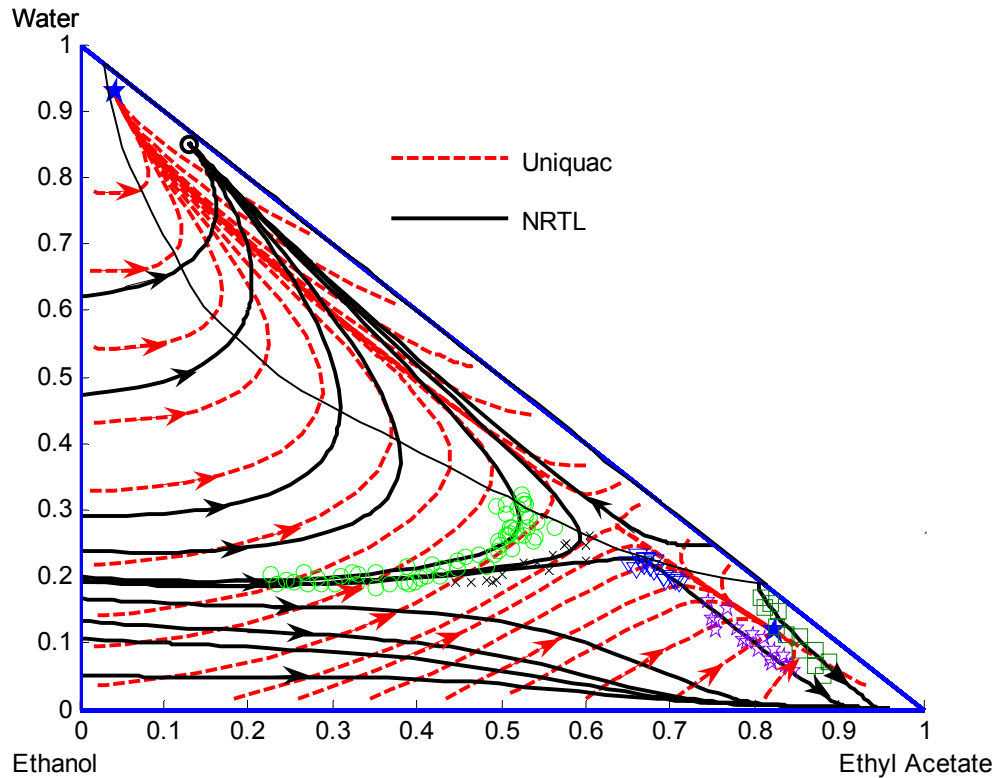


Figure 6.15: Comparison of the experimentally measured and theoretically predicted CPMs for the ethyl acetate, water and ethanol system. The CPMs were predicted using the NRTL and UNIQUAC models. The total pressure is 0.83 bar

A figure 6.15 show further experimental results and superimposes this on the predicted CPMs using both the NRTL and UNIQUAC models. The column profiles were experimentally measured in the region of the node predicted by UNIQUAC model. It can be seen clearly that the experimental results more closely follow the profiles of the NRTL thermodynamic model. In particular the experimental results represented by the purple stars and green squares are measured around the stable node

predicted by the UNIQUAC thermodynamic model: both profiles pass through the region where the stable node is predicted. This shows that there is no stable node around that region which agrees with the results of the NRTL thermodynamic model. The experimental points in Figure 6.15 also show increased scattering along the profiles in the region which is close to, or indeed inside the predicted LLE region. These suggest that there may have been a problem with measured profiles in this region and that there may have been two phases present, even if this was not seen during the experiments.

6.9 Conclusion

It has been shown in this paper that CPMs may be a very powerful tool in discriminating between thermodynamic model for complex systems. A process that is otherwise fully optimized in terms of equipment selection, configuration, and operation can be rendered essentially worthless if the simulation is based on inaccurate thermodynamic models. In this paper we considered a system where the predicted RCMs were quite similar for two different thermodynamic models, namely NRTL and UNIQUAC. The main differences in the RCMs were small differences in the predicted composition of one binary and the ternary azeotrope. The CPMs for these two models were however very different. The curvature was quite different and the UNIQUAC model predicted a node in the CPM that did not appear in the CPM predicted using the NRTL model. A node corresponds to a pinch point in a column; hence the UNIQUAC model predicts the certain column profiles will pinch whereas the NRTL model does not predict any pinching. According to the experimental results, the extra stable node predicted by the UNIQUAC thermodynamic model does not exist. The experimental results around the predicted stable pass through the region, which implies that there is no stable node at this point. Furthermore the curvature of the measured column profiles matches that predicted by the NRTL model. It can therefore be concluded that the NRTL thermodynamic model is a better

thermodynamic model than the UNIQUAC model. We therefore claim that we have introduced a new powerful tool for use in modelling and fitting of VLE data. Thus in addition to measuring and fitting binary data and RCMs, one should and can compare predicted and measured CPMs in order to discriminate between and fit thermodynamic models.

6.10 Nomenclature

A, B, C	:	Antoine Coefficients
A_{ij}	:	Interaction energy
B	:	Bottoms flow rate
d	:	Feed addition flow rate (mol/time)
D	:	Distillate flow rate (mol/time)
dx	:	Change in composition
dt	:	Change in time
dl	:	Change in liquid level
dn	:	Change in number of stages
l	:	Amount of residue in the still (mol)
L	:	Vapour flow rate (mol/time)
n	:	Tray position
P	:	System pressure (Pa)
p_i^{sat}	:	Vapour pressure (Pa)
r	:	Reflux ratio
r_i	:	Size parameter
R	:	Universal gas constant
s	:	Reboil ratio
t	:	Time variable
T	:	Temperature
v	:	Amount of vapour formed (mol/time)
x	:	Liquid mole fraction

x_b	:	Bottoms composition
x_d	:	Distillate flow rate (mol/time)
y	:	Vapour mole fraction
Z	:	Average co-ordination number

6.10.1 Greek letters

γ	:	Liquid phase activity coefficient
ζ	:	Time dependent variable
μ_i^0	:	Chemical potential of pure component
q_i	:	Surface Area
μ_i^{0L}	:	Gibbs energy per mole of liquid
γ_i	:	Activity Coefficient
ϕ	:	Segment or volume fraction
θ	:	Fractional Area

6.11 References

1. Aslam, N and Sunol, A.K. "Sensitivity of azeotropic states to activity coefficient model parameters and system variables". (2006).240,1-14.
2. Bushmakin, I. N., & Kish, I. (1957). Isobaric liquid–vapor equilibrium in a ternary system with an azeotrope of the saddlepoint type. *Russian Journal of Applied Chemistry*, 30(2), 205–215 [200–211].
3. Castillo, F.J.L, Thong, D and Towler, G. "Homogenous azeotropic distillation 1. Design procedure for single-feed columns and non total reflux." *Ind. Eng. Chem. Res.* (1998), 37(3), 987-997.
4. Cairns, B.P. and Furzer, I.A. "Sensitivity testing with the predictive thermodynamic models NRTL, UNIQUAC, ASOG and UNIFAC in multicomponent separations of methanol-acetone-chloroform." *Chem. Eng. Sci.* (1988). 43, 3, 495-501.
5. Chronis, T. "The Simple Measurement of Residue Curves and the Associated VLE data for Ternary Liquid Mixtures". (1996), Thesis, University of the Witwatersrand, Johannesburg.
6. Doherty, M.F. and Malone, J.M. "Conceptual Design of Distillation Column Systems". (2001). McGraw-Hill, New York.
7. Franklin, N.L. *The theory of Countercurrent Cascades.* *Chem. Eng. Res. Des.* (1988), 66
8. Furzer, I.A. "Optimization of a wastewater system containing the Ternary Homogenous Azeotropic system Ethyl Acetate-Ethanol-Water." *Ind. Eng. Chem.* (2000).39, 1539-1545.
9. Holland, S.T., Tapp, M., Hildebrandt, D and Glasser, D. "Column Profile Maps. 2. Singular points and phase diagram behaviour in Ideal and Non-ideal systems." *Ind. Eng. Chem.* (2004), 43, 3590-3603.

10. Sandler, S.I., "Chemical Engineering Thermodynamics" 1999, John Wiley & Sons, New Jersey
11. Schreinemakers, F.A.H. ,Z. Phys. Chem. ,43, pp671, 1902
12. Tapp, M., Holland, S.T., Hildebrandt, D and Glasser, D. "Column Profile Maps. 1. Derivation and Interpretation." Ind. Eng. Chem. (2004), 43 (2), 364-374.
13. Van Dongen, D.B. and Doherty, M.F. "Design and synthesis of homogenous azeotropic distillations. 1. Problem formulation for a single column." (1985). Ind. Eng. Chem. Fund. 24, 454-463
14. Widago, S., & Seider, W.D., (1996). Azeotropic distillation. *A.I.Ch.E. Journal*,42(1), 96-130.
15. Zharov, V.T. "Free evaporation of homogenous multicomponent solutions." Russ.J.Phys.Chem. 1967.41(11), 1539.

7 CONCLUSIONS

This thesis is focused on two main parts; (i) the experimental and (ii) the theoretical parts of the column profile maps of a distillation column. A major problem facing the development of new separation systems is the lack of rapid and inexpensive screening and synthesis methods. A simple batch apparatus has been developed to experimentally measure column profile maps. It was shown in this thesis that a stable node which was the apex of the residue curve map's mass balance triangle could be shifted inside the mass balance triangle by transforming the residue curve map to a column profile map. This meant that profiles which were originally outside the mass balance triangle have been moved inside the triangle and profiles which were in the mass balance triangle have been shifted outside the triangle. Experiments were conducted inside the mass balance triangle starting from different initial compositions, all profiles converged to the same node as predicted theoretically. It was also noticed for a particular system used in the thesis that there were no other nodes introduced in the mass balance triangle by the use of column profile as theoretically predicted. This agrees well with the theory which says that column profile maps are linear transformation of the residue curve map.

It has also been shown that the operating leaves of a distillation column can be expanded beyond the pinch point curve by changing the reflux ratio along the length of the column. Column profile curves approaches the pinch point curve along the direction of the eigenvectors with the smallest eigenvalue. When one operates a

column from a fixed feed with different but constant reflux values, this will always approach the pinch point from the same side. However, if one effectively goes past the pinch for a low reflux ratio, using a higher reflux ratio and then reducing the reflux ratio, one must approach the pinch point value along the same eigenvector. The only way to achieve this is to approach the pinch point in this direction from the outside. This means approaching the pinch point from outside the operating leaf. The experimental results have shown that the pinch point curve can be crossed and they approach the pinch point along the direction of the eigenvectors.

Total and minimum reflux ratio serves as limiting case scenarios for determining feasibility in azeotropic distillation columns. A criterion to establish the possibility of crossing the simple-distillation or distillation-line boundaries has been introduced through the use of open leaves in which the total reflux and minimum reflux composition paths diverge towards different final pinch points. It is possible to cross such distillation boundaries without excessive capital penalty if side reboilers or condensers are used to change the reflux or boil-up ratio in the relevant column section. It has been shown in the thesis that the curvature of the simple distillation boundary is very important, the more the curvature of the distillation boundary, the more the possibilities of having open leaves.

It was shown that this behavior is associated with the saddle point region, as column profiles are introduced into the mass balance triangle. Profiles which were in the negative space have been shifted into the mass balance triangle and those which were

in the triangle have moved outside the mass balance triangle. Experiments were conducted around the saddle point region, these results were very interesting from the fundamental point of view. Because the results were so sensitive to the saddle point position, these were an extremely good test of the underlying thermodynamics close to the saddle point.

It is necessary to choose an appropriate thermodynamic model for a process. A process that is fully optimized in terms of equipment selection, configuration, and operation can be rendered essentially worthless if the process is based on an inaccurate thermodynamic model. It is therefore important to ensure that the thermodynamic model is suitable, especially in complex systems. Experimental data is vital in these situations and this can be used to identify the correct model for the complex systems. In such a situation, we believe that one should not only compare experimental and predicted binary VLE and residue curves, but that one should also compare the experimentally measured column profile maps to the predicted ones. It is shown in this thesis that when simulating column profile maps using different thermodynamic models, one can get different column profile topologies, even though the residue curve maps for the models looked fairly similar. Experimental simulations of column profile maps were used to discriminate between thermodynamic models.

We therefore believe that we have shown in this thesis that experimentally measured column profile maps are an important tool for process synthesis and design.

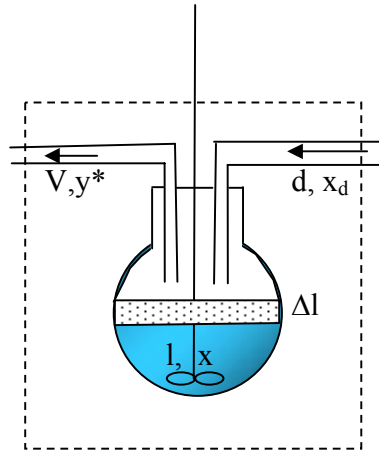
7.1 Future work

It has been shown in the thesis that the batch apparatus can be used to measure column profiles of a continuous distillation column. It was extensively shown in chapters 3,4 and 5 that these profiles can be measure experimentally but it was only shown in one chapter i.e. chapter 6 that the measurement of these profiles can be used to distinguish between different thermodynamic models. More experiments should be conducted on complex systems to discriminate between thermodynamic models, so that this experimental method can be used as standard procedure to distinguish between thermodynamic models.

APPENDIX A

Derivation of the Feed Addition Equation

Derivation of the feed addition equation



$$l_t = l_{\Delta t+t} + v\Delta t - d\Delta t$$

material balance on the still

1

$$l_t = l_t + l_{\Delta t} + v\Delta t - d\Delta t$$

2

$$l_{\Delta t} = d\Delta t - v\Delta t$$

3

$$\frac{dl}{dt} = d - v$$

4

Component balance

$$\frac{d(lx)}{dt} = dx_d - vy \quad 5$$

$$\frac{ldx}{dt} + \frac{xdl}{dt} = dx_d - vy \quad 6$$

but $\frac{dl}{dt} = d - v$ from eq. (4)

$$\frac{ldx}{dt} + x(d - v) = dx_d - vy \quad 7$$

$$\frac{ldx}{dt} = d(x_d - x) + v(x - y) \quad 8$$

$\frac{dx}{dt} = \frac{d}{l}(x_d - x) + \frac{v}{l}(x - y)$	design equation for a rectifying section of a distillation column
---	---

$$\frac{d}{l} \div \frac{v}{l} = \frac{r}{r+1} \div r \quad 10$$

$$\frac{d}{v} = \frac{1}{r+1} \quad 11$$

$$d = \frac{v}{r+1} \quad 12$$

but $\frac{dl}{dt} = d-v$ from eq. (4)

$$d = \frac{d - \frac{dl}{dt}}{r+1} \quad 13$$

$$d(r+1) = d - \frac{dl}{dt} \quad 14$$

$$d = -\frac{\frac{dl}{dt}}{r} \quad 15$$

$\Delta d = d \cdot dt = -\frac{dl}{r}$	16
---	----

APPENDIX B

Derivation of the Composition Equation for GC Calibration

GC calibration

In this thesis ternary systems were evaluated using the HP gas chromatography 6890 model. For a ternary mixture of components A, B and C injected into the GC, the composition or mole fraction of component A for example, was determined by the following Equation 1 below:

$$x_A = \frac{k_A Area_A}{k_A Area_A + k_B Area_B + k_C Area_C} \quad 1$$

where x_A is the mole fraction for component A, k_A , k_B and k_C are the response factor for component A, B and C respectively and $Area_A$, $Area_B$ and $Area_C$ are areas under a peak for components A, B and C respectively obtained from the GC. The response factors are determined by calibrating the GC. The above equation 1 was derived from the following assumption, that the area under each peak is directly proportional to the number of moles for that component. i.e.

$$n_A \propto Area_A$$

$$n_B \propto Area_B$$

$$n_C \propto Area_C$$

The proportionality factor or the response factor, are normally utilized to bring in the equality. The constants are unique for each component, the above equations become the following equations:

$$n_A = k_A Area_A$$

$$n_B = k_B Area_B$$

$$n_C = k_C Area_C$$

where n_i is the number of moles for component i, $Area_i$ is the area under a peak for component i and k_i is the response factor for component i.

The mole fraction of each component can be determined by dividing each component number of moles by the total number of moles for all components. The mole fractions are shown in the following equations:

$$x_A = \frac{k_A \text{ Area}_A}{k_A \text{ Area}_A + k_B \text{ Area}_B + k_C \text{ Area}_C}$$

$$x_B = \frac{k_B \text{ Area}_B}{k_A \text{ Area}_A + k_B \text{ Area}_B + k_C \text{ Area}_C}$$

$$x_C = \frac{k_C \text{ Area}_C}{k_A \text{ Area}_A + k_B \text{ Area}_B + k_C \text{ Area}_C}$$

APPENDIX C

The Methanol, Ethanol and Acetone System

Operating conditions for the GC

Inlet

Carrier Gas used	:	Helium
Mode	:	Split
Heater Temperature	:	100°C
Pressure	:	400 KPa
Total Flow	:	167 ml/min.
Split ratio	:	10:1
Split flow	:	15 ml/min
Gas saver	:	20 ml/min

Column

Type of Column	:	Zebron Capillary Column
Dimensions of the column	:	75m*350µm*1 µm
Mode	:	Constant Pressure
Inlet	:	Front
Detector	:	Back
Pressure	:	400,3 KPa
Flow	:	15 ml/min.
Average velocity	:	85 cm/sec

Oven

Oven Temperature	:	55 °C
Max. Temperature	:	200 °C
Hold up time	:	7 min

Detector

Type of Detector	:	Thermal Conductivity Detector
Heater Temperature	:	200°C
Reference flow	:	17 ml/min
Makeup flow for Helium	:	3 ml/min
Constant Column + Makeup	:	2 ml/min

Auxiliary

Thermal Aux. number	:	1
Heater Setpoint	:	160 °C
Type	:	Valve Box

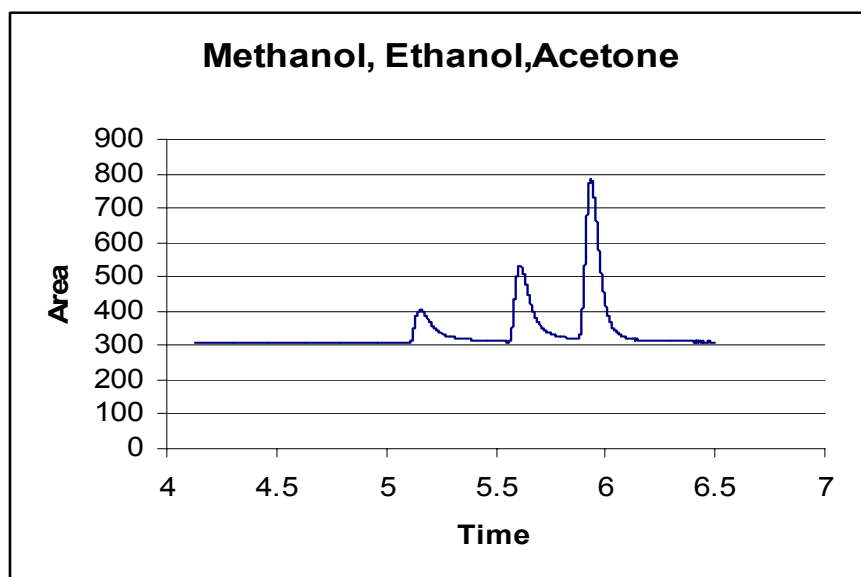


Figure C1: Area vs Time plot from the GC.

The above figure shows traces of GC results for the Methanol, Ethanol and Acetone system. The first peak is Methanol, second peak Ethanol and the last peak is Acetone.

Computer Program used to determine the response factors

The following Mathcad Program was used to calibrate the GC, i.e., determine the component response factors. The response factors are normalized with respect to methanol. Through out this program, M = methanol; E = ethanol; A = acetone.

Samples Compositions in mole fractions:

$x_M :=$	$\begin{bmatrix} 0.581327 \\ 0.791532 \\ 0.483036 \\ 0.695566 \\ 0.214324 \\ 0.255094 \\ 0.362927 \\ 0.462732 \\ 0.659211 \\ 0.797577 \\ 0 \\ 0 \\ 0 \\ 0 \\ 0 \\ 0.356861 \\ 0.449125 \\ 0.590233 \\ 0.228745 \\ 0.200056 \end{bmatrix}$	$x_E :=$	$\begin{bmatrix} 0.418673 \\ 0.208468 \\ 0.516964 \\ 0.304434 \\ 0.785676 \\ 0 \\ 0 \\ 0 \\ 0 \\ 0 \\ 0.259556 \\ 0.433514 \\ 0.60829 \\ 0.7886 \\ 0.666352 \\ 0.4775746 \\ 0.3963821 \\ 0.2457218 \\ 0.4329786 \\ 0.2368045 \end{bmatrix}$	$x_A :=$	$\begin{bmatrix} 0 \\ 0 \\ 0 \\ 0 \\ 0 \\ 0.744906 \\ 0.637073 \\ 0.537268 \\ 0.340789 \\ 0.202423 \\ 0.740444 \\ 0.566486 \\ 0.39171 \\ 0.2114 \\ 0.333648 \\ 0.165565 \\ 0.154493 \\ 0.164045 \\ 0.338277 \\ 0.56314 \end{bmatrix}$
14					

Peak Areas Obtained:

AreaM :=	3249.24	2171.29	0
	6414.8	1848.18	0
	2495.467	2690.35	0
	4178.28	1822.64	0
	964.333	3966.617	0
	2812.7	0	17149
	1868.8	0	7171.56
	3095.46	0	7703.22
	4689.625	0	5205.775
	13897.78	0	7577.24
	0	3075.24	18361.8
	0	2279.32	6263.26
	0	3647.75	5104.95
	0	5178.38	2907.8
	0	4147.2	4396.75
	3765.54	4862.36	3690.34
	3152.35	2896	2500.625
	3633.45	1651.55	2121.975
	1579.9	2578	4264.875
	1080.08	1460.48	6416

n := 0..19

Guess Values for the Normalized response factors with respect to ethanol:

kE := 0.00001

kM := 0.00001

kA := 0.00001

Defining predicted compositions - mole fractions:

$$xM_{p_n} := \frac{kM \cdot \text{Area}M_n}{kM \cdot \text{Area}M_n + kE \cdot \text{Area}E_n + kA \cdot \text{Area}A_n}$$

$$xE_{p_n} := \frac{kE \cdot \text{Area}E_n}{kM \cdot \text{Area}M_n + kE \cdot \text{Area}E_n + kA \cdot \text{Area}A_n}$$

$$xA_{p_n} := \frac{kA \cdot \text{Area}A_n}{kM \cdot \text{Area}M_n + kE \cdot \text{Area}E_n + kA \cdot \text{Area}A_n}$$

Defining the error term:

$$\begin{aligned} \text{Error}(kM, kE, kA) := & \sum_{n=0}^{19} \left[xM_n - \left(\frac{kM \cdot \text{Area}M_n}{kM \cdot \text{Area}M_n + kE \cdot \text{Area}E_n + kA \cdot \text{Area}A_n} \right) \right]^2 \dots \\ & + \sum_{n=0}^{19} \left[xE_n - \left(\frac{kE \cdot \text{Area}E_n}{kM \cdot \text{Area}M_n + kE \cdot \text{Area}E_n + kA \cdot \text{Area}A_n} \right) \right]^2 \dots \\ & + \sum_{n=0}^{19} \left[xA_n - \left(\frac{kA \cdot \text{Area}A_n}{kM \cdot \text{Area}M_n + kE \cdot \text{Area}E_n + kA \cdot \text{Area}A_n} \right) \right]^2 \end{aligned}$$

Iteration loop:

given $\text{Error}(kM, kE, kA) = 0$

$$\frac{d}{dkM} \text{Error}(kM, kE, kA) = 0$$

$$\frac{d}{dkA} \text{Error}(kM, kE, kA) = 0$$

$$\frac{d}{dkE} \text{Error}(kM, kE, kA) = 0$$

The Calculating Function:

$$\begin{bmatrix} kM \\ kE \\ kA \end{bmatrix} := \text{minerr}(kM, kE, kA)$$

The calculated response factors and the error term:

$$\begin{bmatrix} kM \\ kE \\ kA \end{bmatrix} = \begin{bmatrix} 1.4065 \cdot 10^{-5} \\ 1.39347 \cdot 10^{-5} \\ 6.619 \cdot 10^{-6} \end{bmatrix}$$

$$\text{Error}(kM, kE, kA) = 5.03001 \cdot 10^{-3}$$

Recalling the predicted mole fractions:

$$xM_{p_n} := \frac{kM \cdot \text{Area}M_n}{kM \cdot \text{Area}M_n + kE \cdot \text{Area}E_n + kA \cdot \text{Area}A_n}$$

$$xA_{p_n} := \frac{kA \cdot \text{Area}A_n}{kM \cdot \text{Area}M_n + kE \cdot \text{Area}E_n + kA \cdot \text{Area}A_n}$$

$$xE_{p_n} := \frac{kE \cdot \text{Area}E_n}{kM \cdot \text{Area}M_n + kE \cdot \text{Area}E_n + kA \cdot \text{Area}A_n}$$

Calibration Plots: Actual vs. Predicted compositions:

$f(x) := x$

$x := 0, 1 \dots 1$

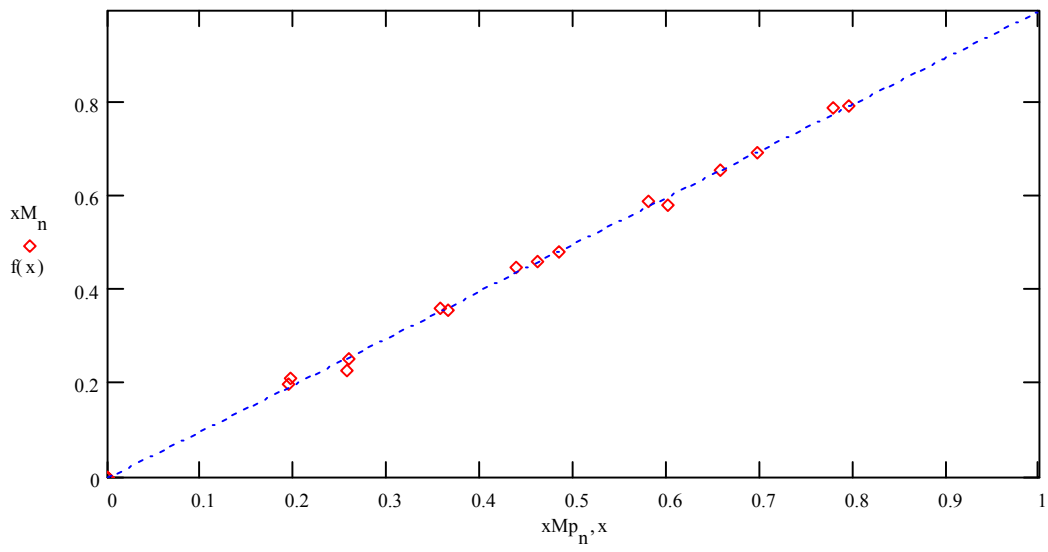


Figure C1: The Methanol Plot

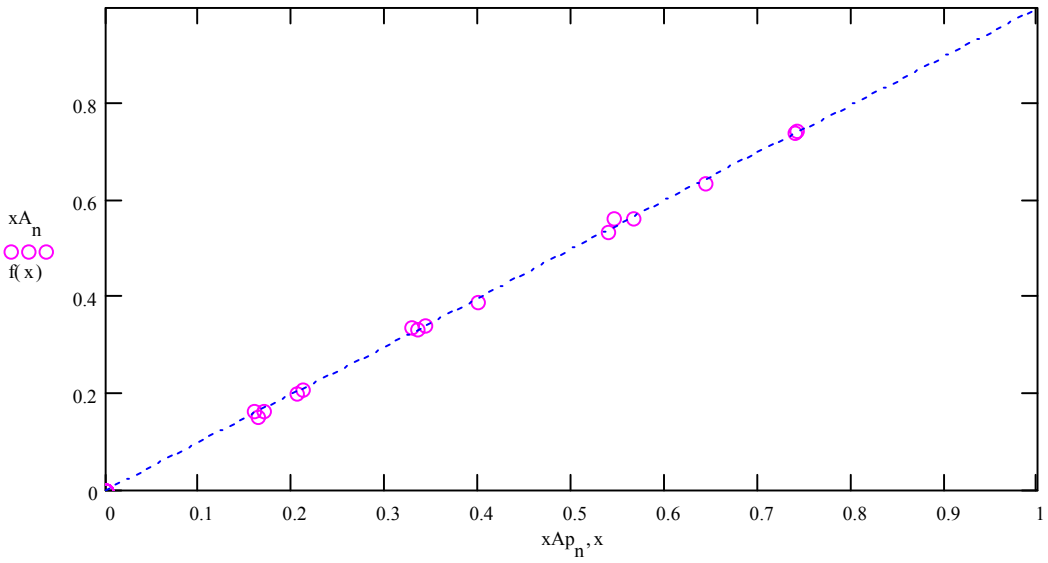


Figure C2: The Ethanol Plot:

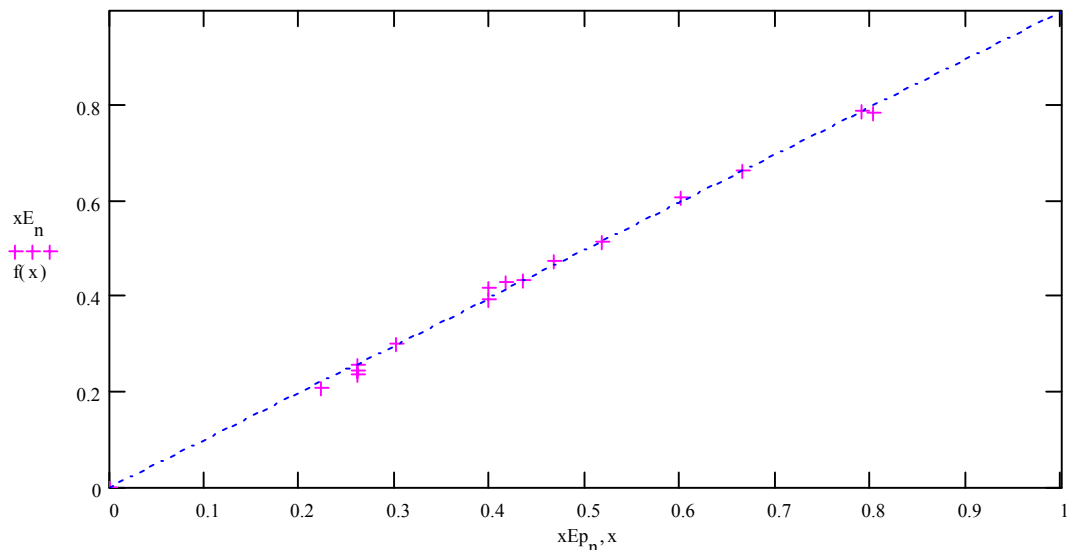


Figure C3: The Acetone Plot:

The Difference between Actual and Predicted Compositions:

$xM_n - xMp_n =$	$ xEn - xEp_n =$	$xAn - xAp_n =$
-0.02034	0.02034	0
0.01359	0.01359	0
$-4.9768 \cdot 10^{-4}$	$4.9768 \cdot 10^{-4}$	0
$-2.6717 \cdot 10^{-3}$	$2.6717 \cdot 10^{-3}$	0
0.01729	0.01729	0
$-3.35386 \cdot 10^{-3}$	0	$3.35386 \cdot 10^{-3}$
$6.54064 \cdot 10^{-3}$	0	$-6.54064 \cdot 10^{-3}$
$2.1397 \cdot 10^{-3}$	0	$-2.1397 \cdot 10^{-3}$
$2.35209 \cdot 10^{-3}$	0	$-2.35209 \cdot 10^{-3}$
$1.76471 \cdot 10^{-3}$	0	$-1.76471 \cdot 10^{-3}$
0	$1.1211 \cdot 10^{-3}$	$1.1211 \cdot 10^{-3}$
0	$2.80427 \cdot 10^{-4}$	$2.80427 \cdot 10^{-4}$
0	$7.60092 \cdot 10^{-3}$	$-7.60092 \cdot 10^{-3}$
0	$8.36592 \cdot 10^{-4}$	$8.36592 \cdot 10^{-4}$
0	$1.27437 \cdot 10^{-3}$	$-1.27437 \cdot 10^{-3}$
$-8.03321 \cdot 10^{-3}$	0.01076	$-2.72544 \cdot 10^{-3}$

The Average Difference between Actual and Predicted Mole Fractions:

$$\text{Mmean} := \frac{\sum_{n=0}^{19} |xM_n - xMp_n|}{20}$$

$$\text{Emean} := \frac{\sum_{n=0}^{19} |xE_n - xEp_n|}{20}$$

$$\text{Amean} := \frac{\sum_{n=0}^{19} |xA_n - xAp_n|}{20}$$

$$\text{Mmean} = 6.70944 \cdot 10^{-3}$$

$$\text{Emean} = 6.74633 \cdot 10^{-3}$$

$$\text{Amean} = 3.69608 \cdot 10^{-3}$$

Experimental Results for the column profile map of the stable node, see Chapter 3

	Mole Fractions		
	Methanol	Ethanol	Acetone
X _o (initial)	0.5956	0.2995	0.10485
X _d (Distillate)	0.3488	0.11141	0.5398

Temp °C		Time (dt),min	dl,mL	distillate, Δd ,mL	Areas			Moles			Mole Fractions		
Still pot	H ₂ O Bath				Methanol	Ethanol	Acetone	Methanol	Ethanol	Acetone	Methanol	Ethanol	Acetone
59	64	8	6.3	6.3	716.8	496.2	237.5	2247.168	1339.74	337.25	0.57265	0.34141	0.08594
59	64	7.5	6.3	6.3	662.2	481.9	259	2075.997	1301.13	367.78	0.554352	0.34744	0.09821
59	64	6.2	6.3	6.3	593.1	407.7	243.3	1859.369	1100.79	345.486	0.562483	0.333	0.10451
59/58	64	8	6.3	6.3	615.7	423	250.6	1930.22	1142.1	355.852	0.563046	0.33315	0.1038
59/58	64	6.5	6.3	6.3	672.8	496.9	318.9	2109.228	1341.63	452.838	0.540316	0.34368	0.116
59/58	64	7.2	6.3	6.3	570	420.4	269.4	1786.95	1135.08	382.548	0.54075	0.34349	0.11576
58	64	7.1	6.3	6.3	675.8	542.7	369.5	2118.633	1465.29	524.69	0.515657	0.35664	0.1277
58	64	6.3	6.3	6.3	704.1	531.8	400.1	2207.354	1435.86	568.142	0.524143	0.34095	0.13491
58	64	7.4	6.3	6.3	571.7	441.4	316.1	1792.28	1191.78	448.862	0.522086	0.34716	0.13075
58	64	6.2	6.3	6.3	835.4	632.6	526.4	2618.979	1708.02	747.488	0.516107	0.33659	0.1473
58	64	6.3	6.3	6.3	643.5	506.8	390.1	2017.373	1368.36	553.942	0.512066	0.34733	0.14061
57	63	6.4	6.3	6.3	543.2	465.8	375.3	1702.932	1257.66	532.926	0.487455	0.36	0.15255
57	63	6.5	6.3	6.3	645.9	496.7	349.1	2024.897	1341.09	495.722	0.524352	0.34728	0.12837
57	63	6.2	6.3	6.3	582.7	516.9	438.2	1826.765	1395.63	622.244	0.475146	0.36301	0.16185
57	63	7.1	6.3	6.3	486.9	432.7	394.4	1526.432	1168.29	560.048	0.468983	0.35895	0.17207
57	63	6.5	6.3	6.3	479.4	445.3	382.8	1502.919	1202.31	543.576	0.462607	0.37008	0.16732

Table C1: Results for the column profile map using the reflux ratio of 1, see figure 3.10

	Mole Fractions		
	Methanol	Ethanol	Acetone
X _o (initial)	0.1009	0.8611	0.038
X _d (Distillate)	0.3494	0.111	0.539

Temp °C		Time (dt),min	dl,mL	distillate, Δd ,mL	Areas			Moles			Mole Fractions		
Still pot	H ₂ O Bath				Methanol	Ethanol	Acetone	Methanol	Ethanol	Acetone	Methanol	Ethanol	Acetone
68	72	8	6.3	6.3	101.7	1029.9	86	318.8295	2780.73	122.12	0.0989638	0.8631306	0.03791
68	72	7	6.3	6.3	148	1213.8	174.3	463.98	3277.26	247.506	0.1163223	0.8216266	0.06205
67/68	72	6.5	6.3	6.3	134.7	1055.4	170.2	422.2845	2849.58	241.684	0.1201875	0.8110262	0.06879
67	71	6.3	6.3	6.3	104.7	769.7	141	328.2345	2078.19	200.22	0.1259222	0.7972664	0.07681
66	70	5.3	6.3	6.3	134.1	906	149	420.4035	2446.2	211.58	0.1365752	0.7946895	0.06874
65	70	6	6.3	6.3	169	1084.8	210.9	529.815	2928.96	299.478	0.1409737	0.7793408	0.07969
65	69	6.3	6.3	6.3	188.3	1194.7	263.7	590.3205	3225.69	374.454	0.1408723	0.7697691	0.08936
65/64	68	8.3	6.3	6.3	205	1302.5	300.7	642.675	3516.75	426.994	0.1401257	0.7667747	0.0931
64	68	8.5	6.3	6.3	164.6	968.3	282.4	516.021	2614.41	401.008	0.146122	0.7403243	0.11355
63	67	7.3	6.3	6.3	186.2	1022.3	272.5	583.737	2760.21	386.95	0.1564602	0.7398248	0.10372
63	67	8.3	6.3	6.3	213.7	1264	383.7	669.9495	3412.8	544.854	0.1447725	0.7374876	0.11774
63/62	67	7.3	6.3	6.3	180.7	843.4	258.8	566.4945	2277.18	367.496	0.1764137	0.7091433	0.11444
62	66	7.3	6.3	6.3	160.7	757.9	231.9	503.7945	2046.33	329.298	0.1749637	0.7106738	0.11436
62	66	7.3	6.3	6.3	197.1	986.1	337.6	617.9085	2662.47	479.392	0.1643474	0.7081469	0.12751
61	65	8.1	6.3	6.3	221.1	1040.8	380.9	693.1485	2810.16	540.878	0.1713938	0.6948641	0.13374

Table C2: Results for the column profile map using the reflux ratio of 1, see figure 3.10

	Mole Fractions		
	Methanol	Ethanol	Acetone
X _o (initial)	0.799	0.1001	0.1005
X _d (Distillate)	0.3476	0.111	0.5412

Temp Still pot	°C H ₂ O Bath	Time (dt),min	dl,mL	distillate, Δd ,mL	Areas			Moles			Mole Fractions		
					Methanol	Ethanol	Acetone	Methanol	Ethanol	Acetone	Methanol	Ethanol	Acetone
57	62	8	6.3	6.3	934.6	139.6	191	2929.971	376.92	271.22	0.81886	0.10534	0.0758
57	62	7.3	6.3	6.3	918.8	145.6	217.4	2880.438	393.12	308.708	0.804083	0.109741	0.086177
57	62	6.3	6.3	6.3	989	170.6	264.4	3100.515	460.62	375.448	0.787616	0.11701	0.095374
57	62	6.3	6.3	6.3	1133.2	210.3	361	3552.582	567.81	512.62	0.766797	0.122557	0.110645
57	62	6.4	6.3	6.3	1017.6	185.1	337.7	3190.176	499.77	479.534	0.765126	0.119864	0.115011
57	62	6.2	6.3	6.3	849.8	146.9	251	2664.123	396.63	356.42	0.779628	0.11607	0.104303
56/57	62	6.3	6.3	6.3	818.8	145.7	264.4	2566.938	393.39	375.448	0.769517	0.117931	0.112552
56	62	6.3	6.3	6.3	911.6	194.2	387.7	2857.866	524.34	550.534	0.726686	0.133327	0.139987
56	61	6	6.3	6.3	849.6	161.6	316.2	2663.496	436.32	449.004	0.75053	0.122948	0.126522
56	61	6	6.3	6.3	826.8	175.7	345.5	2592.018	474.39	490.61	0.728705	0.133367	0.137927
56	61	6.2	6.3	6.3	847.8	198.8	381.8	2657.853	536.76	542.156	0.71127	0.143643	0.145087
56	61	5.3	6.3	6.3	766.6	167.1	319.9	2403.291	451.17	454.258	0.726351	0.136358	0.137291
56	61	5	6.3	6.3	781.1	176.3	358.6	2448.7485	476.01	509.212	0.713095	0.138618	0.148287
56	61	5.3	6.3	6.3	880	233.2	507	2758.8	629.64	719.94	0.671506	0.153257	0.175237
56	61	4.2	6.3	6.3	748.6	184.9	392.2	2346.861	499.23	556.924	0.689642	0.146702	0.163656
56/55	61	4.3	6.3	6.3	709	184.1	411.4	2222.715	497.07	584.188	0.67274	0.150446	0.176814
56/55	61	5	6.3	6.3	751.9	203	417.4	2357.2065	548.1	592.708	0.67387	0.156689	0.169441
56/55	61	5.2	6.3	6.3	676.7	184.5	387.1	2121.4545	498.15	549.682	0.669379	0.15718	0.17344
55	61	5.2	6.3	6.3	692.3	191.3	417.5	2170.3605	516.51	592.85	0.661752	0.157486	0.180762
55	60	5.5	6.3	6.3	689.8	201.6	428.8	2162.523	544.32	608.896	0.652199	0.164162	0.183638
55	60	4	6.3	6.3	670.5	199	446.2	2102.0175	537.3	633.604	0.642245	0.164165	0.19359
55	60	6	6.3	6.3	670.5	211.8	454.4	2102.0175	571.86	645.248	0.633305	0.172292	0.194403
55	60	5	6.3	6.3	662.5	208.8	497.4	2076.9375	563.76	706.308	0.620536	0.168437	0.211027

Table C3 Results for the column profile map using the reflux ratio of 1, see figure 3.10

	Mole Fractions		
	Methanol	Ethanol	Acetone
X _o (initial)	0.785	0.1022	0.113
X _d (Distillate)	0.3453	0.113	0.54

Temp °C	Still pot	H ₂ O Bath	Time (dt),min	dl,mL	distillate, Δd ,mL	Areas			Moles			Mole Fractions		
						Methanol	Ethanol	Acetone	Methanol	Ethanol	Acetone	Methanol	Ethanol	Acetone
56/57	61	9	6.3	6.3	1457.4	295.4	483.8	4568.949	797.58	686.996	0.754758	0.13175	0.113487	
56/57	61	9	6.3	6.3	1411.4	248.9	408.9	4424.739	672.03	580.638	0.779359	0.11837	0.102272	
56/57	61	8.3	6.3	6.3	1404.4	267.8	465.7	4402.794	723.06	661.294	0.760788	0.12494	0.114269	
56	61	8.3	6.3	6.3	1378.4	268.3	460.6	4321.284	724.41	654.052	0.758154	0.1271	0.114751	
56	61	8.3	6.3	6.3	1491.7	319.5	615.1	4676.4795	862.65	873.442	0.729267	0.13452	0.136208	
56	61	8	6.3	6.3	1329.8	286.3	505.7	4168.923	773.01	718.094	0.736555	0.13657	0.126871	
56	61	8	6.3	6.3	1640.6	360.5	698.5	5143.281	973.35	991.87	0.723539	0.13693	0.139533	
56	61	8	6.3	6.3	1326.8	280.2	507.5	4159.518	756.54	720.65	0.737934	0.13422	0.127849	
56	61	7.3	6.3	6.3	1335.4	292.7	563.4	4186.479	790.29	800.028	0.724706	0.1368	0.13849	
56	61	7	6.3	6.3	1392.8	324.5	663.7	4366.428	876.15	942.454	0.705967	0.14166	0.152377	
56	61	6.5	6.3	6.3	1334.9	310.3	602.2	4184.9115	837.81	855.124	0.711981	0.14254	0.145483	
56	61	6.4	6.3	6.3	1205.1	295.6	592.1	3777.9885	798.12	840.782	0.697446	0.14734	0.155215	
56	61	6.3	6.3	6.3	1099.6	266.4	489.1	3447.246	719.28	694.522	0.709157	0.14797	0.142875	
55/56	61	6	6.3	6.3	1331.1	370.1	693.1	4172.9985	999.27	984.202	0.677823	0.16231	0.159865	
55/56	61	6.2	6.3	6.3	987.94	262.4	507.8	3097.1919	708.48	721.076	0.684198	0.15651	0.159292	
55/56	61	6	6.3	6.3	1167	303.1	573.2	3658.545	818.37	813.944	0.691484	0.15468	0.15384	
55/56	60	6.3	6.3	6.3	1111.4	310.9	601.2	3484.239	839.43	853.704	0.672974	0.16213	0.164891	
55/56	60	6.3	6.3	6.3	1015.5	285.5	573.5	3183.5925	770.85	814.37	0.667586	0.16164	0.17077	
55	60	6	6.3	6.3	989.1	288.3	567.8	3100.8285	778.41	806.276	0.66179	0.16613	0.172078	
55	60	7	6.3	6.3	1009.4	302.6	611	3164.469	817.02	867.62	0.652588	0.16849	0.178924	
55	60	6.3	6.3	6.3	1223.8	382.8	623.6	3836.613	1033.56	885.512	0.666578	0.17957	0.15385	
55	60	5.3	6.3	6.3	1236.6	417.8	841.7	3876.741	1128.06	1195.21	0.625279	0.18194	0.192776	
55	60	6.4	6.3	6.3	1276.3	423.6	863.5	4001.2005	1143.72	1226.17	0.628024	0.17952	0.192458	
55	60	6.5	6.3	6.3	1061	356.5	690.4	3326.235	962.55	980.368	0.631266	0.18268	0.186058	
55	60	6.3	6.3	6.3	1197.4	411.4	843.3	3753.849	1110.78	1197.49	0.619231	0.18323	0.197536	
55	60	6.3	6.3	6.3	879.8	358.1	703.2	2758.173	966.87	998.544	0.583915	0.20469	0.211395	
55	60	6	6.3	6.3	1047.1	387.3	715.2	3282.6585	1045.71	1015.58	0.614275	0.19568	0.190044	

Table C4: Results for the column profile map using the reflux ratio of 1, see figure 3.10

Mole Fractions			
	Methanol	Ethanol	Acetone
X _o (initial)	0.3514	0.10798	0.5406
X _d (Distillate)	0.3494	0.1113	0.5393

Temp Still pot	°C H ₂ O Bath	Time (dt),min	dl,mL	distillate, Δd ,mL	Areas			Moles			Mole Fractions		
					Methanol	Ethanol	Acetone	Methanol	Ethanol	Acetone	Methanol	Ethanol	Acetone
51	55	11	6.3	6.3	646.8	320.4	2360.5	2135.669	771.7795	3580.88	0.3291556	0.118949	0.5519
51	55	12	6.3	6.3	657.1	307.6	2221.1	2169.678	740.9469	3369.41	0.3454883	0.117985	0.53653
51/52	55	13	6.3	6.3	699.5	319.5	2259.9	2309.679	769.6116	3428.27	0.3549225	0.118264	0.52681
51/52	56	8	6.3	6.3	1670.5	727.9	4753.7	5515.824	1753.366	7211.36	0.3809125	0.121084	0.498
52	56	7	6.3	6.3	776.7	367.3	2179.5	2564.586	884.7522	3306.3	0.3796215	0.130965	0.48941
52	56	7.3	6.3	6.3	1908.1	838.5	5199.9	6300.355	2019.779	7888.25	0.3887097	0.124613	0.48668
52	56	7.2	6.3	6.3	842.4	416.41	2563.34	2781.521	1003.048	3888.59	0.3625002	0.130722	0.50678
52	56	7.3	6.3	6.3	718.4	346.5	2230.1	2372.085	834.6492	3383.06	0.3599633	0.126658	0.51338
52	56	7.4	6.3	6.3	683.6	304.1	2012.12	2257.179	732.5161	3052.39	0.3735764	0.121236	0.50519
52	56	7.5	6.3	6.3	746.5	377.9	2363.91	2464.868	910.2855	3586.05	0.3540864	0.130766	0.51515
52	56	7.3	6.3	6.3	619.7	320	2043.9	2046.187	770.816	3100.6	0.34578	0.130258	0.52396
52	56	7.2	6.3	6.3	605.02	323.5	2016.2	1997.716	779.2468	3058.58	0.3423362	0.133535	0.52413
52	56	7.4	6.3	6.3	675.2	379.8	2069.3	2229.443	914.8622	3139.13	0.3548129	0.145599	0.49959
52	56	7.3	6.3	6.3	959.2	486	2519.2	3167.182	1170.677	3821.63	0.3881596	0.143474	0.46837
52	56	7.2	6.3	6.3	920.65	443.9	2441.7	3039.894	1069.266	3704.06	0.3890706	0.136853	0.47408

Table C5 Results for the column profile map using the reflux ratio of 1, see figure 3.10

Experimental Results for the expanding of the operating leaves , see Chapter 4

	Mole Fraction		
	Methanol	Ethanol	Acetone
X _o (initial)	0.084	0.8757	0.0403
X _d (Distillate)	0.3458	0.542	0.1122

Temp °C		Time (dt),min	dl,mL	distillate, Δd ,mL	Areas			Moles			Mole Fractions		
Still pot	H ₂ O Bath				Methanol	Ethanol	Acetone	Methanol	Ethanol	Acetone	Methanol	Ethanol	Acetone
68	74	9	6.3	3.2	197	2797.7	273.3	617.595	7553.79	388.086	0.072153	0.882507	0.04534
68	73	9	6.3	3.2	244.4	2959.8	391.5	766.194	7991.46	555.93	0.082266	0.858043	0.05969
68/67	73	8.3	6.3	3.2	249.6	3011.7	357.2	782.496	8131.59	507.224	0.083056	0.863106	0.053838
68/67	73	7	6.3	3.2	232.3	2794	345.5	728.2605	7543.8	490.61	0.083109	0.860902	0.055989
67	73	7.3	6.3	3.2	187.1	2135.3	183.7	586.5585	5765.31	260.854	0.088702	0.871851	0.039447
67	72	7.3	6.3	3.2	216.9	2542.6	345.9	679.9815	6865.02	491.178	0.084615	0.854264	0.061121
66/67	72	7.4	6.3	3.2	227.1	2770	354.5	711.9585	7479	503.39	0.081888	0.860214	0.057899
66	72	6.5	6.3	3.2	160.2	1668.5	274.4	502.227	4504.95	389.648	0.09306	0.834741	0.072199
66	72	6.4	6.3	3.2	215.3	2199.5	351.9	674.9655	5938.65	499.698	0.094888	0.834864	0.070248
66	71	6	6.3	3.2	229.6	2259.2	342.4	719.796	6099.84	486.208	0.098523	0.834926	0.066551
66	71	7	6.3	3.2	224.3	2258.9	339.8	703.1805	6099.03	482.516	0.096528	0.837235	0.066237
66	71	7.3	6.3	3.2	208	2432.3	375.7	652.08	6567.21	533.494	0.084109	0.847078	0.068813
66	71	8	6.3	3.2	340.1	2888.2	494	1066.214	7798.14	701.48	0.111461	0.815208	0.073332

Table C6: Results for expanding the operating leaves using a reflux ratio of 2, see figure 4.9

	Mole Fraction		
	Methanol	Ethanol	Acetone
X _o (initial)	0.2053	0.6766	0.11812
X _d (Distillate)	0.3496	0.1106	0.5398

Temp Still pot	°C H ₂ O Bath	Time (dt),min	dl,mL	distillate, Δd ,mL	Areas			Moles			Mole Fractions		
					Methanol	Ethanol	Acetone	Methanol	Ethanol	Acetone	Methanol	Ethanol	Acetone
62	67	8	6.3	6.3	538.1	2671.2	757.1	1686.9435	7212.24	1075.08	0.1691296	0.723085	0.107786
62	67	6	6.3	6.3	450.2	2231	673.3	1411.377	6023.7	956.086	0.168198	0.717862	0.11394
62	67	8	6.3	6.3	388.1	1836.5	602.8	1216.6935	4958.55	855.976	0.1730416	0.705219	0.121739
62	67	7.3	6.3	6.3	476.9	2141	733	1495.0815	5780.7	1040.86	0.1797699	0.695076	0.125154
62/61	67	7	6.3	6.3	541.4	2305.6	844.5	1697.289	6225.12	1199.19	0.1860736	0.682459	0.131467
62/61	67	7	6.3	6.3	555.3	2418.5	929	1740.8655	6529.95	1319.18	0.1815293	0.680913	0.137558
61	66	6	6.3	6.3	521.6	1995.7	830.2	1635.216	5388.39	1178.88	0.199356	0.656921	0.143723
61	66	7	6.3	6.3	504.5	1884.5	811.6	1581.6075	5088.15	1152.47	0.202194	0.650473	0.147333
61	66	7	6.3	6.3	539.5	1961.5	880.5	1691.3325	5296.05	1250.31	0.2053163	0.642905	0.151779
61	66	7	6.3	6.3	530.4	1844.4	858.7	1662.804	4979.88	1219.35	0.2114978	0.633408	0.155094
60/61	66	6.3	6.3	6.3	555.1	1902.2	907.2	1740.2385	5135.94	1288.22	0.2131495	0.629065	0.157785
60	65	6.3	6.3	6.3	588.3	1980.1	957.7	1844.3205	5346.27	1359.93	0.2156968	0.625256	0.159047
59/60	65	6	6.3	6.3	446.9	1626.4	804.3	1401.0315	4391.28	1142.11	0.2020403	0.633259	0.164701
59/60	65	5.3	6.3	6.3	673.1	2147.4	1117.5	2110.1685	5797.98	1586.85	0.22224	0.610635	0.167125
59	64	5.3	6.3	6.3	545.1	1729.4	860.9	1708.8885	4669.38	1222.48	0.2248317	0.614332	0.160837
59	64	6	6.3	6.3	665.7	2040	1148.5	2086.9695	5508	1630.87	0.2262092	0.597019	0.176772
59	64	6	6.3	6.3	553.4	1628.9	942.8	1734.909	4398.03	1338.78	0.2321969	0.588624	0.179179
58/59	64	5.3	6.3	6.3	673.2	1920.8	1127.2	2110.482	5186.16	1600.62	0.2372057	0.582894	0.179901
58/59	64	5.4	6.3	6.3	731.5	2102.2	1305.7	2293.2525	5675.94	1854.09	0.2334506	0.577805	0.188745
58/59	64	5.5	6.3	6.3	623.3	1683.7	1053.4	1954.0455	4545.99	1495.83	0.244382	0.568543	0.187075
58/59	64	5.4	6.3	6.3	706.7	2006.2	1312.6	2215.5045	5416.74	1863.89	0.2333059	0.570415	0.196279
58/59	64	5.3	6.3	6.3	622.8	1616.4	1051.95	1952.478	4364.28	1493.77	0.2499803	0.558769	0.191251
58	63	5.3	6.3	6.3	609.4	1554.9	1026.1	1910.469	4198.23	1457.06	0.2525151	0.554899	0.192586

Table C7: Results for expanding the operating leaves using a reflux ratio of 1, see figure 4.9

	Mole Fraction		
	Methanol	Ethanol	Acetone
X _o (initial)	0.239	0.646	0.1153
X _d (Distillate)	0.349	0.112	0.5399

Temp °C		Time (dt),min	dl,mL	distillate, Δd ,mL	Areas			Moles			Mole Fractions		
Still pot	H ₂ O Bath				Methanol	Ethanol	Acetone	Methanol	Ethanol	Acetone	Methanol	Ethanol	Acetone
63	68	6.3	6.3	6.3	526.1	2217	598.8	1649.3235	5985.9	850.296	0.1943692	0.70543	0.10021
63	68	7.3	6.3	6.3	512.8	2098.5	611.8	1607.628	5665.95	868.756	0.1974407	0.69586	0.1067
63	68	6	6.3	6.3	492.6	1955.1	614.8	1544.301	5278.77	873.016	0.2006605	0.6859	0.11344
62/63	68	5.3	6.3	6.3	502.7	1892.8	661.3	1575.9645	5110.56	939.046	0.2066684	0.67019	0.12314
62	67	5.3	6.3	6.3	429.9	1532.6	544.9	1347.7365	4138.02	773.758	0.2153101	0.66108	0.12361
61/62	67	5.3	6.3	6.3	512.3	1862.8	722.9	1606.0605	5029.56	1026.518	0.20961	0.65642	0.13397
61/62	67	5.2	6.3	6.3	641.7	2249.6	913.2	2011.7295	6073.92	1296.744	0.2144154	0.64737	0.13821
61	66	6	6.3	6.3	452.3	1598.5	656.2	1417.9605	4315.95	931.804	0.2127245	0.64748	0.13979
60/61	66	6.2	6.3	6.3	670.9	2193.8	1007.9	2103.2715	5923.26	1431.218	0.222386	0.62629	0.15133
60/61	66	6.3	6.3	6.3	548.6	1759.8	837.1	1719.861	4751.46	1188.682	0.2245248	0.62029	0.15518
60	66	5.3	6.3	6.3	533.1	1573.9	750.8	1671.2685	4249.53	1066.136	0.2391991	0.60821	0.15259
60	65	5.4	6.3	6.3	561.8	1684.1	847	1761.243	4547.07	1202.74	0.2344868	0.60538	0.16013
59/60	65	5.3	6.3	6.3	662.9	1937.8	940.4	2078.1915	5232.06	1335.368	0.2403751	0.60517	0.15446
59/60	65	6	6.3	6.3	433.1	1194.3	647.7	1357.7685	3224.61	919.734	0.2467722	0.58607	0.16716
59/60	65	5.3	6.3	6.3	575.8	1628.3	863.8	1805.133	4396.41	1226.596	0.2430128	0.59186	0.16513

Table C8: Results for expanding the operating leaves using a reflux ratio of 1, see figure 4.9

	Mole Fraction		
	Methanol	Ethanol	Acetone
X _o (initial)	0.1739	0.7829	0.04319
X _d (Distillate)	0.35118	0.11202	0.5368

Temp °C		Time (dt),min	dl,mL	distillate, Δd ,mL	Areas			Moles			Mole Fractions		
Still pot	H ₂ O Bath				Methanol	Ethanol	Acetone	Methanol	Ethanol	Acetone	Methanol	Ethanol	Acetone
67/68	73	5	6.3	1.2	515.1	3801.3	318	1700.8087	9156.571	482.406	0.149986	0.80747	0.042541
67/68	73	5	6.3	1.2	474	3675.7	371.5	1565.1006	8854.026	563.5655	0.1425061	0.80618	0.051314
67/68	73	6.3	6.3	1.2	438.4	3151.8	281.3	1447.553	7592.056	426.7321	0.1529158	0.80201	0.045079
68	73	7	6.3	1.2	486.5	3744.9	340.7	1606.3744	9020.715	516.8419	0.1441479	0.80947	0.046379
68	73.5	6	6.3	1.2	461.7	3754.2	354.1	1524.4872	9043.117	537.1697	0.1372821	0.81434	0.048373
69	73.5	7	6.3	1.2	472.2	3773.9	298.5	1559.1572	9090.57	452.8245	0.1404323	0.81878	0.040786
69	73.5	6.3	6.3	1.2	445.7	3975.8	355	1471.6568	9576.907	538.535	0.1270082	0.82651	0.046477
69	73.5	7	6.3	1.2	338.7	3704.6	278.4	1118.3535	8923.64	422.3328	0.106873	0.85277	0.040359
69	74.5	6	6.3	1.2	374.1	3687.8	297.9	1235.2408	8883.173	451.9143	0.1168593	0.84039	0.042753
69	74.5	5.3	6.3	1.2	287.4	3259.3	230.1	948.96606	7851.002	349.0617	0.1037231	0.85812	0.038153
69	74.5	5.3	6.3	1.2	394.7	4234.7	371.4	1303.2599	10200.55	563.4138	0.108	0.84531	0.04669
69	74.5	6	6.3	1.2	381.5	3870.5	327.4	1259.6749	9323.26	496.6658	0.1136932	0.84148	0.044827
69	74.5	5.3	6.3	1.2	344.4	3907.9	317.7	1137.1744	9413.35	481.9509	0.1030752	0.85324	0.043685
70	75	6	6.3	1.2	372.7	3685.1	312.2	1230.6181	8876.669	473.6074	0.1163057	0.83893	0.044761
70	75	6.3	6.3	1.2	323.9	3825.8	275.8	1069.4854	9215.587	418.3886	0.0999196	0.86099	0.039089
70/71	75	7	6.3	1.2	333.3	4141.6	276.7	1100.5233	9976.286	419.7539	0.0957263	0.86776	0.036511
71	75	6	6.3	1.2	271.2	3789	346	895.47528	9126.943	524.882	0.0849009	0.86533	0.049765

Table C9: Results for expanding the operating leaves using a reflux ratio of 5, see figure 4.10

	Mole Fraction		
	Methanol	Ethanol	Acetone
X _o (initial)	0.2937	0.5915	0.1148
X _d (Distillate)	0.349	0.1112	0.5394

Temp °C		Time (dt),min	dl,mL	distillate, Δd ,mL	Areas			Moles			Mole Fractions		
Still pot	H ₂ O Bath				Methanol	Ethanol	Acetone	Methanol	Ethanol	Acetone	Methanol	Ethanol	Acetone
62/63	66.5	7.2	6.3	3.2	868.4	2562.3	699.2	2867.37	6172.068	1060.686	0.2838945	0.611088	0.105017
62/63	66.6	4	6.3	3.2	707.5	2249.5	632.2	2336.0943	5418.596	959.0474	0.2680933	0.621845	0.110062
62/63	66.5	4	6.3	3.2	868.9	2518.4	715	2869.0209	6066.322	1084.655	0.2863295	0.605421	0.108249
62/63	66.5	4.3	6.3	3.2	902.6	2811.6	753.8	2980.2949	6772.582	1143.515	0.2735121	0.621544	0.104944
63	66.5	5.3	6.3	3.2	847.3	2682.4	740.6	2797.6999	6461.365	1123.49	0.2694616	0.622329	0.108209
63	66.5	5.3	6.3	3.2	772.3	2310.8	602.3	2550.0574	5566.255	913.6891	0.2823983	0.616418	0.101184
63	66.5	5.2	6.3	3.2	696.7	2034.7	530.2	2300.4337	4901.185	804.3134	0.2873411	0.612194	0.100465
63	66.5	5	6.3	3.2	854.5	2669.4	696.4	2821.4736	6430.051	1056.439	0.2737179	0.623795	0.102488
63	66.5	5	6.3	3.2	853.4	2661.7	703.5	2817.8415	6411.503	1067.21	0.2736684	0.622684	0.103647
63	66.5	6	6.3	3.2	836.8	2671.3	678.8	2763.0299	6434.627	1029.74	0.2701596	0.629156	0.100684
63	66.5	6	6.3	3.2	866.3	2795.6	784.1	2860.436	6734.041	1189.48	0.2652492	0.62445	0.110301
63	66.5	6	6.3	3.2	806.1	2563.1	697.6	2661.6616	6173.995	1058.259	0.26902	0.624019	0.106961
63	67.4	6.2	6.3	3.2	774.3	2572.7	652.7	2556.6612	6197.12	990.1459	0.2623851	0.635998	0.101617
63	67.4	7	6.3	3.2	847.9	2805.7	708.7	2799.681	6758.37	1075.098	0.2632974	0.635594	0.101108
63	67.7	6	6.3	3.2	829.5	2796.3	689.5	2738.9261	6735.727	1045.972	0.2603387	0.64024	0.099421

Table C10: Results for expanding the operating leaves using a reflux ratio of 2, see figure 4.9

	Mole Fraction		
	Methanol	Ethanol	Acetone
X _o (initial)	0.2606	0.6318	0.1075
X _d (Distillate)	0.3496	0.111	0.5399

Temp Still pot	°C H ₂ O Bath	Time (dt),min	dl,mL	distillate, Δd ,mL	Areas			Moles			Mole Fractions		
					Methanol	Ethanol	Acetone	Methanol	Ethanol	Acetone	Methanol	Ethanol	Acetone
63/64	68	5	6.3	3.2	712.1	2949.9	688.1	2351.283	7105.7191	1043.848	0.2239136	0.67668	0.099406
63/64	67	4	6.3	3.2	737.4	2756.5	643.4	2434.8211	6639.8572	976.0378	0.2422535	0.660635	0.097111
63/64	67	5	6.3	3.2	770.3	2832.2	689.7	2543.4536	6822.2034	1046.275	0.2442826	0.655229	0.100488
63/64	67	6.1	6.3	3.2	919.2	3366.7	744.8	3035.1065	8109.707	1129.862	0.2472657	0.660686	0.092048
63/64	67	6	6.3	3.2	811.1	2943.1	668.8	2678.1711	7089.3393	1014.57	0.248391	0.657511	0.094098
63	67	5	6.3	3.2	871.2	3109.9	780.8	2876.6153	7491.1271	1184.474	0.2490098	0.648458	0.102532
63	67	7	6.3	3.2	778.1	2784.5	691.4	2569.2084	6707.3036	1048.854	0.2488249	0.649595	0.10158
63	67	6.3	6.3	3.2	852.6	3133.9	781.1	2815.1999	7548.9383	1184.929	0.2437599	0.653641	0.1026
63	67	8	6.3	3.2	732.1	2608	670.8	2417.321	6282.1504	1017.604	0.2487704	0.646506	0.104723
63	67	8	6.3	3.2	805.4	2937.3	753	2659.3503	7075.3682	1142.301	0.2444926	0.650488	0.10502
63/64	67	7.3	6.3	3.2	823	3010.3	765.8	2717.4637	7251.2106	1161.719	0.244148	0.651478	0.104374
63/64	67	8	6.3	3.2	773.1	2874.3	680.8	2552.6989	6923.6138	1032.774	0.242904	0.658822	0.098274
63/64	67	9	6.3	3.2	754.8	2781.5	633.2	2492.2741	6700.0772	960.5644	0.2454737	0.659917	0.09461
64	68	6	6.3	3.2	820.2	3132.2	708.9	2708.2184	7544.8434	1075.401	0.2390632	0.666008	0.094929
64	68	5	6.3	3.2	802	3097.2	688.8	2648.1238	7460.5354	1044.91	0.2374239	0.668892	0.093684
64	68	5	6.3	3.2	770.6	2859.7	653.8	2544.4441	6888.4454	991.8146	0.2440783	0.660781	0.095141
64	68	5	6.3	3.2	849.9	3132.2	744.7	2806.2848	7544.8434	1129.71	0.2444321	0.657168	0.0984

Table C11: Results for expanding the operating leaves using a reflux ratio of 2, see figure 4.9

	Mole Fraction		
	Methanol	Ethanol	Acetone
X _o (initial)	0.2241	0.67055	0.1053
X _d (Distillate)	0.3494	0.1105	0.5401

Temp °C		Time (dt),min	dl,mL	distillate, Δd ,mL	Areas			Moles			Mole Fractions		
Still pot	H ₂ O Bath				Methanol	Ethanol	Acetone	Methanol	Ethanol	Acetone	Methanol	Ethanol	Acetone
63/64	67.8	8	6.3	3.2	631	3151.8	643.4	2083.4989	7592.056	976.0378	0.19560445	0.712763	0.091633
64	67.8	7	6.3	3.2	715.4	3287.4	693.1	2362.1793	7918.689	1051.4327	0.20844657	0.698772	0.092782
64.1	67.8	6.3	6.3	3.2	713.5	3322.4	674.7	2355.9057	8002.997	1023.5199	0.20697752	0.703101	0.089921
64.3	67.8	6.3	6.3	3.2	560.6	2541.3	539.9	1851.0451	6121.483	819.0283	0.21054805	0.696291	0.093161
64.2	67.8	6.2	6.3	3.2	709.9	2947.8	638.8	2344.0188	7100.661	969.0596	0.22508907	0.681855	0.093056
64.5	67.8	6.3	6.3	3.2	696.1	3144.6	674.9	2298.4526	7574.712	1023.8233	0.21092549	0.69512	0.093955
64.7	67.8	6.2	6.3	3.2	647.9	3022.7	647.8	2139.301	7281.08	982.7126	0.20564085	0.699896	0.094463
64.4	67.8	6.2	6.3	3.2	665	3058.4	683.7	2195.7635	7367.074	1037.1729	0.2071473	0.695006	0.097846
64.7	67.8	7	6.3	3.2	505.4	2533.7	536.1	1668.7803	6103.177	813.2637	0.19437826	0.710893	0.094728
64.8	67.8	7.3	6.3	3.2	657.8	2988.3	665.1	2171.9898	7198.217	1008.9567	0.20926444	0.693526	0.09721
64.8	67.8	6.3	6.3	3.2	615.3	2840.9	632.8	2031.6591	6843.16	959.9576	0.20657908	0.695812	0.097608
64.9	67.8	7	6.3	3.2	597.2	2678.7	636.4	1971.8947	6452.453	965.4188	0.21000467	0.687179	0.102816
64.7	67.8	8.3	6.3	3.2	664.4	3072.6	674.7	2193.7824	7401.279	1023.5199	0.20659845	0.697012	0.09639
64.8	68.9	6.3	6.3	3.2	695.8	3214.2	701.3	2297.462	7742.365	1063.8721	0.20690961	0.697278	0.095812
64.9	68.9	5	6.3	3.2	616.4	2700.7	577	2035.2912	6505.446	875.309	0.21615135	0.690889	0.092959
64.9	68.9	5.1	6.3	3.2	652.5	2902.6	690.2	2154.4898	6991.783	1047.0334	0.2113632	0.685919	0.102718
64.9	68.9	5	6.3	3.2	668	3125	642.7	2205.6692	7527.5	974.9759	0.20598051	0.70297	0.09105

Table C12: Results for expanding the operating leaves using a reflux ratio of 2, see figure 4.9

	Mole Fraction		
	Methanol	Ethanol	Acetone
X _o (initial)	0.2937	0.5915	0.1148
X _d (Distillate)	0.349	0.1112	0.5394

Temp °C		Time (dt),min	dl,mL	distillate, Δd ,mL	Areas			Moles			Mole Fractions		
Still pot	H ₂ O Bath				Methanol	Ethanol	Acetone	Methanol	Ethanol	Acetone	Methanol	Ethanol	Acetone
69	73	7	6.3	6.3	166.4	3466.7	367.7	549.43616	8350.587	557.8009	0.0580933	0.882929	0.05898
68	73	3	6.3	6.3	241.2	3646.6	502.3	796.41828	8783.9301	761.9891	0.0770056	0.849318	0.07368
67	72	3.3	6.3	6.3	241.8	3561.5	569.9	798.39942	8578.9412	864.5383	0.0779544	0.837634	0.08441
66	71	3.3	6.3	6.3	320	3458.5	607.1	1056.608	8330.8348	920.9707	0.1024996	0.808159	0.08934
66/65	71	3	6.3	6.3	346.3	3506.2	752.7	1143.448	8445.7346	1141.846	0.1065553	0.787039	0.10641
65	69.5	3.3	6.3	6.3	374.2	3703.9	872.7	1235.571	8921.9543	1323.886	0.1076149	0.777078	0.11531
64	69	3.3	6.3	6.3	359.3	3066.6	762	1186.3727	7386.8261	1155.954	0.12194	0.759247	0.11881
64	68	3	6.3	6.3	386.2	2983.7	767	1275.1938	7187.1366	1163.539	0.1324757	0.746648	0.12088
64/63	68	4.2	6.3	6.3	460.3	3081.8	862.5	1519.8646	7423.4398	1308.413	0.1482546	0.724117	0.12763
63	68	4	6.3	6.3	440.8	2634.2	766.4	1455.4775	6345.261	1162.629	0.1623807	0.70791	0.12971
63	67.5	3	6.3	6.3	502.3	3089.5	1014.3	1658.5444	7441.9876	1538.693	0.1558896	0.699486	0.14462
63	67	3.3	6.3	6.3	431.1	2598.3	868.2	1423.4491	6258.785	1317.059	0.1581734	0.695475	0.14635
62	66	4	6.3	6.3	501	2644.3	913.2	1654.2519	6369.5898	1385.324	0.1758128	0.676956	0.14723
62	66	4	6.3	6.3	552.2	2812	1116.3	1823.3092	6773.5456	1693.427	0.1771875	0.658247	0.16457
62/61	66	5	6.3	6.3	694.7	2769.9	1055.1	2293.8299	6672.1351	1600.587	0.2170841	0.631439	0.15148
61	65	3.3	6.3	6.3	525.6	2464.3	1087.7	1735.4786	5936.0058	1650.041	0.1861797	0.636806	0.17701
61	65	4.2	6.3	6.3	556.4	2536.4	1025.5	1837.1772	6109.6803	1555.684	0.1933354	0.642952	0.16371
61	65	5	6.3	6.3	486.2	2044.3	929.7	1605.3838	4924.3098	1410.355	0.2021882	0.620186	0.17763
60	64	4.3	6.3	6.3	559.9	2354.3	1076.1	1848.7338	5671.0378	1632.444	0.2019985	0.619636	0.17837

Table C13: Results for expanding the operating leaves using a reflux ratio of 1, see figure 4.10

APPENDIX D

The Methanol, Di-ethyl ether and Benzene System

Operating conditions for the GC

Inlet

Carrier Gas used	:	Helium
Mode	:	Split
Heater Temperature	:	120°C
Pressure	:	400 KPa
Total Flow	:	190 ml/min.
Split ratio	:	5.7:1
Split flow	:	160 ml/min
Gas saver	:	20ml/min

Column

Type of Column	:	Zebron Capillary Column
Dimensions of the column	:	75m*350µm*1 µm
Mode	:	Constant Pressure
Inlet	:	Front
Detector	:	Back
Pressure	:	400 KPa
Flow	:	14 ml/min.
Average velocity	:	80 cm/sec

Oven

Oven Temperature	:	70 °C
Max. Temperature	:	200 °C
Hold up time	:	9 min

Detector

Type of Detector	:	Thermal Conductivity Detector
Heater Temperature	:	200°C
Reference flow	:	20 ml/min
Makeup flow for Helium	:	2 ml/min
Constant Column + Makeup	:	2 ml/min

Auxiliary

Thermal Aux. number	:	1
Heater Setpoint	:	160 °C
Type	:	Valve Box

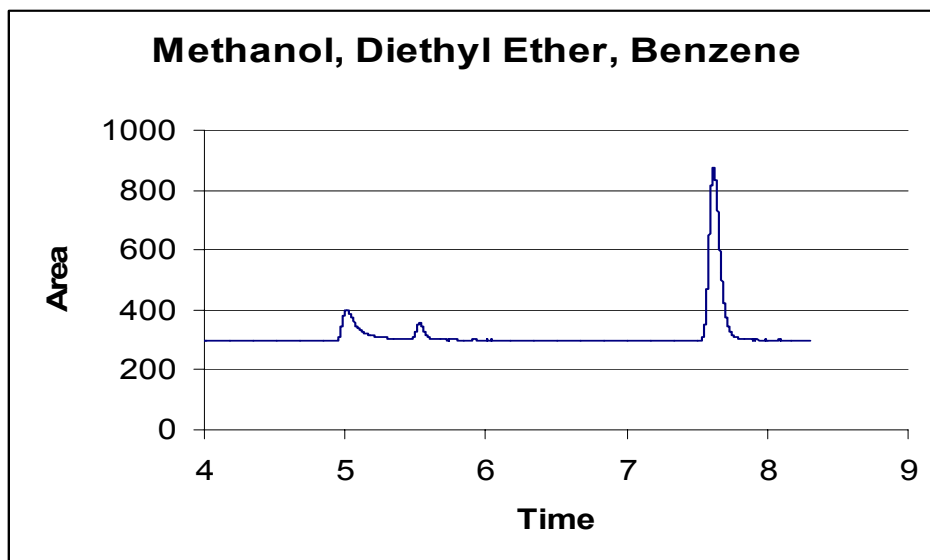


Figure D1: Area vs Time plot from the GC.

The above figure shows traces of GC results for the Methanol, Diethyl Ether and Benzene system. The first peak is Methanol, second peak Diethyl Ether and the last peak is Benzene.

GC Calibration Program

The following Mathcad Program was used to calibrate the GC, i.e., determine the component response factors. The response factors are normalized with respect to methanol. Through out this program, M = methanol; E = diethyl ether; A = Benzene.

Samples Compositions in mole fractions:

$x_M :=$	$\begin{bmatrix} 0.1994 \\ 0.3984 \\ 0.6056 \\ 0.8118 \\ 0.5072 \\ 0.79397 \\ 0.6039 \\ 0.4157 \\ 0.2201 \\ 0.5217 \\ 0 \\ 0 \\ 0 \\ 0 \\ 0 \\ 0.543 \\ 0.327 \\ 0.6827 \\ 0.2574 \\ 0.3129 \end{bmatrix}$	$x_E :=$	$\begin{bmatrix} 0 \\ 0 \\ 0 \\ 0 \\ 0 \\ 0.206 \\ 0.3961 \\ 0.5843 \\ 0.7799 \\ 0.4783 \\ 0.19343 \\ 0.3661 \\ 0.6033 \\ 0.8016 \\ 0.4951 \\ 0.2347 \\ 0.2785 \\ 0.1773 \\ 0.3685 \\ 0.5409 \end{bmatrix}$	$x_A :=$	$\begin{bmatrix} 0.8006 \\ 0.6016 \\ 0.3944 \\ 0.1883 \\ 0.4928 \\ 0 \\ 0 \\ 0 \\ 0 \\ 0 \\ 0.8066 \\ 0.6339 \\ 0.3968 \\ 0.1984 \\ 0.5049 \\ 0.2222 \\ 0.3943 \\ 0.14 \\ 0.3741 \\ 0.1462 \end{bmatrix}$
14					

Peak Areas Obtained:

AreaM :=	225.7	0	3535.56
	574.37	0	2593.63
	1043.9	0	1855.75
	1657.7	0	1011.75
	576.85	0	2109.65
	1477.65	1231.04	0
	824.8	1599.23	0
	292.9	1617.93	0
	112.91	2351.74	0
	526.295	1649.05	0
	0	707.9	3167.85
	0	1211.85	2183.9
	0	1808.12	1317.89
	0	2035.3	572.9
	0	1837.1	1791.5
	651.99	1058.45	1023.25
	286.5	1080.25	1648.65
	1131.27	996.84	740.2
	211.45	1358.3	1486.4
	267	1935.8	547.05

n := 0..19

Guess Values for the Normalized response factors with respect to ethanol:

kE := 1

kM := 1

kA := 1

Defining predicted compositions - mole fractions:

$$xM_{p_n} := \frac{kM \cdot \text{Area}M_n}{kM \cdot \text{Area}M_n + kE \cdot \text{Area}E_n + kA \cdot \text{Area}A_n}$$

$$xE_{p_n} := \frac{kE \cdot \text{Area}E_n}{kM \cdot \text{Area}M_n + kE \cdot \text{Area}E_n + kA \cdot \text{Area}A_n}$$

$$xA_{p_n} := \frac{kA \cdot \text{Area}A_n}{kM \cdot \text{Area}M_n + kE \cdot \text{Area}E_n + kA \cdot \text{Area}A_n}$$

Defining the error term:

$$\begin{aligned} \text{Error}(kM, kE, kA) := & \sum_{n=0}^{19} \left[xM_n - \left(\frac{kM \cdot \text{Area}M_n}{kM \cdot \text{Area}M_n + kE \cdot \text{Area}E_n + kA \cdot \text{Area}A_n} \right) \right]^2 \dots \\ & + \sum_{n=0}^{19} \left[xE_n - \left(\frac{kE \cdot \text{Area}E_n}{kM \cdot \text{Area}M_n + kE \cdot \text{Area}E_n + kA \cdot \text{Area}A_n} \right) \right]^2 \dots \\ & + \sum_{n=0}^{19} \left[xA_n - \left(\frac{kA \cdot \text{Area}A_n}{kM \cdot \text{Area}M_n + kE \cdot \text{Area}E_n + kA \cdot \text{Area}A_n} \right) \right]^2 \end{aligned}$$

Iteration loop:

given $\text{Error}(kM, kE, kA) = 0$

$$\frac{d}{dkM} \text{Error}(kM, kE, kA) = 0$$

$$\frac{d}{dkA} \text{Error}(kM, kE, kA) = 0$$

$$\frac{d}{dkE} \text{Error}(kM, kE, kA) = 0$$

The Calculating Function:

$$\begin{bmatrix} kM \\ kE \\ kA \end{bmatrix} := \text{minerr}(kM, kE, kA)$$

The calculated response factors and the error term:

$$\begin{bmatrix} kM \\ kE \\ kA \end{bmatrix} = \begin{bmatrix} 2.60307 \\ 0.73827 \\ 0.73192 \end{bmatrix}$$

$$\text{Error}(kM, kE, kA) = 0.04667$$

Recalling the predicted mole fractions:

$$xM_{p_n} := \frac{kM \cdot \text{Area}M_n}{kM \cdot \text{Area}M_n + kE \cdot \text{Area}E_n + kA \cdot \text{Area}A_n}$$

$$xA_{p_n} := \frac{kA \cdot \text{Area}A_n}{kM \cdot \text{Area}M_n + kE \cdot \text{Area}E_n + kA \cdot \text{Area}A_n}$$

$$xE_{p_n} := \frac{kE \cdot \text{Area}E_n}{kM \cdot \text{Area}M_n + kE \cdot \text{Area}E_n + kA \cdot \text{Area}A_n}$$

Calibration Plots: Actual vs. Predicted compositions:

$f(x) := x$

$x := 0, 1 \dots 1$

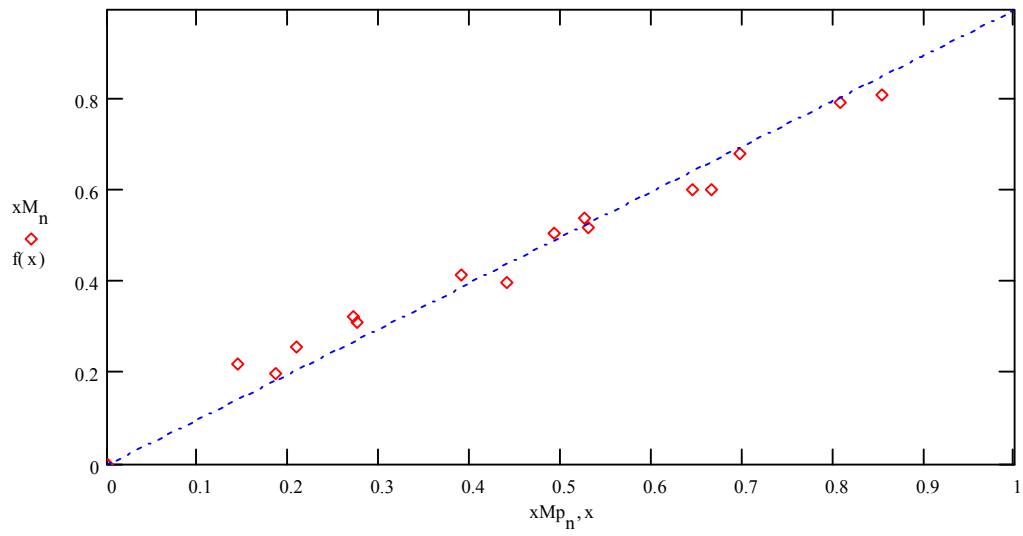


Figure D1: The Methanol Plot:

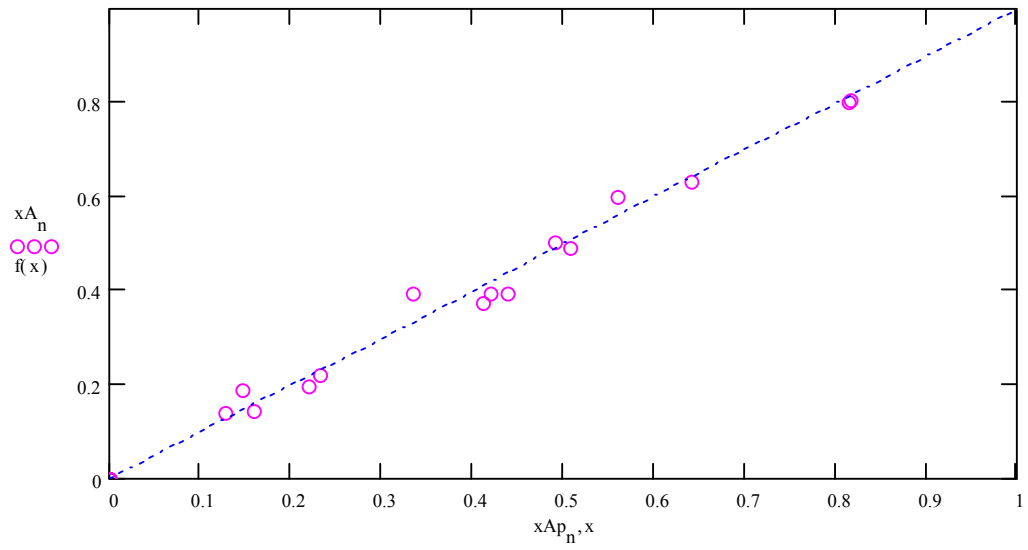


Figure D2: The Diethyl ether Plot:

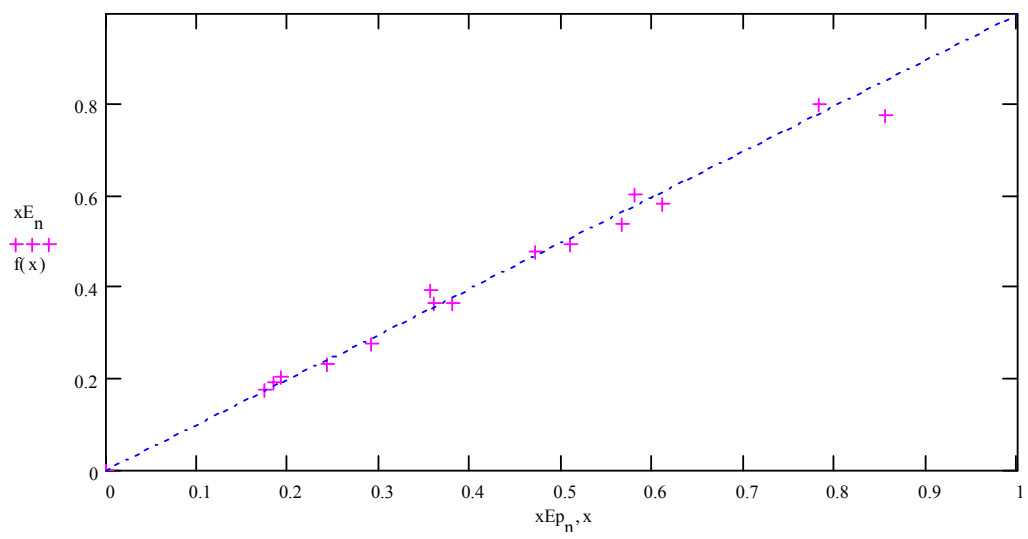


Figure D3: The Benzene Plot:

The Difference between Actual and Predicted Compositions:

$xM_n - xMp_n =$	$ xEn - xEp_n =$	$xAn - xAp_n =$
0.01437	0	-0.01437
-0.04219	0	0.04219
-0.06113	0	0.06113
-0.04173	0	0.04183
0.01418	0	-0.01418
-0.01491	0.01488	0
-0.0413	0.0413	0
0.02608	0.02608	0
0.07532	0.07532	0
$-7.77848 \cdot 10^{-3}$	$7.77848 \cdot 10^{-3}$	0
0	$9.48896 \cdot 10^{-3}$	$-9.45896 \cdot 10^{-3}$
0	$7.24332 \cdot 10^{-3}$	$-7.24332 \cdot 10^{-3}$
0	0.02278	-0.02268
0	0.01978	-0.01978
0	0.01334	0.01334
0.01716	$7.41003 \cdot 10^{-3}$	$-9.84616 \cdot 10^{-3}$

The Average Difference between Actual and Predicted Mole Fractions:

$$M_{\text{mean}} := \frac{\sum_{n=0}^{19} |xM_n - xMp_n|}{20}$$

$$E_{\text{mean}} := \frac{\sum_{n=0}^{19} |xE_n - xEp_n|}{20}$$

$$A_{\text{mean}} := \frac{\sum_{n=0}^{19} |xA_n - xAp_n|}{20}$$

Mmean = 0.02566

Emean = 0.01482

Amean = 0.01812

Experimental Results for the column profile map of the saddle point node, see Chapter 5

	Mole Fractions		
	Methanol	Diethyl ether	Benzene
X _o (initial)	0.2443	0.688	0.0677
X _d (distillate)	0.398	0.4265	0.1753

Temp °C		Time (dt),min	dl,mL	distillate, Δd ,mL	Areas			Moles			Mole Fractions		
Still pot	H ₂ O Bath				Methanol	Diethyl ether	Benzene	Methanol	Diethyl ether	Benzene	Methanol	Diethyl ether	Benzene
38.8	41.5	3	6.3	2.1	300.9	1155.4	461.4	2256.75	2449.448	968.94	0.397655528	0.431610297	0.170734174
38.8	41.5	5	6.3	2.1	616.2	1764.7	895.7	4621.5	3741.164	1880.97	0.451158251	0.365218437	0.183623312
39	41.5	5	6.3	2.1	559.9	1484.9	829.1	4199.25	3147.988	1741.11	0.462047668	0.346376261	0.191576071
39.1	41.5	6	6.3	2.1	459.5	1340.7	799.9	3446.25	2842.284	1679.79	0.432493709	0.356697845	0.210808446
39.4	41.5	7	6.3	2.1	672.4	1698	911.3	5043	3599.76	1913.73	0.477715604	0.340999707	0.181284688
39.6	41.5	7.2	6.3	2.1	617.2	1523.3	950.9	4629	3229.396	1996.89	0.469697176	0.327681612	0.202621213
39.7	42	8.1	6.3	2.1	617.3	1541.7	931.8	4629.75	3268.404	1956.78	0.469790056	0.331651536	0.198558407
40.1	42	8	6.3	2.1	655.3	1422.5	891.9	4914.75	3015.7	1872.99	0.501329125	0.30761651	0.191054365
40.7	42	7.3	6.3	2.1	605.5	1280.7	875.7	4541.25	2715.084	1838.97	0.49929612	0.298514926	0.202188954
41	43.5	5.4	6.3	2.1	650.7	1453.1	1020.7	4880.25	3080.572	2143.47	0.482987823	0.304877571	0.212134606
41.1	43.5	6.2	6.3	2.1	794.3	1557.6	1144.8	5957.25	3302.112	2404.08	0.510762603	0.283116425	0.206120972
41.5	43.5	8.1	6.3	2.1	679.4	1275.8	986.4	5095.5	2704.696	2071.44	0.51617584	0.273986602	0.209837559

Table D1: Results for the column profile map using the reflux ratio of 3, see figure 5.14

	Mole Fractions		
	Methanol	Diethyl ether	Benzene
X _o (initial)	0.243	0.6913	0.0657
X _d (distillate)	0.5387	0.1593	0.302

Temp Still pot	°C H ₂ O Bath	Time (dt),min	dl,mL	distillate, Δd ,mL	Areas			Moles			Mole Fractions		
					Methanol	Diethyl ether	Benzene	Methanol	Diethyl ether	Benzene	Methanol	Diethyl ether	Benzene
46	49	6	6.3	2.1	1260.9	1487.7	2721	9456.75	3153.924	5714.1	0.516063663	0.172112573	0.311823764
46	49	5	6.3	2.1	846.3	763.8	1520.1	6347.25	1619.256	3192.21	0.568815444	0.145111319	0.286073236
47	49	5.2	6.3	2.1	717.1	725.3	1481.5	5378.25	1537.636	3111.15	0.536374857	0.153349006	0.310276137
47.3	49	5.3	6.3	2.1	778.4	755.9	1529.9	5838	1602.508	3212.79	0.547999314	0.150423653	0.301577033
47.5	49	7.1	6.3	2.1	887.8	823.1	1738.6	6658.5	1744.972	3651.06	0.55236487	0.144756511	0.302878619
47.7	50	4.3	6.3	2.1	537.8	463.5	1042.6	4033.5	982.62	2189.46	0.559774508	0.136369314	0.303856178
48.6	51	6	6.3	2.1	850.8	552.1	1548.1	6381	1170.452	3251.01	0.590698676	0.108350485	0.300950839
48.8	52	6.2	6.3	2.1	896.8	594.8	1669.3	6726	1260.976	3505.53	0.585250945	0.109721587	0.305027467
48.9	52	6.3	6.3	2.1	646.4	357.9	963.3	4848	758.748	2022.93	0.635413447	0.099446923	0.26513963
49.2	52	6	6.3	2.1	998.3	540.3	1514	7487.25	1145.436	3179.4	0.633863485	0.096971526	0.269164989
49.6	52	7	6.3	2.1	816.4	550.2	1622.7	6123	1166.424	3407.67	0.572398448	0.109041203	0.318560349
49.7	52	5.2	6.3	2.1	879.7	462.5	1277.7	6597.75	980.5	2683.17	0.642966568	0.095552078	0.261481354
50	53	6	6.3	2.1	908.6	442.8	1301.1	6814.5	938.736	2732.31	0.649894626	0.089526668	0.260578705
50	53	6.3	6.3	2.1	798.6	480.5	1551.7	5989.5	1018.66	3258.57	0.583389258	0.099219518	0.317391224
50	53	7	6.3	2.1	846.5	409.2	1326.7	6348.75	867.504	2786.07	0.634727489	0.086730244	0.278542267
50	53	7.3	6.3	2.1	1680.4	937.6	3002.8	12603	1987.712	6305.88	0.603112699	0.095121348	0.301765953

Table D2: Results for the column profile map using the reflux ratio of 3, see figure 5.14

Mole Fractions			
	Methanol	Diethyl ether	Benzene
X _o (initial)	0.6383	0.08655	0.2751
X _d (distillate)	0.2434	0.6908	0.06581

Temp °C		Time (dt),min	dl,mL	distillate, Δd,mL	Areas			Moles			Mole Fractions		
Still pot	H ₂ O Bath				Methanol	Diethyl ether	Benzene	Methanol	Diethyl ether	Benzene	Methanol	Diethyl ether	Benzene
49.2	52	7	6.3	2.1	1019.4	537	1507.7	7645.5	1138.44	3166.17	0.639784906	0.095266069	0.264949026
49.5	52	6.2	6.3	2.1	844.4	392	941.6	6333	831.04	1977.36	0.692782287	0.090909489	0.216308224
49.6	52	6.1	6.3	2.1	977.5	454.6	1350.2	7331.25	963.752	2835.42	0.658667749	0.086587193	0.254745058
49.5	52	7	6.3	2.1	1155.4	581	1649.9	8665.5	1231.72	3464.79	0.648517701	0.092180742	0.259301557
49.5	52	8	6.3	2.1	1356.8	522.5	1418.1	10176	1107.7	2978.01	0.713518926	0.077669508	0.208811566
49.7	52	8.3	6.3	2.1	1426.4	681.9	1844.7	10698	1445.628	3873.87	0.667894574	0.090253047	0.241852379
50	53	7	6.3	2.1	868.7	325.4	850.5	6515.25	689.848	1786.05	0.72462938	0.076725241	0.198645379
50	53	7.1	6.3	2.1	990.3	432.9	1190.7	7427.25	917.748	2500.47	0.684825219	0.084620415	0.230554366
50	53	7.3	6.3	2.1	1349	564.6	1586.8	10117.5	1196.952	3332.28	0.690768425	0.081721438	0.227510137
50.1	53	8	6.3	2.1	1054.9	379.8	1274.7	7911.75	805.176	2676.87	0.694391053	0.070667932	0.234941015
50.3	54	6.3	6.3	2.1	1614.2	530.5	1726.7	12106.5	1124.66	3626.07	0.718178491	0.066716774	0.215104735
50.4	54	6	6.3	2.1	1128.6	427.5	1247.5	8464.5	906.3	2619.75	0.705930921	0.075584523	0.218484557
50.7	54	7	6.3	2.1	1327.6	461.5	1353.3	9957	978.38	2841.93	0.722710021	0.071013863	0.206276116
50.7	54	8.1	6.3	2.1	1571.9	526.4	1369.8	11789.25	1115.968	2876.58	0.747015644	0.070712348	0.182272007
50.6	54	8.2	6.3	2.1	1227.4	401.2	1099.9	9205.5	850.544	2309.79	0.744430178	0.068781774	0.186788048
50.7	55	6.3	6.3	2.1	1096.5	415	1001	8223.75	879.8	2102.1	0.73389317	0.078513964	0.187592866
50.7	55	7	6.3	2.1	1346.7	455	1223	10100.25	964.6	2568.3	0.740859596	0.070754008	0.188386396
50.9	55	8	6.3	2.1	1730.97	510.9	1320.5	12982.275	1083.108	2773.05	0.770990685	0.064323563	0.164685752

Table D3: Results for the column profile map using the reflux ratio of 3, see figure 5.14

	Mole Fractions		
	Methanol	Diethyl ether	Benzene
X _o (initial)	0.4472	0.1561	0.3966
X _d (distillate)	0.2403	0.6905	0.06914

Temp °C		Time (dt),min	dl,mL	distillate, Δd ,mL	Areas			Moles			Mole Fractions		
Still pot	H ₂ O Bath				Methanol	Diethyl ether	Benzene	Methanol	Diethyl ether	Benzene	Methanol	Diethyl ether	Benzene
47.5	50	7	6.3	2.1	618.3	1025.3	1365.2	4637.25	2173.636	2866.92	0.47916336	0.2246001	0.2962366
47.5	50	6.3	6.3	2.1	900.2	1423.8	1941.5	6751.5	3018.456	4077.15	0.4875748	0.2179846	0.2944406
47.6	50	6.3	6.3	2.1	805.6	1256.1	1780.9	6042	2662.932	3739.89	0.48550313	0.2139791	0.3005178
47.5	50	6	6.3	2.1	590.5	752.9	1298.7	4428.75	1596.148	2727.27	0.50601748	0.1823717	0.3116108
47.5	50	6	6.3	2.1	998.6	1243.7	2354.8	7489.5	2636.644	4945.08	0.49694039	0.1749456	0.328114
47.6	51	5.3	6.3	2.1	911.2	1045.1	2217.8	6834	2215.612	4657.38	0.49857766	0.161641	0.3397813
47.7	51	6	6.3	2.1	642.7	623.8	1498.7	4820.25	1322.456	3147.27	0.51886571	0.142353	0.3387813
47.7	51	6	6.3	2.1	910.3	998.1	2419.3	6827.25	2115.972	5080.53	0.48683476	0.1508849	0.3622804
47.7	51	6.2	6.3	2.1	752.8	765.7	2078.4	5646	1623.284	4364.64	0.48530487	0.1395302	0.3751649
47.7	51	6.3	6.3	2.1	455.2	412.3	1346.8	3414	874.076	2828.28	0.47973991	0.1228263	0.3974337
47.8	51	6.4	6.3	2.1	643.7	572.9	1920.1	4827.75	1214.548	4032.21	0.47920454	0.1205566	0.4002389
47.8	51	7	6.3	2.1	782.4	724.9	2381.7	5868	1536.788	5001.57	0.47298329	0.123871	0.4031457
47.8	51	8	6.3	2.1	514.8	567.1	1921.3	3861	1202.252	4034.73	0.42437982	0.1321449	0.4434753
47.8	51	7	6.3	2.1	546.3	657.8	2410.1	4097.25	1394.536	5061.21	0.38825467	0.132146	0.4795993
47.8	51	8	6.3	2.1	355.6	471.8	1778.6	2667	1000.216	3735.06	0.36029459	0.1351228	0.5045826
47.8	51	8.3	6.3	2.1	378.5	521.4	1981.3	2838.75	1105.368	4160.73	0.35025333	0.1363836	0.5133631

Table D4 Results for the column profile map using the reflux ratio of 3, see figure 5.14

	Mole Fractions		
	Methanol	Diethyl ether	Benzene
X _o (initial)	0.6076	0.0249	0.3675
X _d (distillate)	0.24012	0.6946	0.06528

Temp °C		Time (dt),min	dl,mL	distillate, Δd ,mL	Areas			Moles			Mole Fractions		
Still pot	H ₂ O Bath				Methanol	Diethyl ether	Benzene	Methanol	Diethyl ether	Benzene	Methanol	Diethyl ether	Benzene
47.7	50	7	6.3	2.1	1235.7	218.3	2615.4	9267.75	462.796	5492.34	0.6088037	0.0304013	0.3607949
47.7	50	8	6.3	2.1	925.6	198.5	1850.3	6942	420.82	3885.63	0.6171517	0.0374114	0.3454369
47.5	50	6.3	6.3	2.1	1125.8	320.8	2347.6	8443.5	680.096	4929.96	0.6008088	0.0483932	0.350798
47.5	50	7.2	6.3	2.1	914.8	232.8	1772.4	6861	493.536	3722.04	0.6194152	0.0445567	0.336028
47.4	50	8.1	6.3	2.1	901.3	341.6	1901.6	6759.75	724.192	3993.36	0.5889668	0.0630978	0.3479354
47.4	50	7.5	6.3	2.1	724.8	270.8	1426.4	5436	574.096	2995.44	0.6036287	0.0637492	0.3326221
47.3	51	7.4	6.3	2.1	571.39	275.4	1107.5	4285.425	583.848	2325.75	0.5956096	0.0811461	0.3232443
47.3	51	8	6.3	2.1	1189.7	582.1	2398.7	8922.75	1234.052	5037.27	0.5872521	0.0812193	0.3315286
47.4	51	8.3	6.3	2.1	772.8	439.8	1595.1	5796	932.376	3349.71	0.5751092	0.0925152	0.3323756
47.6	51	8	6.3	2.1	821.3	380	1666.1	6159.75	805.6	3498.81	0.5886521	0.0769866	0.3343613
47.6	51	7.3	6.3	2.1	851.6	467.2	1804.9	6387	990.464	3790.29	0.5719145	0.0886896	0.3393959
47.7	51	7	6.3	2.1	734.7	372.8	1345.9	5510.25	790.336	2826.39	0.6037323	0.0865934	0.3096743
47.8	51	7.2	6.3	2.1	1005.1	461.7	2035.2	7538.25	978.804	4273.92	0.5893414	0.076523	0.3341356
47.8	51	7.4	6.3	2.1	678.4	309.9	1271.6	5088	656.988	2670.36	0.6046096	0.0780702	0.3173202
47.8	51	8.1	6.3	2.1	992.4	437.8	1959.9	7443	928.136	4115.79	0.5960634	0.0743286	0.3296079

Table D5: Results for the column profile map using the reflux ratio of 3, see figure 5.13 & figure 5.14

	Mole Fractions		
	Methanol	Diethyl ether	Benzene
X _o (initial)	0.584	0.0278	0.3882
X _d (distillate)	0.2412	0.6932	0.06798

Temp °C		Time (dt),min	dl,mL	distillate, Δd ,mL	Areas			Moles			Mole Fractions		
Still pot	H ₂ O Bath				Methanol	Diethyl ether	Benzene	Methanol	Diethyl ether	Benzene	Methanol	Diethyl ether	Benzene
47.6	50	7.3	6.3	2.1	1024.8	267.4	2464.7	7686	566.888	5175.87	0.5723538	0.042214	0.3854318
47.6	50	7	6.3	2.1	1332.1	389.7	2940.6	9990.75	826.164	6175.26	0.5879618	0.04862	0.3634179
47.6	50	4.5	6.3	2.1	785.2	312.4	1961.8	5889	662.288	4119.78	0.551866	0.062064	0.3860701
47.5	51	6.2	6.3	2.1	619.7	249.8	1543.7	4647.75	529.576	3241.77	0.5520486	0.062902	0.3850497
47.5	51	6.4	6.3	2.1	721.9	320.8	1703.4	5414.25	680.096	3577.14	0.5598157	0.07032	0.3698646
47.4	51	7.3	6.3	2.1	902.8	416.8	2189.1	6771	883.616	4597.11	0.5526568	0.072122	0.3752214
47.4	50	6.3	6.3	2.1	602.3	278.9	1403.1	4517.25	591.268	2946.51	0.5607988	0.073404	0.3657976
47.5	50	6.4	6.3	2.1	1028.9	521.8	2315.9	7716.75	1106.216	4863.39	0.5638279	0.080826	0.3553459
47.5	50	7.2	6.3	2.1	823.7	435.7	1946.7	6177.75	923.684	4088.07	0.5521022	0.082549	0.3653486
47.7	51	7.1	6.3	2.1	635.9	340.8	1473.4	4769.25	722.496	3094.14	0.5554756	0.084149	0.3603752
47.7	51	6.4	6.3	2.1	813.3	465.8	1920.1	6099.75	987.496	4032.21	0.5485655	0.088808	0.3626266
47.7	51	7.3	6.3	2.1	931.2	624.7	2231	6984	1324.364	4685.1	0.537501	0.101925	0.3605736
47.9	51	8.1	6.3	2.1	621.3	412.5	1450	4659.75	874.5	3045	0.5431419	0.101932	0.3549261
47.9	51	7.4	6.3	2.1	927.8	631.8	2410.1	6958.5	1339.416	5061.21	0.5208799	0.100262	0.3788579
47.9	51	8.2	6.3	2.1	998.1	701.8	2655.8	7485.75	1487.816	5577.18	0.5144582	0.10225	0.3832917
47.9	51	8.3	6.3	2.1	1489.7	1049.1	4006	11172.75	2224.092	8412.6	0.5122896	0.101978	0.385732

Table D6: Results for the column profile map using the reflux ratio of 3, see figure 5.13 & figure 5.14

APPENDIX E

The Water, Ethanol and Ethyl Acetate System

Operating conditions for the GC

Inlet

Carrier Gas used	:	Helium
Mode	:	Split
Heater Temperature	:	130°C
Pressure	:	326.2 KPa
Total Flow	:	222 ml/min.
Split ratio	:	10:1
Split flow	:	15 ml/min
Gas saver	:	20 ml/min

Column

Type of Column	:	Zebron Capillary Column
Dimensions of the column	:	75m*350µm*1 µm
Mode	:	Constant Pressure
Inlet	:	Front
Detector	:	Back
Pressure	:	326.2 KPa
Flow	:	10 ml/min.
Average velocity	:	69 cm/sec

Oven

Oven Temperature	:	70 °C
Max. Temperature	:	200 °C
Hold up time	:	10 min

Detector

Type of Detector	:	Thermal Conductivity Detector
Heater Temperature	:	170°C
Reference flow	:	17 ml/min
Makeup flow for Helium	:	20 ml/min
Constant Column + Makeup	:	2 ml/min

Auxiliary

Thermal Aux. number	:	1
Heater Setpoint	:	160 °C
Type	:	Valve Box

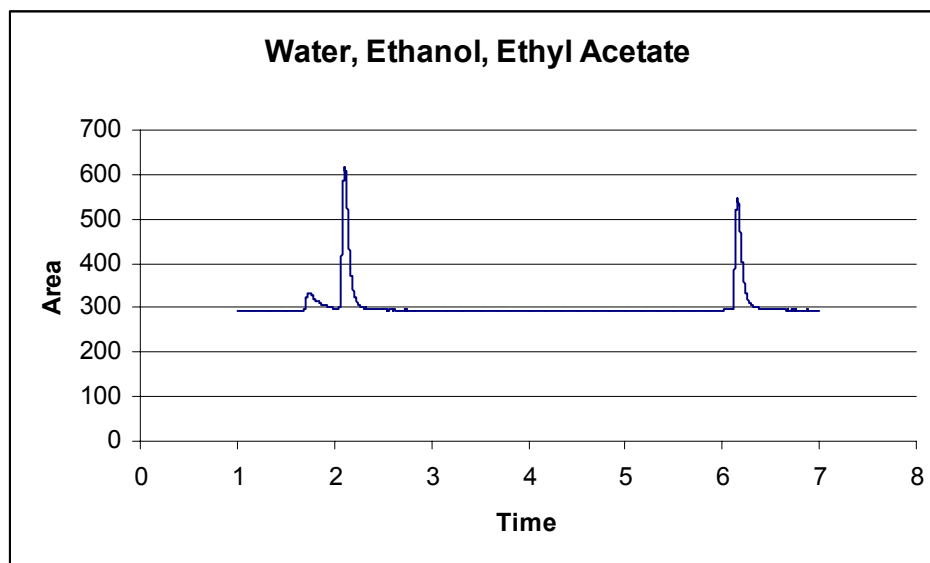


Figure E1: Area vs Time plot from the GC.

The above figure shows traces of GC results for the Water, Ethanol and Ethyl Acetate system. The first peak is Water, second peak Ethanol and the last peak is Ethyl Acetate.

GC Calibration Program

The following Mathcad Program was used to calibrate the GC, i.e., determine the component response factors. The response factors are normalized with respect to water. Through out this program, A =Water; B = Ethanol; C = Ethyl Acetate.

Samples Compositions in mole fractions:

$$\begin{array}{l} x_A := \begin{bmatrix} 0 \\ 0 \\ 0 \\ 0 \\ 0 \\ 0.8037 \\ 0.6092 \\ 0.4074 \\ 0.2122 \\ 0.51002 \\ 0.9357 \\ 0.9606 \\ 0.9711 \\ 0.6262 \\ 0.3938 \\ 0.5565 \\ 0.2495 \\ 0.322 \end{bmatrix} \end{array}$$
$$\begin{array}{l} x_B := \begin{bmatrix} 0.7985 \\ 0.60496 \\ 0.3915 \\ 0.2016 \\ 0.5037 \\ 0.1963 \\ 0.3908 \\ 0.5926 \\ 0.7878 \\ 0.48998 \\ 0 \\ 0 \\ 0 \\ 0.2453 \\ 0.2975 \\ 0.2171 \\ 0.652 \\ 0.4166 \end{bmatrix} \end{array}$$
$$\begin{array}{l} x_C := \begin{bmatrix} 0.2015 \\ 0.39504 \\ 0.6085 \\ 0.7984 \\ 0.4963 \\ 0 \\ 0 \\ 0 \\ 0 \\ 0 \\ 0.06425 \\ 0.03941 \\ 0.0289 \\ 0.12851 \\ 0.3087 \\ 0.2263 \\ 0.0985 \\ 0.26115 \end{bmatrix} \end{array}$$

14

Peak Areas Obtained

AreaA :=	$\begin{bmatrix} 0 \\ 0 \\ 0 \\ 0 \\ 0 \\ 1784.73 \\ 939.6 \\ 461.067 \\ 83.507 \\ 587.9 \\ 4122.45 \\ 4414.4 \\ 4044.67 \\ 795.45 \\ 193.8 \\ 558.925 \\ 101.733 \\ 99.4 \end{bmatrix}$	AreaB :=	$\begin{bmatrix} 1733.3 \\ 833.367 \\ 451.867 \\ 234.267 \\ 724.5 \\ 1608.47 \\ 2342.57 \\ 2762.8 \\ 1967.49 \\ 2583.55 \\ 0 \\ 0 \\ 0 \\ 1343.075 \\ 896.4 \\ 924.75 \\ 2721.77 \\ 1239.3 \end{bmatrix}$	AreaC :=	$\begin{bmatrix} 829.733 \\ 1165.2 \\ 1767.8 \\ 2946.63 \\ 1644.2 \\ 0 \\ 0 \\ 0 \\ 0 \\ 0 \\ 276.95 \\ 355.33 \\ 221.8 \\ 990.31 \\ 1544.77 \\ 1202.73 \\ 667.1 \\ 1228.48 \end{bmatrix}$
----------	--	----------	---	----------	--

n := 0..17

Guess Values for the Normalized response factors with respect to benzene:

kE := 0.1

kM := 0.1

kA := 0.1

Defining predicted compositions - mole fractions:

$$xM_{p_n} := \frac{kM \cdot \text{Area}M_n}{kM \cdot \text{Area}M_n + kE \cdot \text{Area}E_n + kA \cdot \text{Area}A_n}$$

$$xE_{p_n} := \frac{kE \cdot \text{Area}E_n}{kM \cdot \text{Area}M_n + kE \cdot \text{Area}E_n + kA \cdot \text{Area}A_n}$$

$$xA_{p_n} := \frac{kA \cdot \text{Area}A_n}{kM \cdot \text{Area}M_n + kE \cdot \text{Area}E_n + kA \cdot \text{Area}A_n}$$

Defining the error term:

$$\begin{aligned} \text{Error}(kM, kE, kA) := & \sum_{n=0}^{19} \left[xM_n - \left(\frac{kM \cdot \text{Area}M_n}{kM \cdot \text{Area}M_n + kE \cdot \text{Area}E_n + kA \cdot \text{Area}A_n} \right) \right]^2 \dots \\ & + \sum_{n=0}^{19} \left[xE_n - \left(\frac{kE \cdot \text{Area}E_n}{kM \cdot \text{Area}M_n + kE \cdot \text{Area}E_n + kA \cdot \text{Area}A_n} \right) \right]^2 \dots \\ & + \sum_{n=0}^{19} \left[xA_n - \left(\frac{kA \cdot \text{Area}A_n}{kM \cdot \text{Area}M_n + kE \cdot \text{Area}E_n + kA \cdot \text{Area}A_n} \right) \right]^2 \end{aligned}$$

Iteration loop:

given $\text{Error}(kM, kE, kA) = 0$

$$\frac{d}{dkM} \text{Error}(kM, kE, kA) = 0$$

$$\frac{d}{dkA} \text{Error}(kM, kE, kA) = 0$$

$$\frac{d}{dkE} \text{Error}(kM, kE, kA) = 0$$

The Calculating Function:

$$\begin{bmatrix} kM \\ kE \\ kA \end{bmatrix} := \text{minerr}(kM, kE, kA)$$

The calculated response factors and the error term:

$$\begin{bmatrix} kM \\ kE \\ kA \end{bmatrix} = \begin{bmatrix} 0.12882 \\ 0.09581 \\ 0.08451 \end{bmatrix}$$

$$\text{Error}(kM, kE, kA) = 4.5159910^{-4}$$

Recalling the predicted mole fractions:

$$xM_{p_n} := \frac{kM \cdot \text{Area}M_n}{kM \cdot \text{Area}M_n + kE \cdot \text{Area}E_n + kA \cdot \text{Area}A_n}$$

$$xA_{p_n} := \frac{kA \cdot \text{Area}A_n}{kM \cdot \text{Area}M_n + kE \cdot \text{Area}E_n + kA \cdot \text{Area}A_n}$$

$$xE_{p_n} := \frac{kE \cdot \text{Area}E_n}{kM \cdot \text{Area}M_n + kE \cdot \text{Area}E_n + kA \cdot \text{Area}A_n}$$

Calibration Plots: Actual vs. Predicted compositions:

$f(x) := x$

$x := 0..1..1$

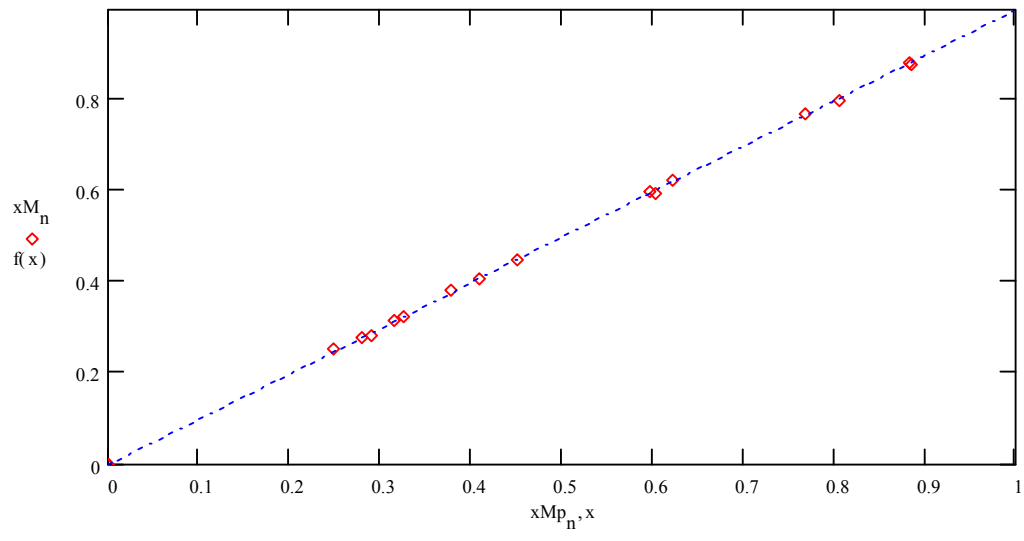


Figure E2: The Water Plot

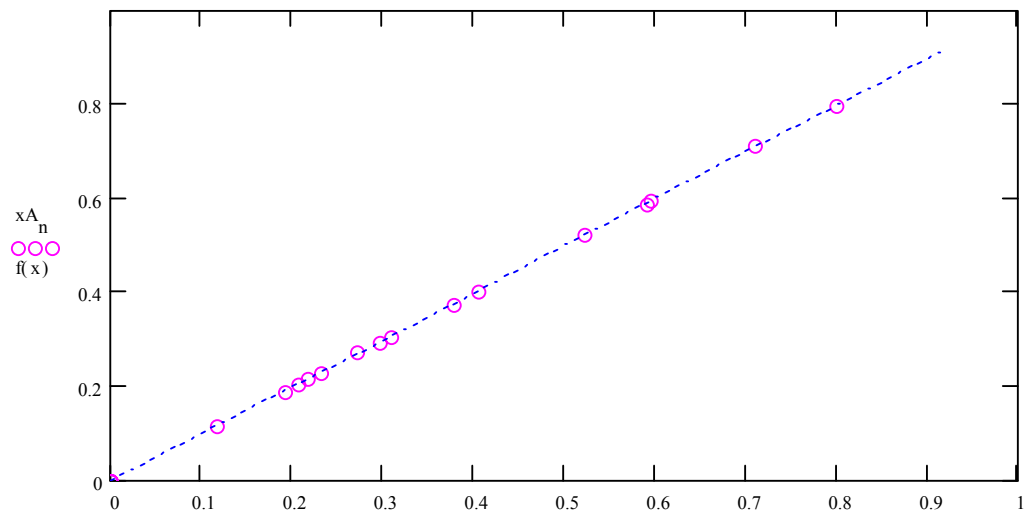


Figure E3: The Ethanol Plot:

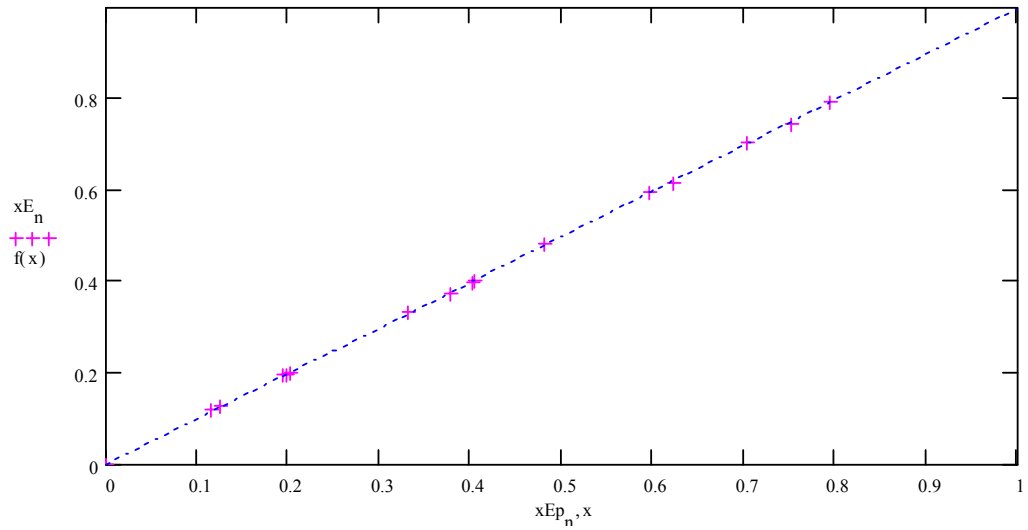


Figure E4: The Ethyl Acetate Plot:

The Difference Between Actual and Predicted Compositions:

$xM_n - xMp_n =$	$ xEn - xEp_n =$	$xAn - xAp_n =$
$-7.14563 \cdot 10^{-3}$	$7.14563 \cdot 10^{-3}$	0
$-4.27936 \cdot 10^{-3}$	$4.27936 \cdot 10^{-3}$	0
$4.73177 \cdot 10^{-3}$	$4.73177 \cdot 10^{-3}$	0
$2.16369 \cdot 10^{-3}$	$2.16369 \cdot 10^{-3}$	0
$6.66568 \cdot 10^{-3}$	$6.66568 \cdot 10^{-3}$	0
$-6.34942 \cdot 10^{-4}$	0	$6.34942 \cdot 10^{-4}$
$1.71403 \cdot 10^{-3}$	0	$-1.71403 \cdot 10^{-3}$
$1.90783 \cdot 10^{-3}$	0	$-1.90783 \cdot 10^{-3}$
$1.02898 \cdot 10^{-3}$	0	$-1.02898 \cdot 10^{-3}$
$-4.94528 \cdot 10^{-3}$	0	$4.91528 \cdot 10^{-3}$
0	$1.27446 \cdot 10^{-3}$	$-1.25446 \cdot 10^{-3}$
0	$2.09302 \cdot 10^{-3}$	$-1.99302 \cdot 10^{-3}$
0	$1.02877 \cdot 10^{-3}$	$-1.02877 \cdot 10^{-3}$
0	$3.83249 \cdot 10^{-4}$	$-3.83249 \cdot 10^{-4}$
0	$1.50868 \cdot 10^{-3}$	$1.50868 \cdot 10^{-3}$
$-1.00797 \cdot 10^{-3}$	$1.93756 \cdot 10^{-3}$	$-8.29594 \cdot 10^{-4}$

The Average Difference between Actual and Predicted Mole Fractions:

$$M_{\text{mean}} := \frac{\sum_{n=0}^{19} |xM_n - xMp_n|}{20}$$

$$E_{\text{mean}} := \frac{\sum_{n=0}^{19} |xE_n - xEp_n|}{20}$$

$$A_{\text{mean}} := \frac{\sum_{n=0}^{19} |xA_n - xAp_n|}{20}$$

$$M_{\text{mean}} = 2.2966810^{-3}$$

$$E_{\text{mean}} = 2.0536410^{-3}$$

$$A_{\text{mean}} = 1.1826110^{-3}$$

Experimental Results for the column profile map, see Chapter 6

	Mole Fractions		
	Ethanol	Water	Ethyl Acetate
x_o (initial)	0.0774	0.1714	0.7512
x_d (distillate)	0.0966	0.1132	0.7902

Temp °C		Time (dt),min	dl,mL	distillate, Δd , mL	Areas			Moles			Mole Fractions		
Still pot	H ₂ O Bath				Ethanol	Water	Ethyl Acetate	Ethanol	Water	Ethyl Acetate	Ethanol	Water	Ethyl Acetate
68	72	6.3	6.3	6.3	243.6	576.4	3016.4	314.244	552.1912	2548.858	0.092010841	0.161682	0.746307228
68.1	72	6.3	6.3	6.3	302.3	768.2	4421.8	389.967	735.9356	3736.421	0.080201778	0.151355	0.768443507
68.2	72	6	6.3	6.3	254.6	405.7	2541.1	328.434	388.6606	2147.2295	0.1146637	0.13569	0.749646138
68.3	72	6	6.3	6.3	270.8	435.7	2801.3	349.332	417.4006	2367.0985	0.111471228	0.133192	0.755336974
68.4	72	6.2	6.3	6.3	256.8	325.7	2351.8	331.272	312.0206	1987.271	0.125931949	0.118614	0.755454459
68.4	72.5	5.3	6.3	6.3	276.7	455.8	3342.8	356.943	436.6564	2824.666	0.098650309	0.120681	0.780668549
68.7	72.5	5	6.3	6.3	187.6	315.4	2557.3	242.004	302.1532	2160.9185	0.089462931	0.111699	0.798838458
69.3	72.5	5.3	6.3	6.3	428.9	543.8	4678.1	553.281	520.9604	3952.9945	0.110056701	0.103628	0.786315697
69.3	72.5	4.2	6.3	6.3	345.3	401.5	4072.5	445.437	384.637	3441.2625	0.104285158	0.090051	0.805664105
69.5	72.5	4.3	6.3	6.3	330.1	422.3	3745	425.829	404.5634	3164.525	0.106592692	0.10127	0.79213778
69.5	72.5	5	6.3	6.3	172	300.1	2588.9	221.88	287.4958	2187.6205	0.082269301	0.106599	0.811132184

Table E1: Results for column profile map using a reflux ratio of 1, see figures 6.13, 6.14 & 6.15

	Mole Fractions		
	Ethanol	Water	Ethyl Acetate
x_o (initial)	0.1161	0.2235	0.6604
x_d (distillate)	0.093	0.1049	0.8021

Temp °C		Time (dt),min	dl,mL	distillate, Δd ,mL	Areas			Moles			Mole Fractions		
Still pot	H ₂ O Bath				Ethanol	Water	Ethyl Acetate	Ethanol	Water	Ethyl Acetate	Ethanol	Water	Ethyl Acetate
66.8	70	7.3	6.3	6.3	274.6	628.4	2105.1	354.234	602.0072	1778.8095	0.129516	0.220108	0.650375329
66.8	70	6.3	6.3	6.3	302.3	908.3	3047.2	389.967	870.1514	2574.884	0.101686	0.226897	0.671416529
66.8	70	6.3	6.3	6.3	282.7	730.8	2541.7	364.683	700.1064	2147.7365	0.113519	0.21793	0.668550719
67.1	70	6.4	6.3	6.3	297.1	863.4	2801.3	383.259	827.1372	2367.0985	0.107131	0.231206	0.661663734
67	70	6.2	6.3	6.3	466.3	1025.7	3646.5	601.527	982.6206	3081.2925	0.128933	0.210617	0.660450554
67.1	70	6.3	6.3	6.3	331.8	889.7	3047.4	428.022	852.3326	2575.053	0.111019	0.221075	0.667906812
67.3	71	6.3	6.3	6.3	254.7	778.9	2613.8	328.563	746.1862	2208.661	0.100068	0.22726	0.672672881
67.4	71	6	6.3	6.3	428.9	1125.7	4017.5	553.281	1078.421	3394.7875	0.110073	0.214547	0.675379461
67.4	71	6	6.3	6.3	354.8	1145.8	3931.8	457.692	1097.676	3322.371	0.093833	0.225038	0.681129254
67.4	71	6.2	6.3	6.3	320.3	805.7	2989.4	413.187	771.8606	2526.043	0.111338	0.207988	0.680674032
67.5	71	5.3	6.3	6.3	261.7	660.4	2588.9	337.593	632.6632	2187.6205	0.106905	0.200344	0.692750448
67.5	72	5	6.3	6.3	371.6	892.3	3610.4	479.364	854.8234	3050.788	0.10932	0.194944	0.695736628
67.5	72	5.3	6.3	6.3	384.2	1045.4	4219.3	495.618	1001.493	3565.3085	0.097901	0.197829	0.70426964
67.6	72	4.2	6.3	6.3	302.5	813.2	3334.5	390.225	779.0456	2817.6525	0.097876	0.1954	0.706723563
67.6	72	4.3	6.3	6.3	257.9	672.8	2846.6	332.691	644.5424	2405.377	0.098353	0.190546	0.711100811

Table E2: Results for column profile map using a reflux ratio of 1, see figures 6.13, 6.14 & 6.15

	Mole Fractions		
	Ethanol	Water	Ethyl Acetate
x_o (initial)	0.5599	0.2089	0.2312
x_d (distillate)	0.0912	0.0987	0.8101

Temp °C		Time (dt),min	dl,mL	distillate, Δd , mL	Areas			Moles			Mole Fractions		
Still pot	H ₂ O Bath				Ethanol	Water	Ethyl Acetate	Ethanol	Water	Ethyl Acetate	Ethanol	Water	Ethyl Acetate
58.2	62	5	6.3	6.3	2746.8	1324.7	1678.4	3543.372	1269.063	1418.248	0.568697	0.20368	0.227623
58.2	62	6.3	6.3	6.3	2346.7	1025.6	1456.7	3027.243	982.5248	1230.9115	0.577643	0.18748	0.234876
58.2	62	7	6.3	6.3	2946.3	1546.3	2264.6	3800.727	1481.355	1913.587	0.528196	0.205868	0.265936
58.3	62	6	6.3	6.3	3547.5	1672.8	2715.8	4576.275	1602.542	2294.851	0.540058	0.18912	0.270821
58.3	63	7	6.3	6.3	2648.7	1309.6	2399.1	3416.823	1254.597	2027.2395	0.510076	0.187291	0.302634
58.5	63	6.3	6.3	6.3	3018.5	1508.5	2741.6	3893.865	1445.143	2316.652	0.508626	0.188768	0.302606
58.5	63	7	6.3	6.3	2785.4	1535.8	2699.9	3593.166	1471.296	2281.4155	0.48914	0.200289	0.310571
58.7	63	6	6.3	6.3	2257.1	1322.5	2431.5	2911.659	1266.955	2054.6175	0.467119	0.203258	0.329623
58.7	63	5.3	6.3	6.3	3714.5	2213.7	3931.8	4791.705	2120.725	3322.371	0.468178	0.207207	0.324615
60	64	5.3	6.3	6.3	3201.3	1689.4	3311.6	4129.677	1618.445	2798.302	0.483205	0.189371	0.327424
60	64	6	6.3	6.3	2167.2	1364.5	2634.9	2795.688	1307.191	2226.4905	0.441701	0.206528	0.351771
60.2	64	5.3	6.3	6.3	2418.6	1768.7	3610.4	3119.994	1694.415	3050.788	0.396684	0.215432	0.387885
60.2	64	6	6.3	6.3	1897.8	1521.5	3325.1	2448.162	1457.597	2809.7095	0.364556	0.217051	0.418394
60.5	64	6.3	6.3	6.3	1603.3	1169.2	2803.4	2068.257	1120.094	2368.873	0.372175	0.201556	0.426269
60.5	64	7	6.3	6.3	2322.4	1868.2	4272.4	2995.896	1789.736	3610.178	0.356832	0.21317	0.429998

Table E3: Results for column profile map using a reflux ratio of 1, see figures 6.13, 6.14 & 6.15

	Mole Fractions		
	Ethanol	Water	Ethyl Acetate
x_o (initial)	0.3476	0.2098	0.4426
x_d (distillate)	0.742	0.1121	0.8137

Temp °C		Time (dt),min	dl,mL	distillate, Δd ,mL	Areas			Moles			Mole Fractions		
Still pot	H ₂ O Bath				Ethanol	Water	Ethyl Acetate	Ethanol	Water	Ethyl Acetate	Ethanol	Water	Ethyl Acetate
61.4	65	7.5	6.3	6.3	1201.7	1010.9	2418.7	1550.193	968.4422	2043.8015	0.339773	0.212264	0.447963
61.4	65	6.2	6.3	6.3	1826.4	1664.2	3812.4	2356.056	1594.304	3221.478	0.328515	0.222301	0.449184
61.6	65	8	6.3	6.3	1901.6	1893.5	4265.8	2453.064	1813.973	3604.601	0.311633	0.230444	0.457923
61.6	65	6.5	6.3	6.3	1306.3	1402.8	3216.4	1685.127	1343.882	2717.858	0.293225	0.233846	0.472929
61.8	65	7.2	6.3	6.3	1823.6	1721.6	4399.1	2352.444	1649.293	3717.2395	0.304761	0.213667	0.481572
62	66	7.1	6.3	6.3	1128.4	1548.5	3439.7	1455.636	1483.463	2906.5465	0.249012	0.253772	0.497216
62	66	6.3	6.3	6.3	1055.9	1276.8	3022.8	1362.111	1223.174	2554.266	0.265025	0.237992	0.496982
62.2	66	7.4	6.3	6.3	1341.7	2047.4	4521.2	1730.793	1961.409	3820.414	0.230385	0.261082	0.508533
62.2	66	6.2	6.3	6.3	1434.6	1614.6	3899.3	1850.634	1546.787	3294.9085	0.276531	0.231128	0.492341
62.2	66	6.3	6.3	6.3	1001.3	1499.3	3300.6	1291.677	1436.329	2789.007	0.234126	0.260345	0.505528
62.4	67	6.4	6.3	6.3	916.4	1194.5	2883.7	1182.156	1144.331	2436.7265	0.248185	0.240243	0.511572
62.4	67	6.5	6.3	6.3	883.3	1539.6	3621.6	1139.457	1474.937	3060.252	0.200798	0.259917	0.539285
62.4	67	6.2	6.3	6.3	697.8	1132.9	2728.3	900.162	1085.318	2305.4135	0.209784	0.252935	0.53728
62.6	67	7.1	6.3	6.3	673.8	1269.4	2803.4	869.202	1216.085	2368.873	0.195144	0.273022	0.531834
62.6	67	6.5	6.3	6.3	1113.9	1897.3	4027.9	1436.931	1817.613	3403.5755	0.215816	0.272992	0.511192

Table E4: Results for column profile map using a reflux ratio of 1, see figures 6.13, 6.14 & 6.15

	Mole Fractions		
	Ethanol	Water	Ethyl Acetate
x_o (initial)	0.2667	0.2412	0.4921
x_d (distillate)	0.0955	0.1059	0.7986

Temp Still pot	°C H ₂ O Bath	Time (dt),min	dl,mL	distillate, Δd ,mL	Areas			Moles			Mole Fractions		
					Ethanol	Water	Ethyl Acetate	Ethanol	Water	Ethyl Acetate	Ethanol	Water	Ethyl Acetate
63.2	67	7.3	6.3	6.3	1347.2	1749.7	4023.9	1737.888	1676.2126	3400.1955	0.255035586	0.245984703	0.498979711
63.3	67	7.1	6.3	6.3	1033.6	1751.3	3812.4	1333.344	1677.7454	3221.478	0.213931742	0.269190093	0.516878165
63.3	68	7.5	6.3	6.3	1209.5	1957.7	4412.1	1560.255	1875.4766	3728.2245	0.217792373	0.261793424	0.520414202
63.3	68	6.2	6.3	6.3	929.3	1583.5	3367.9	1198.797	1516.993	2845.8755	0.215546404	0.272758763	0.511694833
63.5	68	7.4	6.3	6.3	827.3	1321.3	2879.4	1067.217	1265.8054	2433.093	0.223917574	0.265584295	0.51049813
63.5	68	7.3	6.3	6.3	1017.6	1693.2	3863.8	1312.704	1622.0856	3264.911	0.211736676	0.261639344	0.526623979
63.5	68	7.2	6.3	6.3	667.2	1446.8	3052.8	860.688	1386.0344	2579.616	0.178331466	0.287181355	0.53448718
63.5	68	6.3	6.3	6.3	728.8	1572.1	3431.2	940.152	1506.0718	2899.364	0.175874391	0.281741102	0.542384506
63.6	68	6.3	6.3	6.3	869.1	1953.8	4576.8	1121.139	1871.7404	3867.396	0.16342478	0.272837502	0.563737718
63.6	69	6	6.3	6.3	732.3	1593.2	3292.6	944.667	1526.2856	2782.247	0.179826976	0.290543995	0.529629028
63.6	69	5.3	6.3	6.3	764.7	1934.2	3745.2	986.463	1852.9636	3164.694	0.164297666	0.30861532	0.527087014
63.6	69	5.3	6.3	6.3	813.5	1599.6	3129.7	1049.415	1532.4168	2644.5965	0.200790088	0.293205362	0.50600455
63.6	69	6	6.3	6.3	900.4	2062.9	4012.7	1161.516	1976.2582	3390.7315	0.177914526	0.302712181	0.519373292
63.7	69	6	6.3	6.3	855.8	1892.4	3528.8	1103.982	1812.9192	2981.836	0.187155651	0.307340222	0.505504127
63.7	69	5.3	6.3	6.3	687.7	1727.8	3368.9	887.133	1655.2324	2846.7205	0.1646166	0.307145299	0.528238101
63.7	70	5.4	6.3	6.3	1151.3	2396.5	4387.9	1485.177	2295.847	3707.7755	0.198319771	0.306570766	0.495109463
63.9	70	5.5	6.3	6.3	716.7	1894.6	3606.1	924.543	1815.0268	3047.1545	0.159769665	0.313653581	0.526576754
63.9	70	5.4	6.3	6.3	629.2	1805.1	3299.4	811.668	1729.2858	2787.993	0.152313024	0.324507987	0.523178989

Table E5: Results for column profile map using a reflux ratio of 1, see figure 6.13, 6.14 & 6.15

	Mole Fractions		
	Ethanol	Water	Ethyl Acetate
x_o (initial)	0.3681	0.1892	0.4427
x_d (distillate)	0.0959	0.1019	0.8022

Temp °C	Still pot	H ₂ O Bath	Time (dt),min	dl,mL	distillate, Δd ,mL	Areas			Moles			Mole Fractions		
						Ethanol	Water	Ethyl Acetate	Ethanol	Water	Ethyl Acetate	Ethanol	Water	Ethyl Acetate
62.3	67	7.3	6.3	6.3	1698.8	1213.1	3198.7	2191.45	1162.1	2702.9	0.3618345	0.1918846	0.44628086	
62.3	67	7	6.3	6.3	1402.9	1047.8	2883.7	1809.74	1003.8	2436.73	0.3446955	0.1911891	0.46411541	
62.5	67	7.3	6.3	6.3	1792.5	1329.6	3673	2312.33	1273.8	3103.69	0.3456511	0.1904038	0.46394517	
62.5	67	7.3	6.3	6.3	1799.6	1474.9	4118.5	2321.48	1413	3480.13	0.3217772	0.1958473	0.48237555	
62.5	68	7	6.3	6.3	1377.2	1112.2	3218.9	1776.59	1065.5	2719.97	0.3194127	0.191564	0.48902336	
62.7	68	7.2	6.3	6.3	1782.8	1493.2	4315.3	2299.81	1430.5	3646.43	0.3117659	0.1939188	0.49431529	
62.7	68	7.3	6.3	6.3	1307.6	1223.1	3399.1	1686.8	1171.7	2872.24	0.2943414	0.2044628	0.5011958	
62.8	68	7	6.3	6.3	1252.9	1488.7	4016.4	1616.24	1426.2	3393.86	0.2511144	0.2215839	0.5273017	
63.1	68	7.1	6.3	6.3	1109.1	1392.8	3892.2	1430.74	1334.3	3288.91	0.2363315	0.2204019	0.54326659	
63.2	69	7.3	6.3	6.3	1021.8	1219.2	3699.4	1318.12	1168	3125.99	0.2348711	0.2081203	0.55700864	
63.4	69	7	6.3	6.3	737.1	1134.7	3097	950.859	1087	2616.97	0.204272	0.2335282	0.56219978	
63.4	69	7.25	6.3	6.3	861.1	1688.1	4417.2	1110.82	1617.2	3732.53	0.1719387	0.2503191	0.5777422	
63.6	69	7.3	6.3	6.3	765.3	1442.4	3782.8	987.237	1381.8	3196.47	0.1773844	0.248282	0.57433353	
63.6	70	7.3	6.3	6.3	811.3	1375.9	4217.6	1046.58	1318.1	3563.87	0.1765314	0.2223326	0.60113607	
63.8	70	7	6.3	6.3	645.8	1409.4	3897.1	833.082	1350.2	3293.05	0.152124	0.2465526	0.60132342	
63.8	71	7.3	6.3	6.3	509.1	1334.6	3498.2	656.739	1278.5	2955.98	0.1342677	0.2613939	0.60433837	

Table E6: Results for column profile map using a reflux ratio of 1, see figure 6.13, 6.14 & 6.15